POLITECNICO DI TORINO

Automotive Engineering

Master of Science [Class LM-33]

Energy Management Strategy for a High-Performance Hybrid Vehicle

Master Thesis

Supervisors:

Chiar.mo prof. Stefano Malan

Ing. Claudio Manzali

Candidate:

Francesco Bertolini

“La vita è come il caffè. Puoi metterci tutto lo zucchero che vuoi, ma se lo vuoi far diventare dolce, devi girare il cucchiaino. A stare fermi non succede niente”

(Alex Zanardi)

20 Luglio 2020

Table of Contents

Nomenclature

ICE	Internal Combustion Engine
BEV	Battery Electric Vehicle
PHEV	Plug-In Hybrid Electric Vehicle
DCT	Dual Clutch Transmission
WLTP	Worldwide harmonized Light vehicles Test Procedures
SOC	State Of Charge
CS	Charge Sustain
CD	Charge Depleting
EU	European Union
EC	European Commission
EM	Electric Motor
AWD	All Wheel Drive
RWD	Rear Wheel Drive
DoD	Depth of Discharge
SoH	State of Health
RDE	Real Driving Emission cycle

1. Introduction

The first section delivers a brief overview of the working context inside and outside Automobili Lamborghini, as well as an explanation of the aim of the project.

1.1 Context

1.1.1 Automobili Lamborghini: history and products

Automobili Lamborghini is an Italian manufacturer of high-performance vehicles that was established in 1963 in Sant'Agata Bolognese.

As Onion, Missy and Mullen (2009) report, Ferruccio Lamborghini started his own business producing tractors for agriculture purpose, even using old military machines components, few years after World War II.

Since the very beginning of its history, the company's logo recalls the founder's zodiac sign, and therefore shows a bull, also recalled as *Taurus,* shown in Fig. 1. Consistently to the logo's meaning, many Lamborghinis are named as famed bulls.

Fig.1 Lamborghini's logo (retrieved from Wikipedia.org)

It is important to remember that no passenger cars were produced by Lamborghini initially, but air-conditioning and heating systems, in addition to tractors, came out of the original production lines. Nevertheless, as the business grew more and more solid, Ferruccio Lamborghini became a wealthy entrepreneur, able to purchase luxury and sports car such as those from Enzo Ferrari.

The traditional story reports that the rivalry - that still goes on - between Ferrari and Lamborghini companies started after a meeting between the two founders (Harvey, 2016). When Lamborghini (still a tractors-only producer at the time) met Ferrari to complain about various mechanical defects discovered on his new car, the two men had a strong dispute: from that moment on, Lamborghini

decided to expand his own business plans towards luxury sports cars too, meant to be better than Ferrari's cars.

As Smeyers recalls (2015), many famous engineers entered Automobili Lamborghini during the following years and most interestingly, many came from Ferrari. The company's founder was able to recruit Giotto Bizzarrini, a former Ferrari's engineer who built the company's first V-12 engine. Giampaolo Dallara, the future founder of Dallara Automobili in Varano dè Melegari, was engaged from Ferrari by Ferruccio Lamborghini too. Bob Wallace, former Ferrari's and Maserati's chief mechanic, became Lamborghini's chief tester.

The first Lamborghini car concept debuted in 1963, with the name *' Lamborghini 350 GTV, a two-seater coupe with a V12 engine '*. One year later the first production car was completed in the new plant, with the name of Lamborghini 350 GT, depicted in Fig.2.

Fig.2 Lamborghini 350 GT (Smeyers, 2015)

The 30 initial years of history of the new Lamborghini car brand were, on one side, characterized by very successful models. One of the most popular and appreciated cars was without doubt the 1969 Miura P400s, that is often seen as the first supercar, which opened the way for mid-engine road cars (Jurnecka, 2019), since such design was mainly adopted by racing teams for their Le-Mans cars. Among the most successful cars produced by Lamborghini, it is worth remembering the 1975 Countach LP400 and 1990 Diablo, which were all powered by class-leading V12 engines and were admired for their extreme and sporty exterior design.

On the other side, financial and production conditions were rapidly deteriorating by the end of the 1960s. Such difficulties became even more evident after two main events: one regarding the change of ownership of the company, and one due to external factors.

Between 1972 and 1973, Ferruccio Lamborghini sold his own company to Georges-Henri Rossetti and René Leimer, two Swiss entrepreneurs; in addition to that, the oil crisis occurred in 1973 determined a sudden drop in sales and, consequently, revenues.

From those years on, there were a couple of decades of financial troubles and production instability. Between 1981 and 1998, the ownership was repeatedly changed. One after the other, the two Swiss brothers, then a couple of French entrepreneurs, then the Chrysler company, and later on the Indonesian Megatech group stepped into the company and left it few years later.

Eventually in 1998 the company was purchased – and still is- by the German automaker Volkswagen Group, and assigned under the control of Audi division.

As it is shown in Fig.3 a positive trend in terms of new vehicle sales was established, and continued up to the start of the Covid-19 crisis.

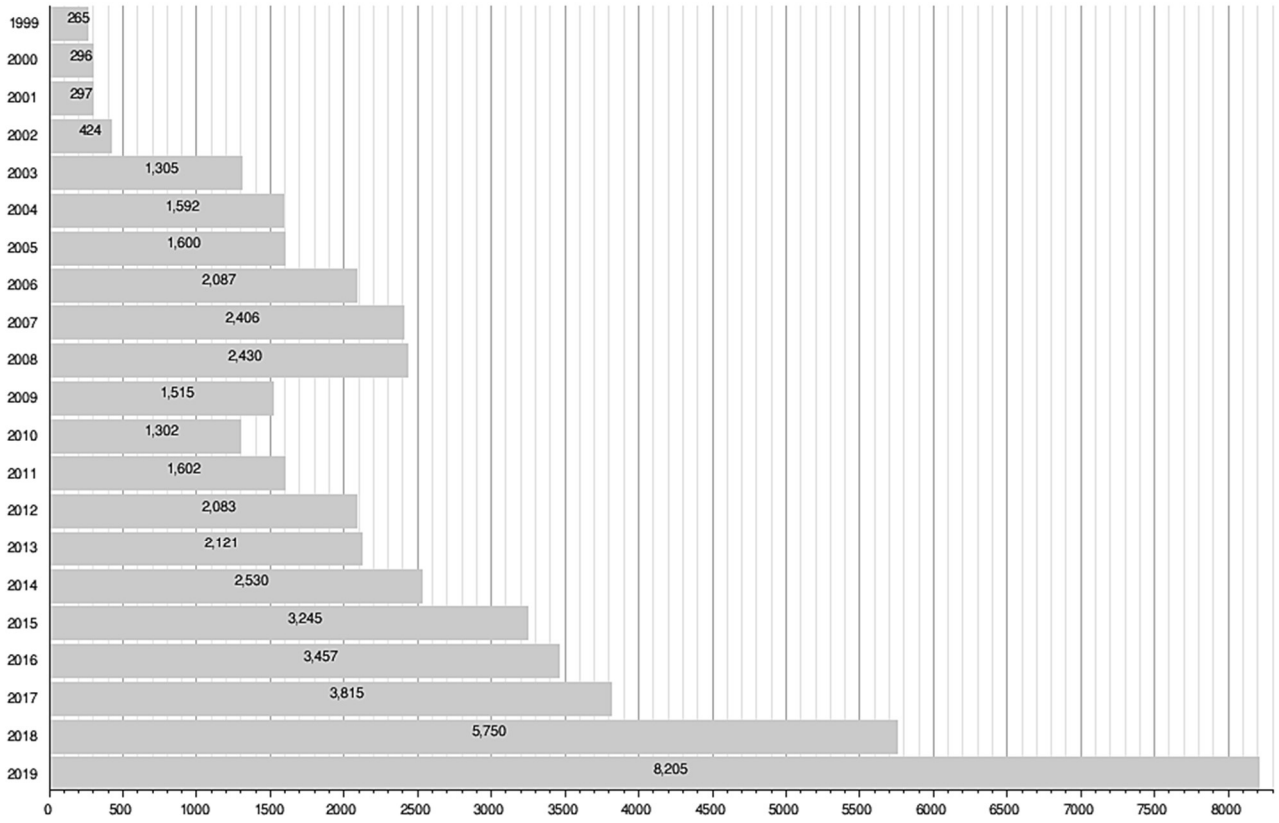

Fig.3 Annual Lamborghini new car sales (retrieved from https://en.wikipedia.org/wiki/Lamborghini)

The latest data available from Lamborghini Press Release documents (PressRelease, Automobili Lamborghini S.p.A MediaCenter, 2020) report that the company delivered 8,205 cars in 2019 and it is selling worldwide through a 165 dealership network.

The current car range is divided depending on the engine typology, and includes:

- V8: Lamborghini Urus, the first Super-SUV launched in 2017 and the currently best-selling product of the range
- V10: Lamborghini Huracán, debuted in 2014, available in AWD, RWD and Spyder version
- V12: Lamborghini Aventador, launched in 2011 and available both with coupé and roadster body in S and SVJ (Super Veloce Jota) versions
- The few-off build of only 63 units Lamborghini Siàn FKP 37, unveiled in 2019 and ' *featuring the world-first application of a supercapacitor for hybridization* ' combined with a V12 gasoline engine

All the vehicles currently under production feature a naturally aspirated gasoline engine (apart from the Urus model, which employs a bi-turbo unit) and no manual gearbox: while the Urus is provided with a eight-speed torque-converter automatic gearbox from ZF, the Huracán is driven by a eight-speed dual clutch transmission, and the Aventador by the proprietary ISR (Independent Shifting Rods), that is seven-speed automated manual gearbox. Another common feature of Lamborghini cars is that they are all four-wheel drive: only a dedicated RWD version of the Huracan does not feature AWD.

It is very important to mention also the first, actual step into the "hybrid" sector that Lamborghini made: the plug-in hybrid Asterion Concept debuted in 2014 at the Paris Motor Show. Powered by a V10 derived from the Huracán and three electric motors, it was capable of driving in full electric mode up to 50km long and with a 125km/h top speed.

During that event, as Buzzetti reports (2014, p. 292-293), engineer Reggiani declared that ' *the underlying problem has always been not to lose sight of the heart of Lamborghini with the requirements of new rules for type-approval of cars, which will definitely arrive in the future. Rules that are naturally linked to consumption and therefore to CO_2 emissions.* '

Such declaration of intent represents a clear guideline for new Lamborghini hybrid cars.

1.1.2 2020 New Emission Standards and Automotive Industry Reaction

The rising demand for lowering greenhouse gases emissions and local pollution has determined increasingly strict emission standards, forcing the automotive sector to come up with alternative solutions to Internal Combustion Engine powered cars. The push from national and international governments towards a more sustainable mobility comes from both the costumer and the producer side: while the former can benefit from subsidies and tax reductions when purchasing EM-powered vehicles such as BEV and PHEV, the latter must avoid considerable fines when crossing specific emission limits.

For sake of simplicity, EU standards are adopted in this paper as the main reference for emission limits: however, it must be clear that being Lamborghini products available worldwide, they must also fulfil all the other requirements imposed by different American and Asian regulations. According to

that, fig. 4 gives a worldwide overview on recent and future emission regulations and fuel consumption trends.

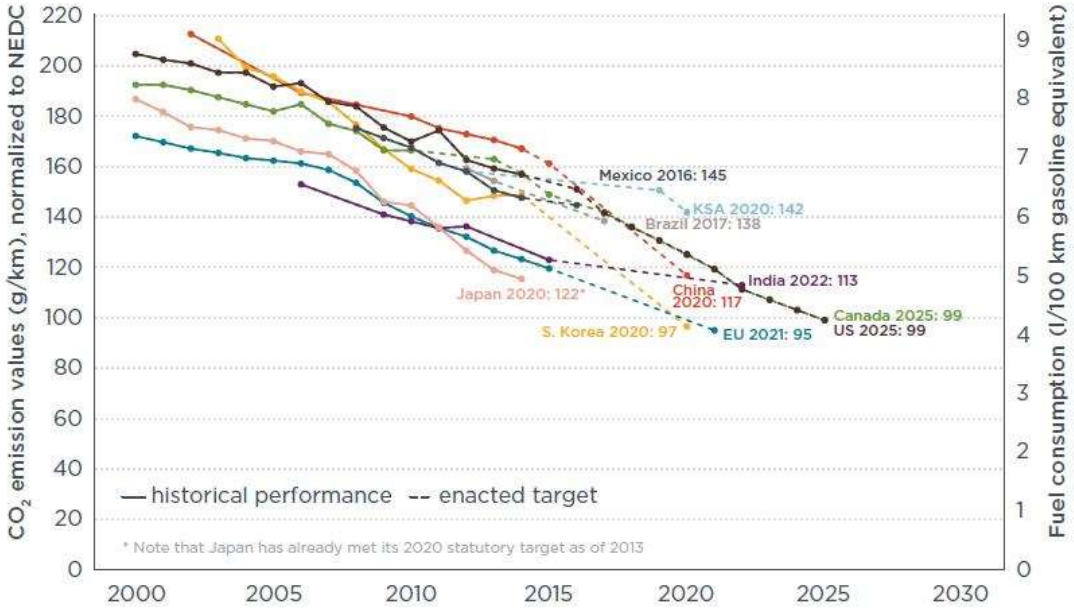

Fig. 4 CO_2 emission standards and fuel consumption worldwide trends ((EUCommission, 2017)

Coming back to the European example, the European Commission states that *' cars are responsible for around 12% of total EU emissions of carbon dioxide (CO_2), the main greenhouse gas '* (2018). This is the reason why Regulation 2019/631 was adopted by the European Parliament and the Council on 17 April 2019: it *' introduces CO_2 emission performance standards for new passenger cars and new vans for 2025 and 2030. The new Regulations started applying on 1 January 2020 '*.

According to these new targets, *' from 2021, phased in from 2020, the EU-fleet-wide average emission target for new cars will be 95g CO_2/km. This emission level corresponds to a fuel consumption of around 4.1l/100 km of petrol […] '*. The phase-in period of 2020 will apply the emission targets *' for each manufacturer's 95% least emitting new cars. From 2021 on, the average emissions of all newly registered cars of a manufacturer will have to be below the target. '*

As the overview of Lamborghini's product range pointed out, the company mainly relies on naturally aspirated gasoline engines, which are the least suitable power units for the ambitious CO_2 emission reduction targets that modern regulations demand. Another possible problem in terms of homologation issues comes from the fact that

' […] targets for manufacturers are set according to the average mass of their vehicles, using a limit value curve. This means that manufacturers of heavier cars are allowed higher emissions than manufacturers of lighter cars'

Exceeding such limits is payed, since 2019, at a very high price. *' The penalty is 95€ for each g/km of targed exceedance '* for each car registered by the manufacturer.

What is crucially important to clarify the context of the research made, is the fact that EU regulations also state that:

‘ Manufacturers are given additional incentives to put on the market zero- and low-emission cars emitting less than 50g/km through a “super-credits” system. This already applied between 2012 and 2015 and will apply again for the period 2020-2022 ’

In addition to that, the rules include some exceptions for low-volumes manufacturers:

‘ Manufacturers responsible for between 1 000 and 10 000 cars registered per year (“small volume” manufacturers) can propose their own derogation target, which has to be approved by the Commission based on the criteria set in the Regulation ’

1.2 Aim of the study

Lamborghini's Research and Development department already started the development of plug-in hybrid vehicles several years from now: the 2014 Asterion concept mentioned in the "Context" paragraph provides an example of how Lamborghini approaches the PHEV idea. What is different, with respect to the earlier stages of study and development that were already performed by the company, is that now a stronger effort is put into the energy management strategies. The main focus is no more related to the layout definition, namely the position of the electric motors, their number, the type of electric motors adopted; nor the sizing of the components has to be defined either, since the vast majority of the technical characteristics were defined and constrained from the very start of the project: such constrains include battery capacity, power and torque of both Internal Combustion Engine and Electric Motors, gear ratios for the thermal and the electric mechanical power transmission.

The purpose of the project is to provide a real-time strategy working with "trained" rules and parameters, so that it can accomplish its driving mission optimizing energy consumption, despite the lack of *a priori* knowledge of the route.

In order to design and optimize the aforementioned rules, it is necessary to create a fully virtual vehicle model first, that simulates the vehicle dynamic behaviour, and, most importantly, determines with adequate accuracy its energy consumption during various driving cycles. Such model accuracy can be achieved only implementing close-to-reality components and parameters: before even creating the model, it is mandatory to gather the latest and most detailed experimental data, available from bench tests on real vehicle components – in particular engine, electric motors, the battery and the gearbox too. This process is never ending in practice: new data, more precise or simply updated up to the latest version, require continuous updates to the virtual model.

To sum up, the final aim of energy optimization is achieved through the data collection phase first, then to the virtual model creation, and is finally reached with rules optimization via recurring testing.

2. High-Performance Hybrid Vehicles: state-of-the-art

This section provides with some insights into the hybrid powertrain technical characteristics, and how such concept has been applied over the past few years to the high-performance vehicle category. This section does not deliver an exhaustive overview of HEV classification: as a suggestion for those looking for further information, a more complete outline is available thanks to the work of Dai-Duong Tran et al. (Thorough state-of-the-art analysis of electric and hybrid vehicle powertrains: Topologies and integrated energy management strategies, 2019).

2.1 Hybridization Degree: Mild, Full and Plug-In Hybrid Vehicles

The Lamborghini Siàn (see Fig.5) is an example of a Mild-Hybrid supercar. As it happens for vehicles with similar hybridization degree, the ICE remains the main source of power. Mild-Hybrid vehicles generally feature a low-capacity electric energy storage: in the case of the Siàn, such role is played by a supercapacitor, that combines high charge/discharge rate with low weight and size.

This is due to the fact that Lamborghini applies the mild-hybrid concept mainly keeping performance as a top-priority target, and not just focusing on efficiency: the electric motor is '*coming directly out of the gearbox, for an immediate and better performance during acceleration and gear shifting* ' (PressRelease, Siàn FKP 37 - Ahead of its time, 2019).

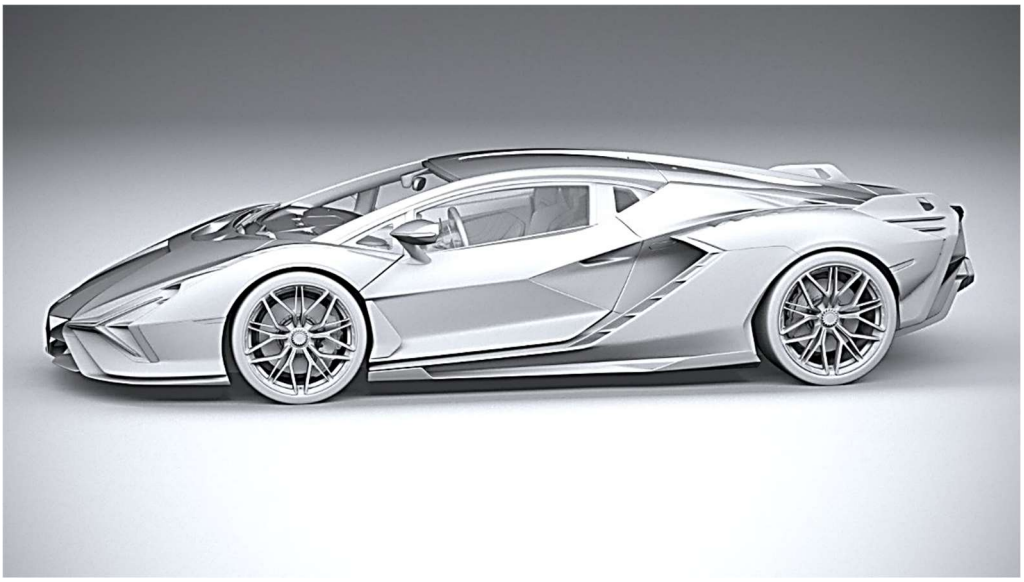

Fig. 5 2019 Lamborghini Siàn (Squir Team, 2020)

Other manufacturers usually adopt a small-size lithium-ion battery instead, which has much lower power rates, it is heavier and usually features around 0.5kWh of storage capacity; anyway such battery is always inexpensive when compared to supercapacitors.

All these systems employ a 48V electric motor, that is mainly used to start the engine and run the auxiliaries, or allow the so-called *coasting* phase for a limited period of time (Lee, Cherry, Safoutin, McDonald, & Olechiw, 2018).

Full-hybrid vehicles differ from the mild-hybrid ones in terms of battery and motor capability. According to Genta (2009) they employ a much more powerful electric unit, able to move the car even without involving the ICE, and the EM is frequently applied to the other axle to provide four-wheel drive capability. Battery storage capacity is higher too, and it is usually adequate to allow EM-only driving even for medium-to-high speed profiles.

The most diffused implementation of the full-hybrid concept is the Plug-In Hybrid vehicle: electric energy is stored not only via regenerative braking, but also by external chargers that are the same of BEVs. This allows the car to have a larger battery, and one (or more) powerful electric motor that allows high speed driving in EM-only mode. At the price of an increase in complexity and weight, the vehicle can be more efficient if the battery is always charged at the driving start.

Over the last decade, many Plug-In Hybrid supercars were launched or are almost ready for homologation procedures, including:

- the 2019 Ferrari SF90 Stradale: it integrates a 573kW V8 engine with a 162kW electric propulsion unit. In particular, the electric powertrain features three electric motors, two of them installed on the front axle, and one between the ICE and the 8-speed dual-clutch gearbox; the Lithium-Ion battery stores 7.9 kWh, and guarantees a 25km in eDrive mode
- the 2013 Porsche 918: it combines a 600 hp 4.6-litre V8 with a couple of synchronous motors that output 282 hp: with such layout, and a 6.8 kWh battery, such vehicle was able to travel for more than 25 km (even though this was measured along the old and far-from-reality New European Driving Cycle) and it can achieve '*astonishing*' performance due to the ' *rampant electric motors instant torque* ' (Prior, 2013)
- the McLaren Speedtail and the Aston Martin Valyrie: they both feature powerful electric motors, combined with a V8 and a V12 gasoline engine. The former produces over 772kW and the latter around 865kW. EM-only range is yet to be specified, as well as most of their technical data (Allan, 2020)

Common traits among the cited supercars are the presence of a battery chosen with the weight reduction target, thus small and with medium-to-low (under 20-15kWh) capacity, and the electric motors moving independently the front axle to improve traction.

2.2 Powertrain Configurations: Series, Parallel and Power-Split

In a Series-Hybrid vehicle, the EM is the only propelling motor. The ICE power is used to charge the battery, maintain its SOC or avoid rapid battery discharging when high requests of power come from the driver. As it is shown in Fig. 6 the ICE is mechanically independent from the wheels and thus, no gearbox is required. This also means that its speed can be tuned according to the energy management strategy.

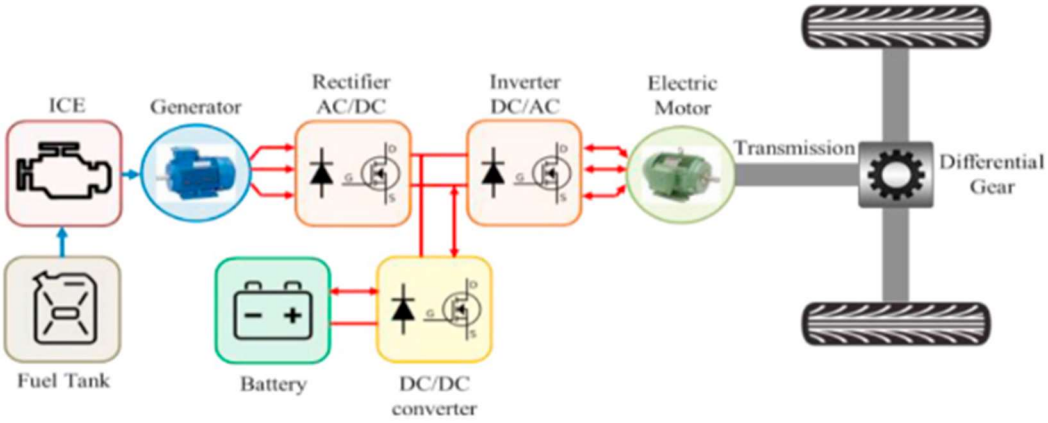

Fig. 6 Series-HEV configuration (Tran, et al., 2019)

Therefore, the series-hybrid configuration allows the ICE to operate at its best efficiency point, and its size can be considerably reduced. However, energy conversion losses that result from this solution make it less efficient than the parallel configuration and as Tran et al. report (2019), series-hybrid vehicles '*are not suitable for highway or inter-urban driving owing to higher conversion losses and the need for a large EM at high speeds*'. Therefore, it is almost straightforward to understand why no modern supercar features this type of configuration: the complete disconnection between engine speed and vehicle velocity, as well as the absence of the gearbox, has a dramatic impact on vehicle performance, sound and driving experience.

As an alternative, Parallel-Hybrid Vehicles utilize both the EM and ICE to drive the vehicle. In this case, the EM size is generally lower than that of the ICE, but it is still able to guarantee zero-emission driving with the ICE turned off, with speed and range depending on EM and battery sizing. The parallel configuration is depicted in Fig. 7: the main difference from the previous model arises in the presence of the two torque lines, that are connected to the differential gear by specific clutches.

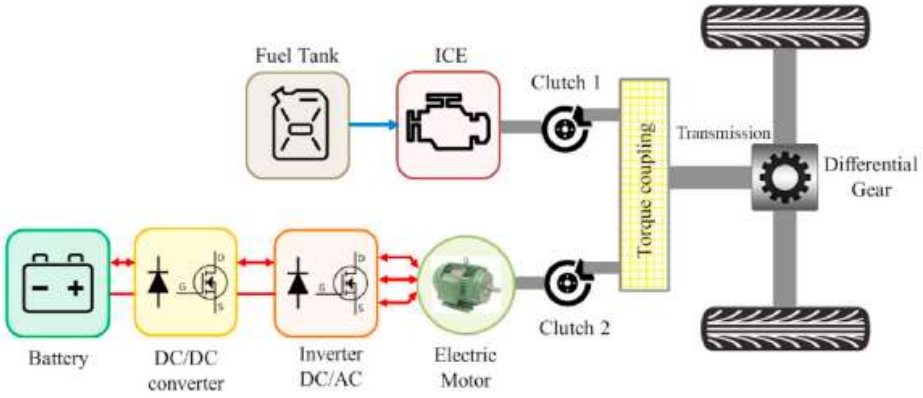

Fig. 7 Parallel-HEV configuration (Tran, et al., 2019)

The third and last configuration is the so-called Power-Split one. As it happened for series-hybrids, this option will not be discussed into details, since it is not considered as suitable for high performance hybrid vehicles by modern automotive companies. As a general overview, it employs a planetary gear set instead of a common gearbox, and it allows both series and parallel powertrain running modes. The replacement of the gearbox with a Continuously Variable Transmission (CVT) makes it a less appealing option for performance and driving involvement targets too, together with the complexity and overall weight of its components.

2.3 E-Motor Layout: P1, P2, P3 and P4 topologies

Focusing on parallel implementations, Fig. 8 shows that E-Motors can be installed in five major locations (Stark, 2016): a brief explanation of each case will be provided, as well as few examples of how such concepts are applied to nowadays supercars.

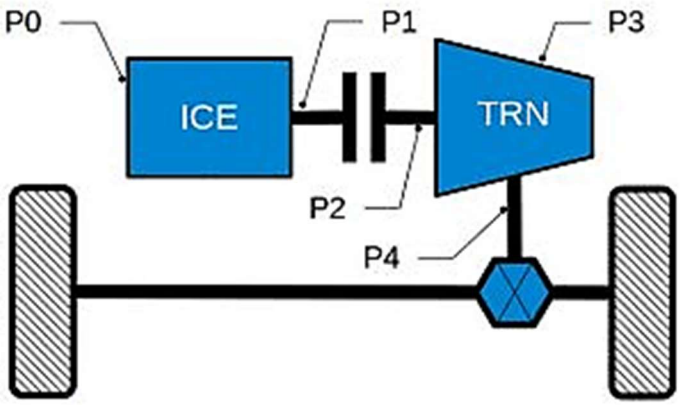

Fig. 8 EM placement among various layouts (Stark, 2016)

P0 and P1 configurations are those typical of Mild-Hybrid vehicles already seen beforehand. Fig.9 shows that the electric motor is mechanically connected to the engine, either via the auxiliary belt (P0) or directly crankshaft mounted (P1), as it is represented in Fig.8. These configurations usually adopt 48V electric devices, that optimize the cranking phase of the internal combustion engine and provide the energy for the auxiliary devices on board. A 48V system allows for an increase power output, while keeping similar current values to the 12V devices and thus reduce cable sizing. For example, a belt-alternator starter 48V system is adopted by the 2019 Audi RS6, powered by the same engine that is mounted onto the Lamborghini Urus.

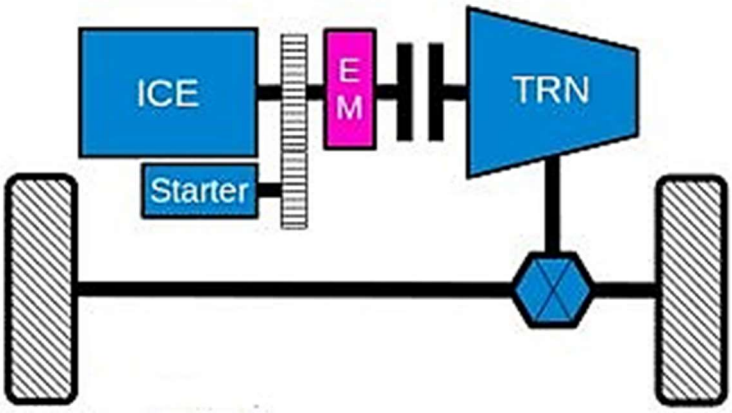

Fig. 9 P1 layout (Stark, 2016)

Alternatively, the P2 option allows the EM to be integrated into the transmission, and so with the possibility to be disconnected from the engine. In this case, at a price of an ' *higher integration cost of such a system* ', Stark (2016) highlights the advantage of the ' *increased energy recuperation potential and the availability of additional hybrid control functions'* such as electric creep or driving.

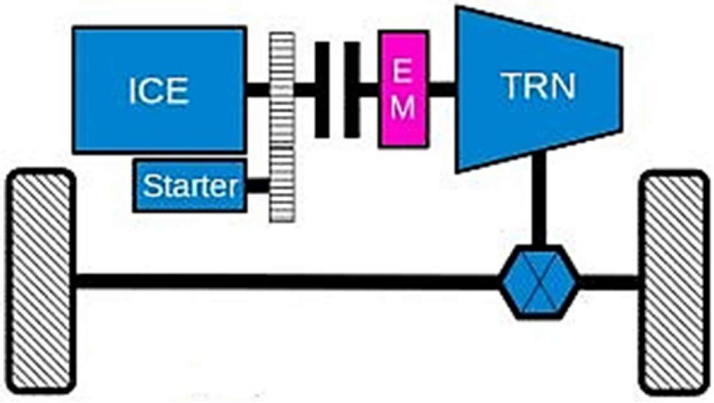

Fig. 10 P2 layout (Stark, 2016)

The P2 configuration, visible in Fig. 10, is adopted by two class leading supercars, namely the 2019 Ferrari SF90 Stradale and the 2013 Porsche 918. They both feature multiple EMs, and both were designed with the P2 configuration at the rear axle: this means that they integrated the rear EM, smaller than those on the front, between the ICE and the gearbox. This option is still very compact and weight efficient, thus complex to design.

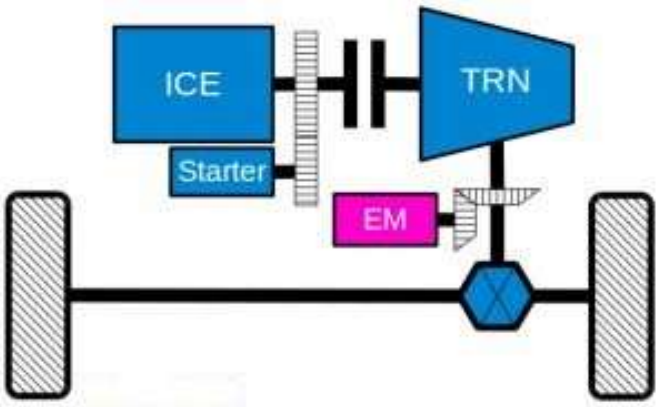

Fig. 11 P3 layout (Stark, 2016)

As Fig. 11 depicts, no engine and transmission losses affect power transmission from P3 and P4 configurations, where the ICE is not propelling the car: this is due to the fact that the EM is installed on the transmission output shaft in the P3 case, or connecting the EM directly on the axle drive is the case of P4.

Wheel-hub EMs, such as those adopted by the 2013 Mercedes-Benz SLS AMG Electric Drive, are generally considered P4-mounted, because they are not in contact with ICE or the gearbox too.

Coming back to the Porsche and Ferrari that served as an application of the P2 layout, it is interesting to notice that they also implemented the P4 configuration at the front axle. This means that all-wheel drive is available, as well as pure EM-only driving, without adding a dedicated mechanic transmission. Fig. 12 clearly shows how Porsche engineers installed P4 and P2 motors into the car.

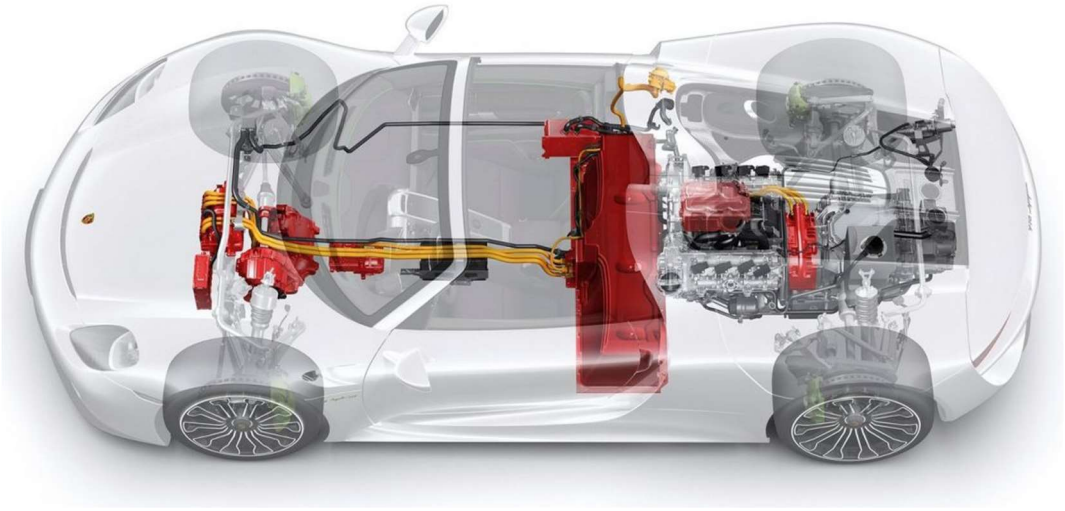

Fig. 12 Porsche 918: the electric powertrain is highlighted in red (Baroni, 2018)

With respect to simpler architectures, P2, P3 and P4 require more powerful electric motors and capable electronics, as well as an increase in the powertrain management complexity. It is not questionable though, that the P4 layout can avoid the usage of mechanical parts to provide 4WD, thus improving lightness and freeing up space for other components along the passenger's compartment. It is worth mentioning that while the SF90 Stradale actually adopts two EMs in parallel at the front axle, so three EMs in total on the car, the 918 adopts one EM only (two EMs).

As it was mentioned earlier on, the dimension of the battery is a question of major concern for supercar design. The dimensioning of this component must consist in a well-balanced trade-off between battery size and weight. Under the hypothesis that size increase is directly proportional to capacity increase, a bigger battery is beneficial in terms of:

- e-drive range, that can be greatly useful when facing homologation tests
- charge and discharge capability: a small size battery generally tolerates lower currents, and thus power outputs and inputs that are linked to EMs intervention
- battery aging: the higher the battery capacity, the greater the possibility to remain into the so-called Constant Current (CC) working phase, avoiding the CV phase that is estimated to feature '*more than 90% of the cyclable lithium*; also, DoD during daily driving would be clearly lower too, and again the lower the DoD, the better the aging behaviour of the battery (Kabitz, et al., 2013)

On the other hand, battery size should be reduced because:

- lateral dynamics and braking performance are worsened
- the car design does not easily allow room for the battery compartment, which must be designed in compliance with all safety rules too
- the overall car cost, even if less problematic for this category of cars, would be higher

3. Vehicle model

The first section of this chapter summarizes how the vehicle model was conceived from the very beginning of the project, in terms of method, software and hardware adopted.

Then, the following sections offer an overview of the model structure, and the in-depth analyses of each major subsystem.

3.1 Modelling Approach and Tools

The model utilized during this project is defined as a longitudinal-only model. None of the blocks utilized takes into account lateral dynamics nor in general vehicle behaviour during manoeuvres and cornering. This is because the focus of the project always remained on the propulsion components, and how they interact with the propelling trust of the vehicle. Such approach is consistent to Lamborghini R&D internal organization: each department works within its specific field, producing its own virtual model. Therefore models used by safety division or vehicle dynamics engineers are independent from each other, and different from those utilized by powertrain engineers as well.

Simulation data regarding engine, electric motors, battery and wheels were utilized when possible. Such values were obtained by powertrain virtual models and in-house testing from other departments and/or external suppliers, and were then reported into detailed and extensive lookup tables.

This choice of using look-up tables was agreed at the project start according to three main reasons:

- first reason was that most of the parameters needed to virtually build a complete physical model of the thermal engine, or the one of the electric motors, were either unavailable or very difficult to obtain: a continuous and time-consuming phase of data collection among suppliers, designers and other departments would have been out of the scope of this study and would have delayed tremendously the model preparation. This stands, without even considering the great complexity of designing the ICE virtual model
- secondly, even though some complete models would have been available at the time of the project, they would have been too complex and impacting on the simulation performance when implemented in a complete car model as the one used in this case. A slowdown in simulation speed would have had a negative impact on the overall project feasibility
- third and last reason, lookup tables were used by the R&D department to simulate powertrain layouts on their own model already before this project started. This choice of consistency permitted more efficient comparison and update processes between the two models

Vehicle layout remained fixed and constrained from the very beginning of the project, and so did most of the technical characteristics of the vehicle. In fact, as it was stated earlier on, neither components dimensioning nor choice was targeted. The strategy was aimed to manage and employ

the actuators and the energy sources available in the most efficient way, without the possibility to add or remove, or even change, existing components.

Still, a noticeable amount of components were continuously updated and revised throughout the course of the project, thanks to new data arrival coming from other departments. The following list specifies the most significant changes occurred:

- **Internal Combustion Engine**: engine torque map and consumption map, rpm range
- **Wheels**: tire radius, rolling resistance coefficients, wheels inertia
- **Vehicle Dynamics**: aerodynamic coefficient (vehicle shape), vehicle mass, frontal area
- **Gearbox**: gear ratios, mechanical efficiencies
- **Electric Motors**: torque maps, current maps, inverter efficiencies, gear ratios, efficiencies
- **Auxiliaries**: other devices consumption, in terms of kW load on the electric powertrain

While some variations had low impact on consumption values, other did have an heavy effect on simulation results, and thus on how all the strategy parameters were set. This meant that the strategy definition was revised multiple times, in order to keep the new model - created for this project - aligned to the already existing one developed by the R&D earlier on, that was continuously kept updated too. The following chapters will provide a detailed overview of the strategy, and how it was adapted together with the model evolution.

The model was created using Matlab-Simulink R2019b, running on a 2014 computer with 8 Gb of RAM. As the model became more complex and the computational load rose up, the computer performances became progressively inadequate, up to a point when it was no more possible to run the simulation. This required an hardware intervention on the computer itself, so that to expand the former 8 Gb RAM up to a 16 Gb value.

A great obstacle to data processing, as well as model design, was the necessity to simulate the model with a *Variable-step solver*, and variable *absolute tolerance*. This led to frequent incompatibilities between external blocks supplied by third party manufacturers and internal model blocks, as well as data logging issues when examining them, with respect to a fixed-step solver model.

Simulink “Model Advisor” was utilized to check model performances, and helped checking for inefficient block design. Last but not least, the model strategy rules and parameters were optimized via the dedicated Add-On “Sensitivity Analyzer”, which works seamlessly inside the Matlab-Simulink environment as it is part of its apps.

3.2 Model overall structure

The vehicle model is composed by eight major functional subsystems: each of them groups a different subset of blocks. Fig. 13 provides an overview of how those blocks are positioned into the Simulink environment, while each of the following paragraphs will take a closer look at each of them. The letters in red above each subsystem are linked to the following list.

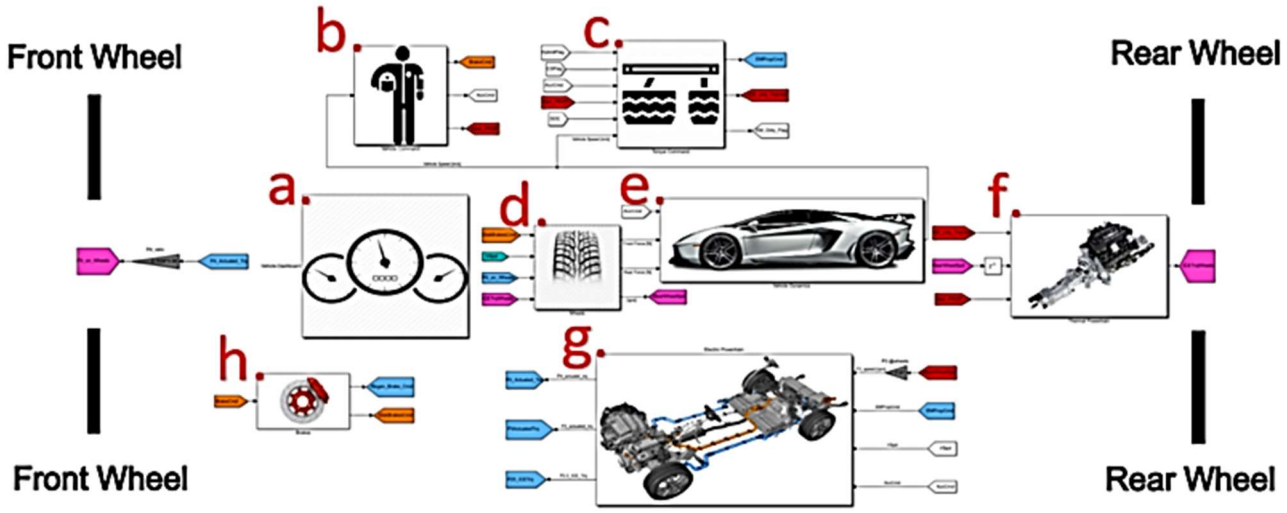

Fig. 13 Simulink model overview

The main subsystems are defined as listed:

a. **Vehicle Dashboard**: real-time output values of powertrain units, brakes, vehicle status and other important information can be any time checked during and after the simulation via scopes, display and signal logging that are here implemented
b. **Vehicle Command:** it includes virtual driver and route inputs to the car
c. **Torque Command:** it assigns torque requests to the different powertrain units depending on the information from “Vehicle Command” subsystem
d. **Wheels:** positive and negative torques coming from propulsion and braking units converge here and are transformed in longitudinal forces acting on the vehicle
e. **Vehicle Dynamics:** all the forces acting on the vehicle are summed to obtain the overall acceleration applied longitudinally to the vehicle mass
f. **Thermal Powertrain**: it features the Internal Combustion Engine and the gearbox
g. **Electric Powertrain:** it is primarily composed by electric motors and the storage system
h. **Brakes**: it simulates regenerative braking, as well as the traditional disk braking system

The *Thermal Powertrain* and the *Electric Powertrain* subsystems will be also recalled from now on as *actuators*.

A detailed description of each subsystem follows. It is clear that it would be impossible to show in figures, nor describe the entire model in all its blocks and subsystems: therefore a selection of the most significant ones will be made.

A couple of disclaimers must be provided:

- subsystem masks adopted are not in any way representative of the real components installed on the actual car
- sensible data were omitted or replaced by letters and symbols

3.3 Vehicle Dashboard

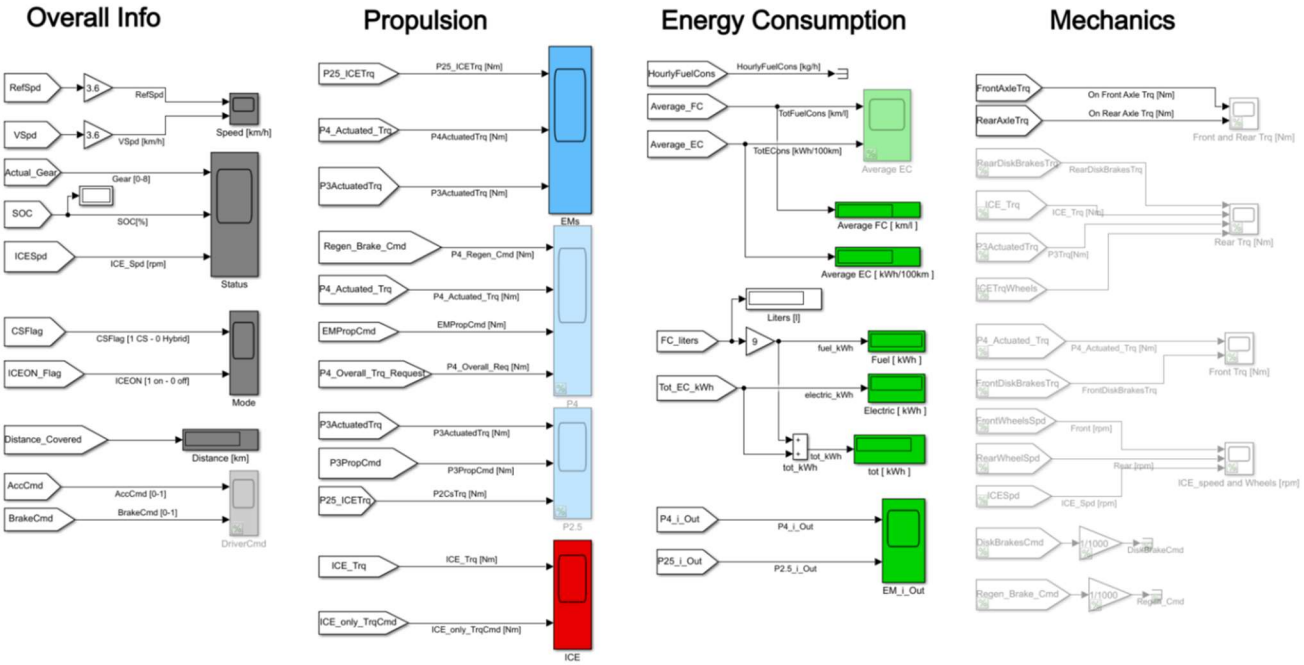

Fig. 14 Vehicle Dashboard overview

As Fig.14 shows, this subsystem groups all the various scopes and displays that are needed to keep under control the vehicle parameters during and after the model run. Those indicators are organised in four main columns.

The first column regards the *Overall Info*. General parameters, such as reference and actual speed, battery State of Charge (SOC) and engine speed are reported. In addition, this particular section allows to monitor the inputs coming from *Vehicle Command* subsystem, such as the gear engaged, acceleration and braking commands, as well as vehicle operating modes .

The second column comprises all the scopes that keep under control the input and output values from both the thermal engine and the three electric motors: information such as the relation between torque demand and torque actuated are fundamental to ensure that the propulsion system behaves in a correct way.

The most important column is nevertheless the third one, that is defined as the *Energy Consumption*. Simulation results are monitored here, and are immediately visible thanks to the creation of many displays. Fig. 15 shows the core blocks from this subsystem, that outputs the final results of energy consumption calculations, which are determined depending on the two different powertrains and combined in the overall kWh amount too.

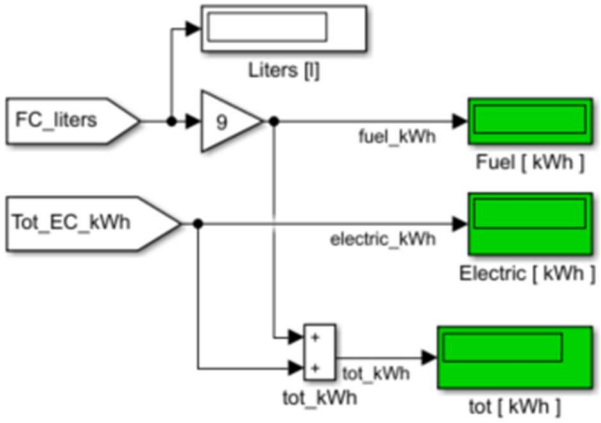

Fig. 15 Overall energy consumption monitoring

Furthermore, scopes that monitor the currents that enter and exit the front and rear EMs are included too.

The *Mechanics* column played an important role during the early stages of development. Back to when bugs and lack of controls made the model unstable, unreliable and even completely blocked, information coming from axle torques, speeds of the wheels and disk brakes intervention were often precious to analyse the model. When the simulation progressively became more precise and controllable, most of these scopes underwent the process of 'commenting', that means they do not take part into the simulation anymore. Still, they were not removed, in case of future needs. This choice helped in speeding up the simulation, while maintaining older problem solving tools.

3.4 Vehicle Command

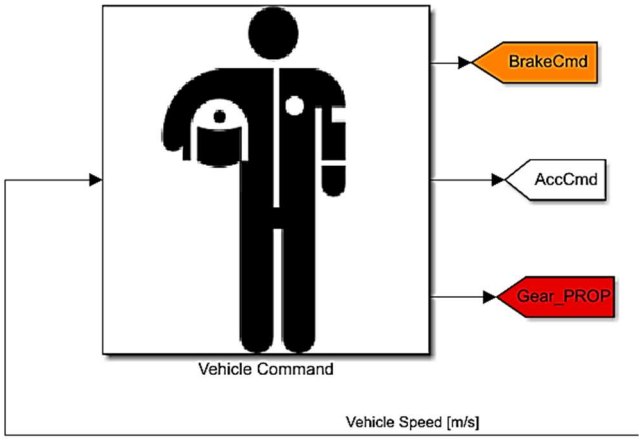

Fig. 16 Vehicle Command subsystem and ports

Fig. 16 shows that the *Vehicle Command* subsystem receives as the main input the vehicle current speed, and outputs driver commands for the other model subsystems.

3.4.1 Vehicle speed tracing

The key parameter that drives the entire model is of course the reference speed provided by the block *Drive Cycle Source*, that directly enters the *PI controller* block simulating driver's reactions. The two blocks are reported in Fig. 17.

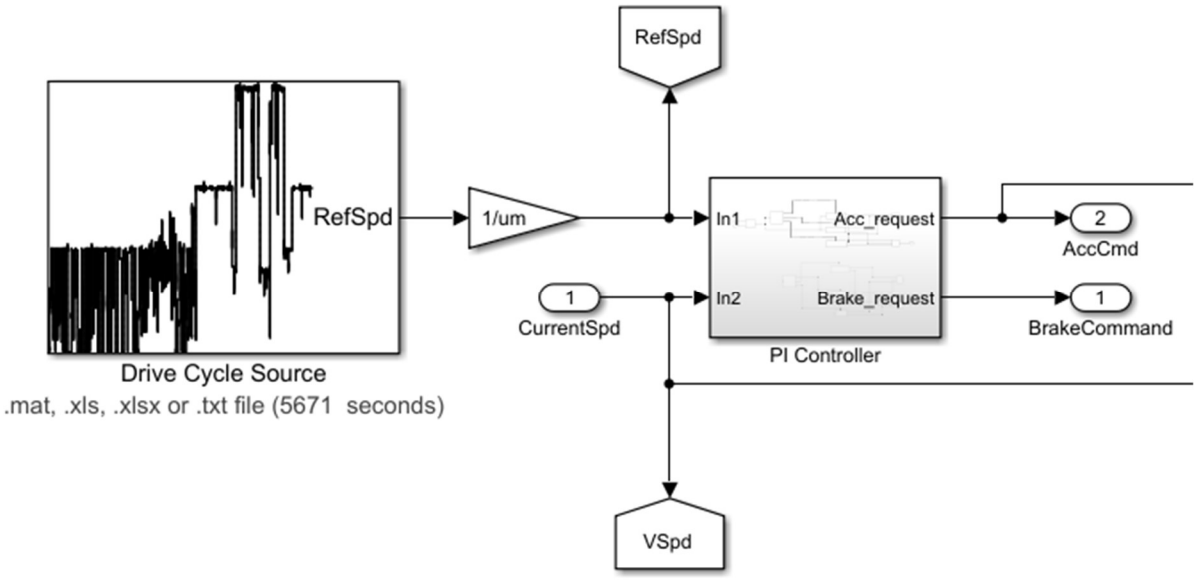

Fig. 17 Drive Cycle Source and PI Controller blocks

The *Drive Cycle Source* block outputs the speed profile corresponding to the homologation cycle selected. Since the model was tested and developed running through several different cycles[1], each requiring a dedicated vehicle mass, it became logic to implement a dedicated Matlab code able to switch automatically vehicle mass, simulation time and the speed output depending on the cycle chosen (see Fig. 18).

In particular, for sake of having the widest and most complete possible range of driving conditions where to train the model strategy, these cycles were employed:

- US06 cycle, for aggressive driving scenarios
- WLTP Class 03, for gentle to normal driving scenarios
- RDE cycles, registered in A and B cities
- Multiples of US06 and WLTP Class 03 employed to simulate homologation performances[2]

While US06 and WLTP Class 03 where already included in the *Drive Cycle Source* block (which comes with the *Simulink Powertrain Blockset*), all the other driving cycles were uploaded separately. The parameter *um* converts the speed trace output units of measurement from km/h to m/s, for those external cycles.

```
%Drive Cycle Choice
cycle=4;  % 1:WLTP; 2:US06; 3:RDE Aachen; 4: RDE Bologna; 5: WLTP_CD

if cycle==1 %WLTP
    cycle_mass=2053;
    sim_time=1800;
    um=1;
elseif cycle==2 %US06
    cycle_mass=1953;
    sim_time=600;
    um=1;
elseif cycle==3 %RDE Aachen
    cycle_mass=1970;
    sim_time=6594;
    um=3.6;
elseif cycle==4 %RDE Bologna
    cycle_mass=1970;
    sim_time=5671;
    um=3.6;
elseif cycle==5 %WLTP_CD
    cycle_mass=2053;
    sim_time=3600;
    um=3.6;
end
```

Fig. 18 Drive Cycle choice Matlab code

[1] See the Appendix 9.1 to compare the different speed profiles.

[2] Homologation procedure for hybrid cars mainly consists in a depleting phase and a sustaining phase. The car runs in EV Mode until the ICE turns on. Then, it is mandatory to maintain the battery SOC almost constant and end the cycle.

Depending on the relation between the reference and the real speed of the car, the PI controller that receives the two signals as input, outputs the corresponding acceleration or brake command which ensures a correct signal tracing. PI controller proportional and integral gains progressively decreased up to the value 1, as the vehicle model behaved more regularly and precisely.

3.4.2 Driveline Control

Accelerator pedal position, vehicle speed and engaged gear are respectively the first, second and third inputs of the gearbox-related group of blocks, that is composed by the shifting map and the gear control subsystem. The shifting map analyses the vehicle cinematic parameters to output the correct gear to be engaged to satisfy the driver's will of longitudinal acceleration. The gear control subsystem instead monitors that such choice does not determine too frequent oscillation and irregularities, mainly blocking recurring gearshifts in a limited period of time.

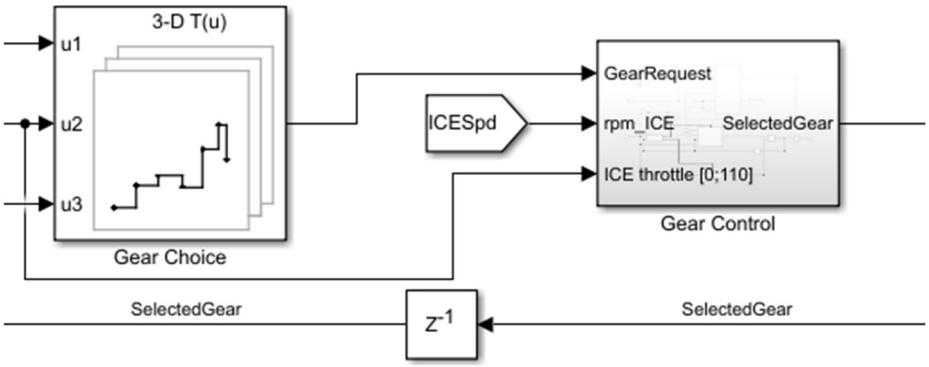

Fig. 19 Gear Choice and Control blocks

As shown In Fig. 19, gearshifts are allowed only after having examined specific conditions, that include ICE current speed and throttle position. However, the main reference parameter is the *gearbox_time*, that specifies the minimum time interval between two gear changes. It was particularly challenging to implement the Gear Control block, as the model works with a variable-step solver and continuous time: instead of using a Matlab function, it was necessary to implement a dedicated subsystem that depending on ICE throttle request, running speed and gear requested chooses whether to actuate a gearshift or not, and when to do it. This is done internally by an *if mode* subsystem, which allows either *Change gear* operations, or the *Keep gear* ones. While the internal logic of the *Keep gear* is trivial and can thus be omitted, it is important to mention the *Change gear* inner principles. The inner structure is reported in fig. 20.

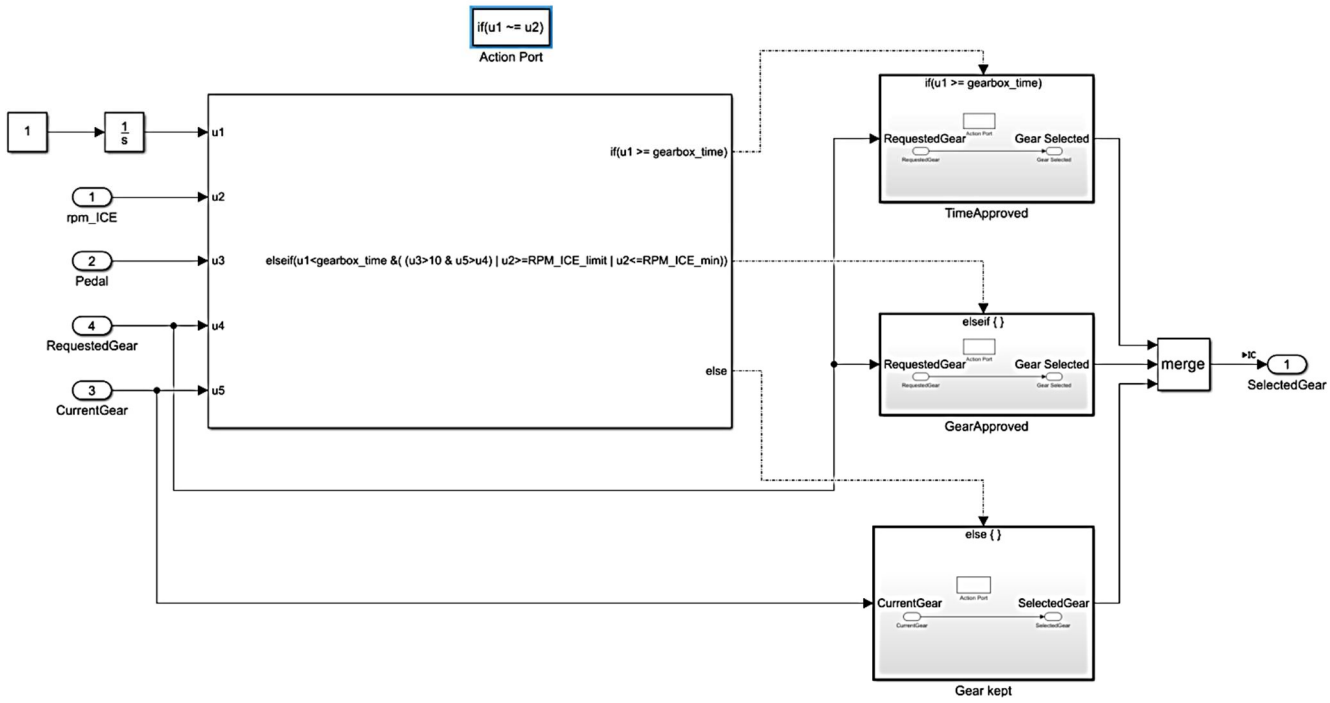

Fig. 20 Change Gear block inner structure

An integrator block is meant to work as a timer, that is reset each time a gear change occurs. As it was mentioned before, the main parameter is the *gearbox_time*: it was set to 2 seconds. In normal operating conditions, the Change gear logic allows a gearshift only when it is required 2 seconds after the previous gear engagement: this is the case of the *TimeApproved* block on the top end corner of fig.20. The block *GearApproved* is activated only when specific conditions are reached, that allow the gearbox to shift gear even before the 2s period. This is authorized only in case of strong acceleration command, or when ICE speed limits are reached. If none of the aforementioned conditions is satisfied, the *Change Gear* block enters the *Gear kept* action block and no gearshift is allowed.

3.4.3 Strategy-related blocks: EM-ICE shift and Discharge Prevention Mode

Next to the gearbox blocks, the *EM-ICE shift* block is there to decide whether to turn on the ICE or not. Such decision is taken thanks to two input data, namely the *Brake Command* and the *EM_only_flag*. When braking command is applied, or the torque applied by the electric motors is adequate to satisfy the driver's requests, the gear chosen by the previous blocks is substituted with the idle one, that disconnects the engine from the rear wheels and mechanically avoids the superimposition of the thermal and the electric powertrains.

The last section of the *Vehicle Command* subsystem is also a core block for the strategy: the *Discharge Prevention Mode*. While its meaning will be discussed later on in the strategy chapter, it is important to notice that the *If* block that mainly constitutes the *Discharge Prevention Mode* requires several data, from minimum and maximum SOC indicated by the driver, to the vehicle speed and type of motor currently running the car.

3.5 Torque Command

The *Torque Command* subsystem is another core part for the model and the strategy. It converts the acceleration command from the driver into a torque command for the actuators. It is also a core subsystem for the strategy actuation too.

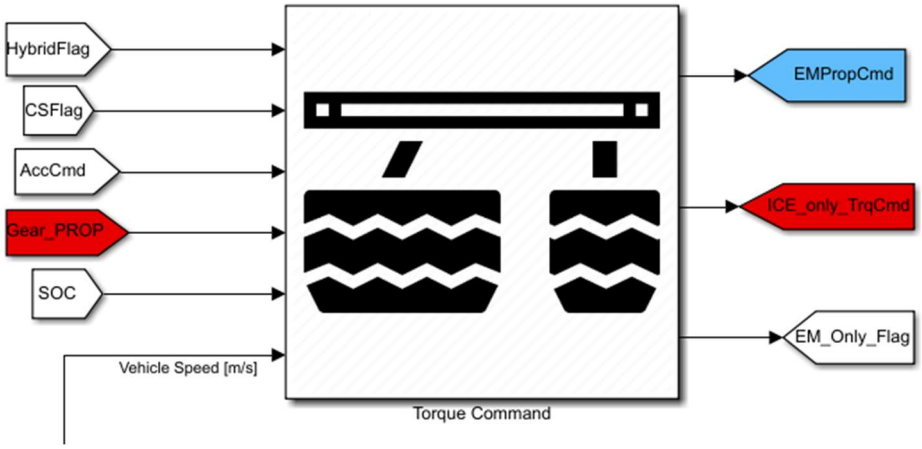

Fig. 21 Torque Command input and output ports

As it is clear from Fig. 21, this subsystem requires almost all data from the *Vehicle Command* one: the way the torque command is assigned strongly depends on the mode chosen, as well as the power required from the driver too. For this reason, the *Torque Command* block is immediately mirrored into two different sections, *Hybrid* and *CS running mode* (see Fig. 22).

The two subgroups share most of their inner structures and working principles, and mainly differ by the torque limits assigned to the electric motors and the internal combustion engine. The *if case* block decides which mode to enter, depending on the input values above mentioned. As it will be the case in many other subsystems, the *delay* blocks inserted where vital to avoid the generation of algebraic loops and system malfunctions.

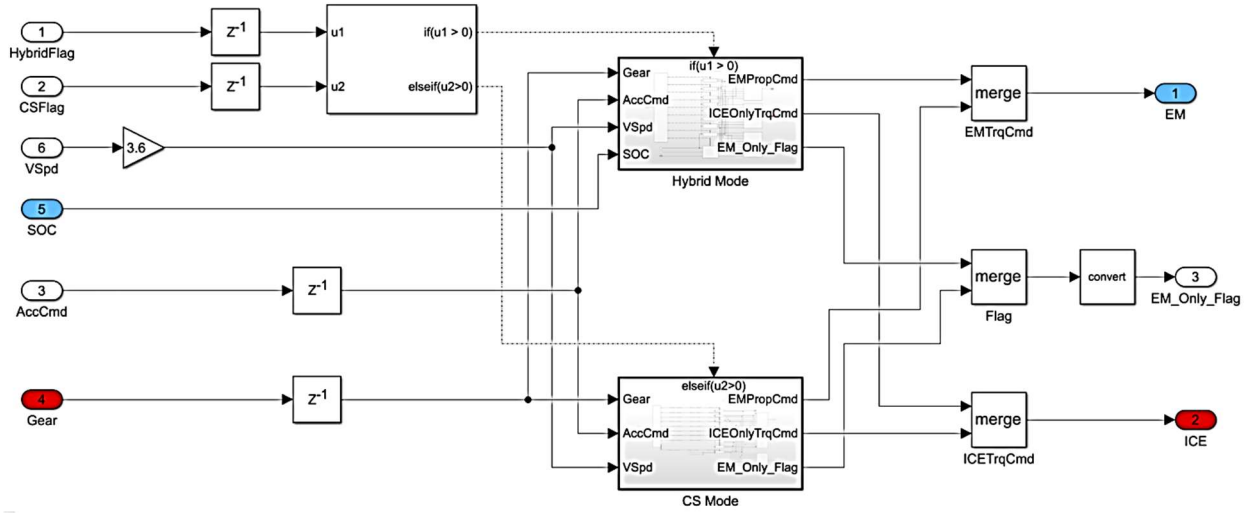

Fig. 22 Differentiation between Hybrid and Charge Sustaining Mode

3.4.4 In-gear torque command

Entering the two modes, the switch case block reported in Fig. 23 processes the input gear and allows the input to enter the correct case among the nine possible (8 gears, and the idle gear case when electric-only propulsion is active).

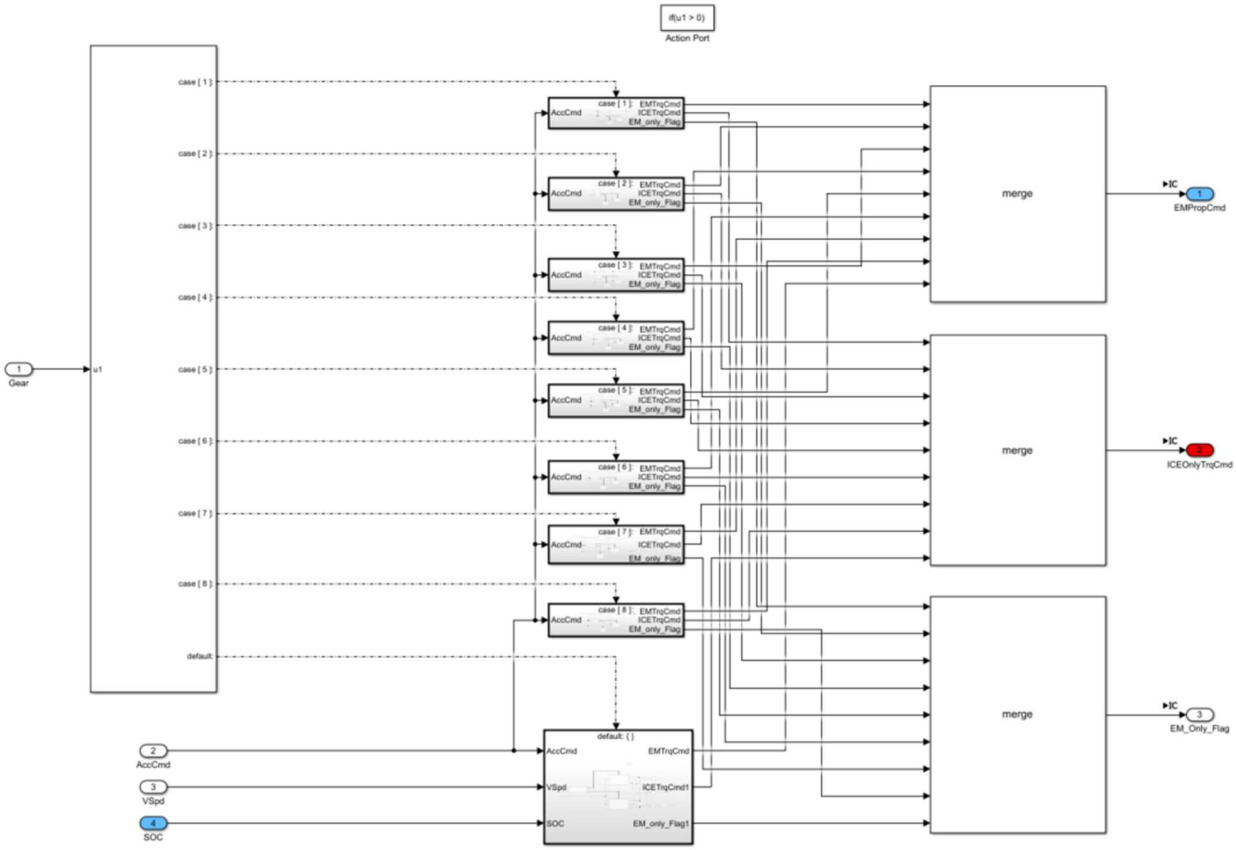

Fig. 23 Switch case (Hybrid Mode, similar structure for CS Mode)

Fig. 24 graphically reports in a flowchart the idea that drives each of the eight in-gear cases. The acceleration command is compared to the available torque from thermal engine in that gear, as well as the torque coming from the electric motors. As it was clarified in the *Vehicle Command* subsystem description, acceleration command comes as a number varying between 0 and 1, where 0 corresponds to no acceleration required, and 1 to maximum acceleration.

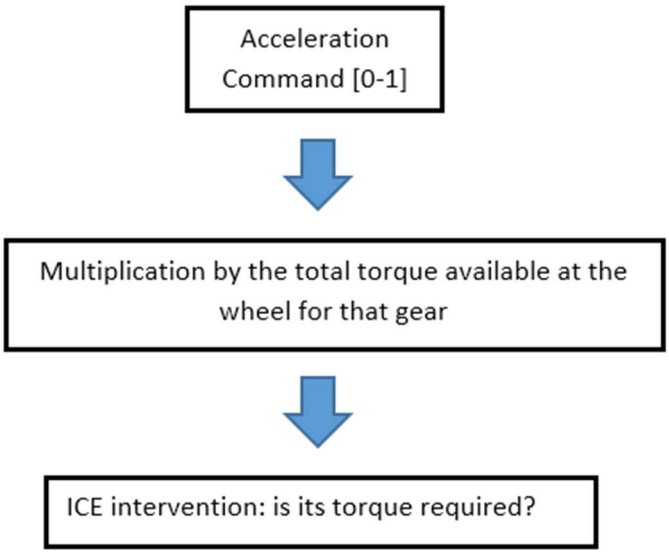

Fig. 24 Principle behind in-gear running cases

The last step of the flow chart is the most important, a crucial point for the rule-based strategy: if the ICE engine torque is required, a 'turning on' message (the *EM_only_flag* already mentioned) is sent to the *Vehicle Command* subsystem, torque is demanded to the engine and applied to the rear axle.

3.4.5 ICE disconnected case

It was often the case, during the drive cycles examined along the project, that the EMs propulsion was sufficient, and the answer to the last step of fig. 24 flowchart was thus no. Then, the *default case* is activated and, as Fig. 25 shows, the *default* block converts the acceleration command in torque command for the electric powertrain only. The electric-only propulsion is possible only when the idle gear (numerically 0 in the model) is engaged. Notice that this case is never utilized when Charge Sustaining mode is activated, since the engine is never turned off as long as the battery SOC remains under the target chosen by the driver. This will be repeated and clarified when entering the *Thermal Powertrain* subsystem.

What is shared by all cases is the presence of the dedicated flag EM_only_flag, which notifies whenever the EMs torque is no more adequate to satisfy the driver's will. The *compare* block that is visible in fig. 24 outputs such flag, and therefore monitors the current value.

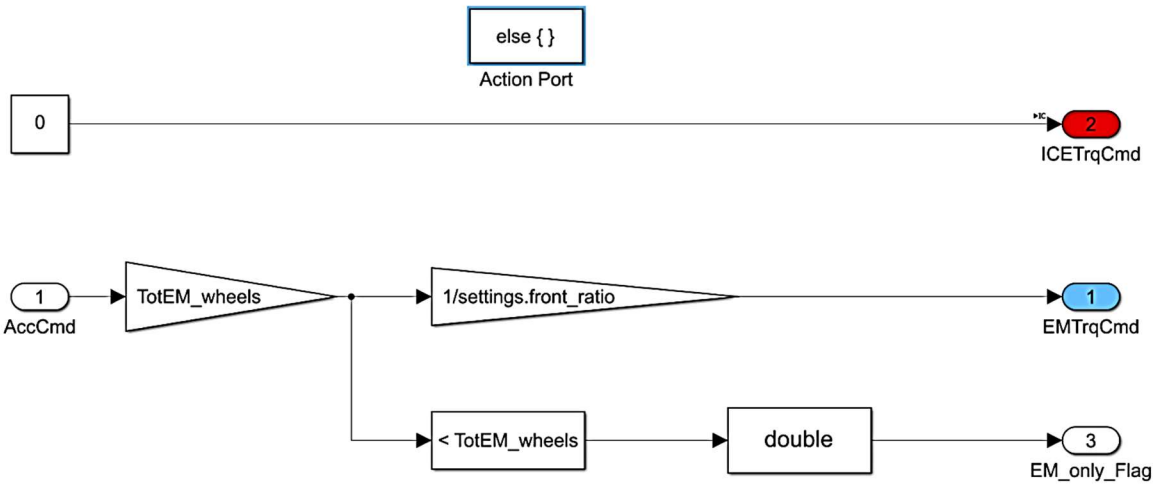

Fig. 25 Electric-only (idle gear) switch case

3.6 Wheels

The *Wheels* subsystem is the one responsible for the torque transmission via the tires, and therefore its transformation into longitudinal forces acting on the vehicle. As the *Wheels* subsystem mask shows in fig. 26 indicates, the tires take into account propulsion torques coming from both thermal and electric powertrain and braking torques coming from both disk and regenerative brakes. Having such inputs, it outputs the front and rear axle forces to be applied to the car, that will be later on processed by the *Vehicle Dynamics* subsystem.

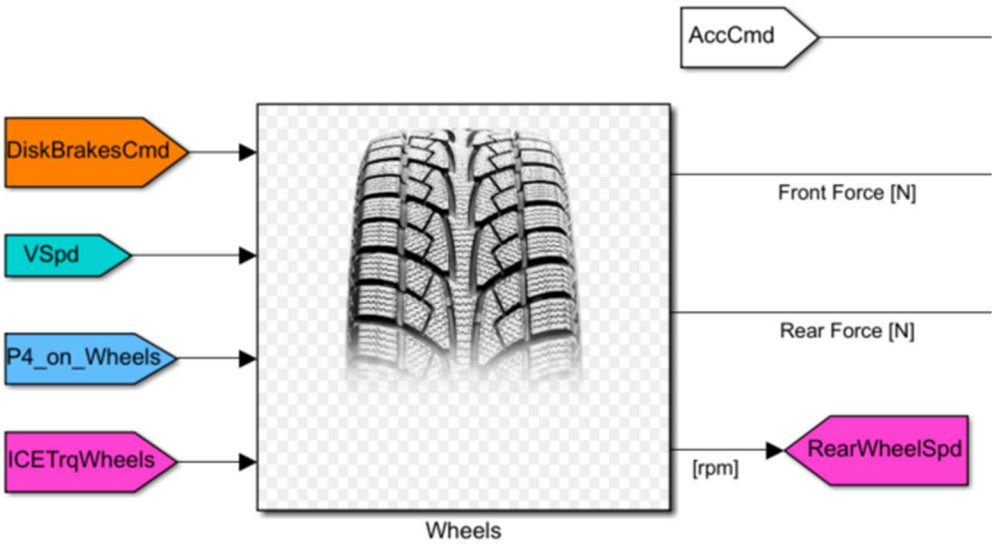

Fig. 26 Wheels subsystem input and output ports

The *Wheels* subsystem runs along two different paths: the cinematic path and the dynamic path.

3.5.1 Cinematic path

The cinematic path starts from the vehicle speed and converts that speed into the different wheel speeds on each axle. This is done thanks to the *Tire Radius* function, provided by external suppliers, that utilizes the vehicle speed to automatically adapt the tire radius.

$$\frac{C0 + C1 * u + C2 * u^2}{2\pi} = tire\ radius\ [m]$$

where the C0, C1 and C2 coefficients are experimentally tuned by the tire supplier and u represents the function input, i.e. vehicle speed in [m/s].

The tire radius value is also utilized to compute the wheel inertia, that is computed as follows:

$$\frac{\Delta\omega}{\Delta t} * I = Single\ wheel\ inertia\ force\ [N]$$

where ω is the wheel rotational speed, and I is the wheel inertia value provided by the tire supplier.

3.5.2 Dynamic path

Along the previously defined cinematic path, tire radius and inertia forces values are then utilized in the overall computation of the forces acting on the wheel. The following list reports those forces:

- Front and rear rolling resistance force
- P4 (front axle) motors force
- P3 (rear axle) motor force
- ICE (rear axle) force
- Disk brakes force

The rolling resistance force is computed via the vehicle mass and the rolling resistance coefficient f_{roll}:

$$vehicle\ mass * g * f_{roll} = Rolling\ resistance\ force\ [N]$$

In particular, the rolling resistance coefficient is provided by the tire supplier via the experimental formula here reported, that includes the two dedicated empirical coefficients T0 and T1:

$$f_{roll} = T0 + T1 * vehicle\ speed$$

EMs torques, differently from the rolling resistance and the engine forces, are applied both with the positive sign (propulsion forces) and with the negative sign (braking torques). Another difference from the ICE torque is that the electric powertrain does not feature any gearbox and thus variable gear ratio.

The ICE torque instead strongly varies depending on the gear engaged: this variation is computed in the *Thermal Powertrain* subsystem, so the value that enters the *Wheels* subsystem already takes into account such condition. As it happens for the other torques, this value is divided by the wheel radius to obtain the driving force.

Last force, the least relevant for the project, is the braking force coming from the disks calipers. Such force is almost never employed during the driving cycles examined along the tests, since the regenerative braking proved to be sufficient in most cases. Still, the friction braking system plays an important role in idle situations and few more cases. It was numerically estimated on the basis of previous experimental data (no real data from the brakes were available, nor particularly useful for the project purposes) and assigned respectively 60% on the front axle, 40% on the rear axle.

All the forces computed converge into a saturation block, that bounds the total force to be exerted inside the tire slip limits.

3.7 Vehicle Dynamics

Fig. 27 shows the Vehicle Dynamics subsystem mask and ports: it is the one that processes the forces coming from the front and rear wheels, as well as those from the aerodynamic force, and outputs vehicle acceleration. In particular, the value of acceleration is then integrated to compute the current vehicle speed, and the distance covered. While the former is fundamental to run the simulation, as it is the main input of the previously examined *Vehicle Command* subsystem, the latter is essential to compute average energy consumption values during the driving cycles.

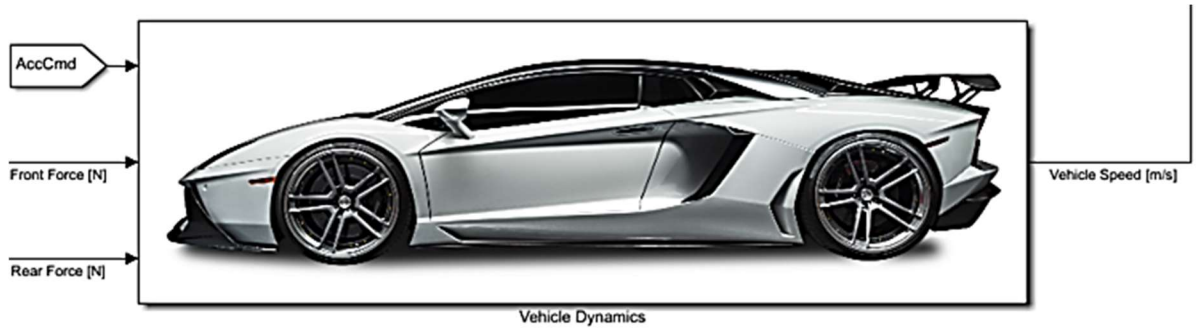

Fig. 27 Vehicle Dynamics mask and ports

3.6.1 Inner structure and brakes control

Among the forces that must be considered, it was mandatory to insert a dedicated control able to manage the low-speed braking phenomenon. When approaching null speed, as the car stops the brakes must be able to exert a small positive force to avoid the car moving backwards. It is clear that for the vast majority of the driving cycles the vehicle brakes exert a negative force on the wheels: still, when the car is blocked in idle phases, a small positive force can be also applied. This is the aim of the *Backwards* and *Forward Motion* blocks visible on the left end side in fig. 28.

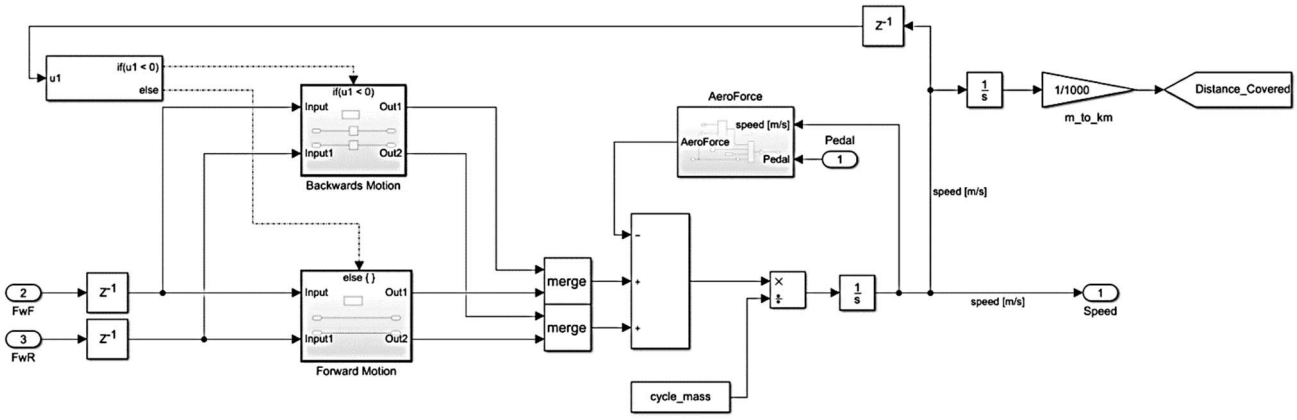

Fig. 28 Vehicle Dynamics inner structure

3.6.2 AeroForce block

In addition, the *AeroForce* block takes into account the negative force that comes from the car frontal area and shape impact against ambient air. Since vehicle aerodynamics can severely impact the fuel consumption during the drive cycles taken into account during the project, it is worth entering into the *AeroForce* block and understand how it was designed. As fig. 29 shows, the aerodynamic force is computed via the following formula:

$$\frac{1}{2}\rho A C_x V^2 = Aerodynamic\ force\ [N]$$

(Genta, 2009)

where:

- ρ: air density at $T_{environment}$ = 25 °C
- A: vehicle frontal area
- Cx: vehicle aerodynamic coefficient: it takes into account vehicle shape
- V: vehicle speed

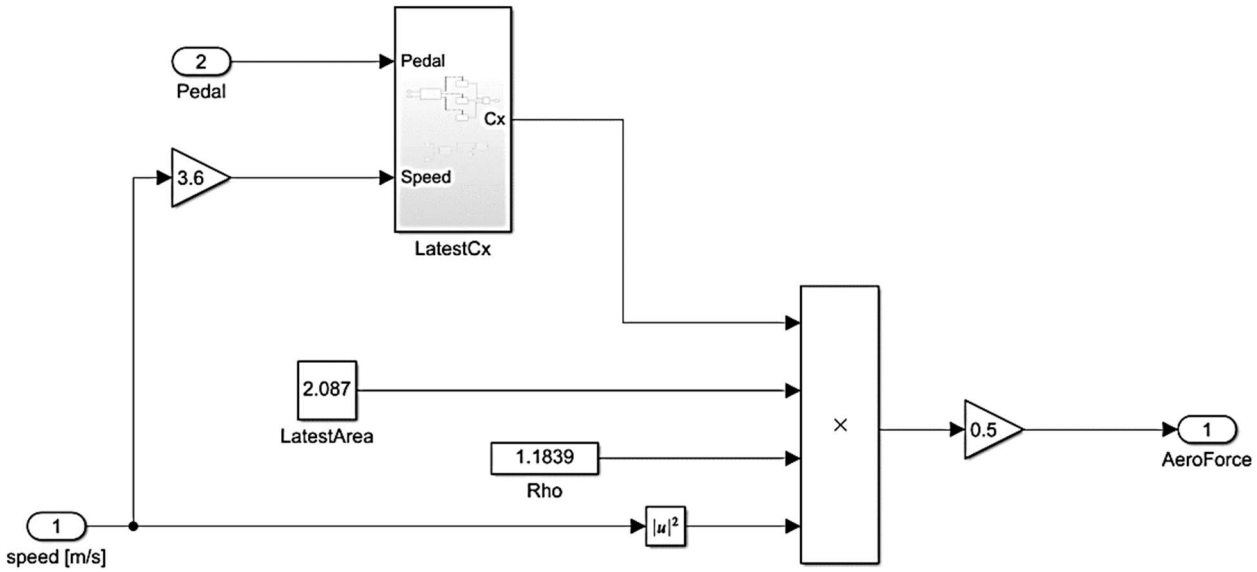

Fig. 29 AeroForce block inner structure

The *LatestCx* block takes into account the car behaviour depending on the speed and the accelerator command: depending on the various combinations of those inputs, the external shape is modified and thus the drag increases or decreases correspondingly. This was one of the last blocks implemented into the model, as the virtual development was following the actual vehicle development done in parallel by other departments.

3.8 Thermal Powertrain

The internal combustion engine installed onto the vehicle is a high-performance V12, naturally aspirated and mid-mounted. Its torque is directly applied to the rear axle, and no mechanical linkages transmit it to the front axle too: therefore, if the car had the thermal powertrain only, it would be rear wheel drive.

The engine transmits its torque through a dual-clutch automatic gearbox, with eight speeds. The in-depth mechanic simulation of this system was not developed: gearshifts and clutch intervention were simplified and no further model design work was done for this component.

The *Thermal Powertrain* subsystem mask is shown in fig. 30: it also puts in evidence some of the most relevant output and input ports, which are torque requested and torque applied, wheels speed and gear engaged.

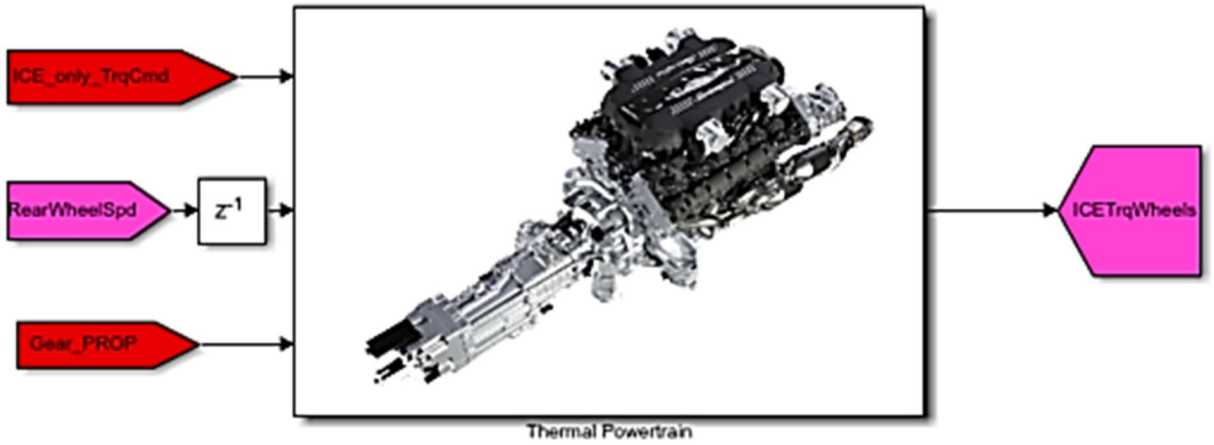

Fig. 30 Thermal Powertrain subsystem mask and ports

3.7.1 Two running modes: Hybrid and Charge Sustaining

As it happened with the Torque Command subsystem, the Thermal Powertrain subsystem behaves differently depending on the current vehicle mode. The thermal powertrain is tuned in two ways, depending on one main criterion: whether the battery needs to be charged in load shift (so CS Mode) or not (Hybrid Mode) by the internal combustion engine. Fig. 31 shows that an *If* block first checks the current running mode: then, the correct block is entered and input data are processed there. Once outputs are determined, some of them (namely engine speed and torque) are utilized by the green block, that computes fuel consumption and will be later on examined.

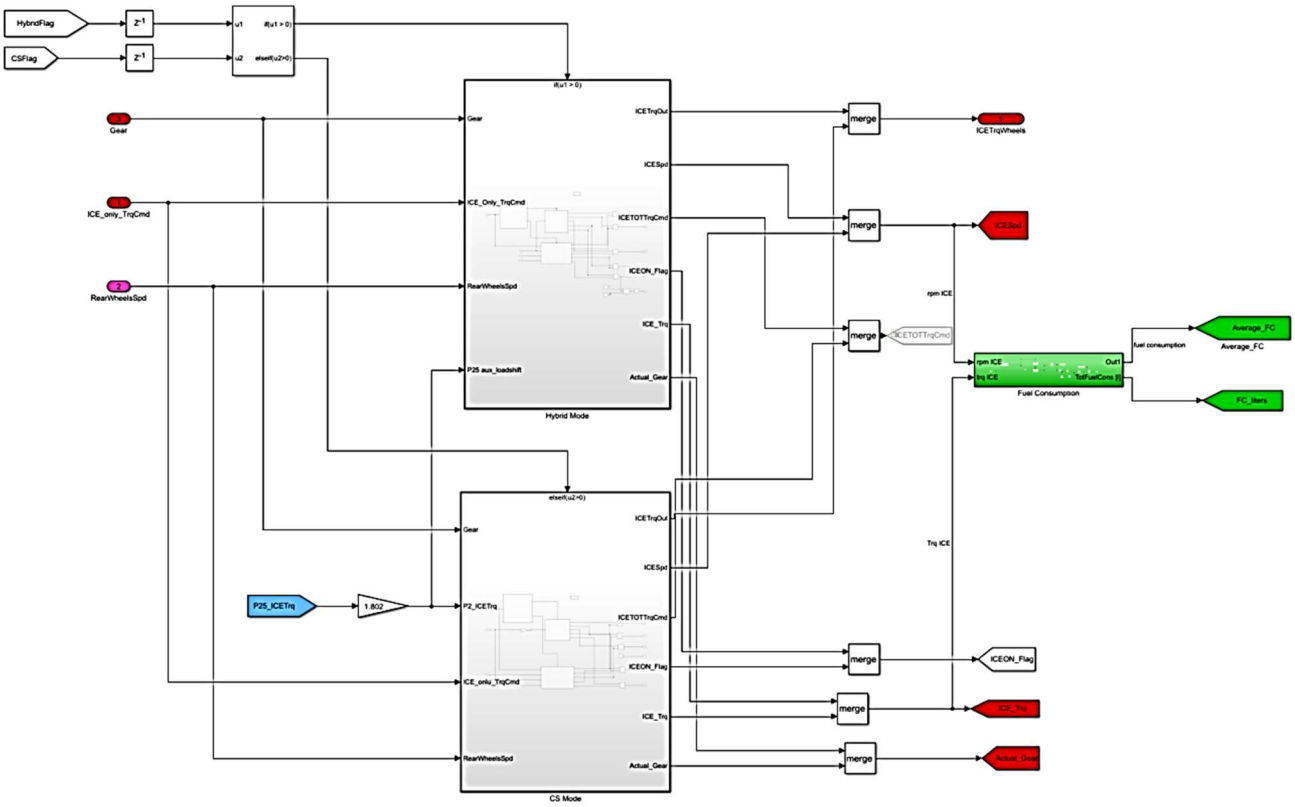

Fig. 31 Thermal Powertrain subsystem inner structure

Once that the current running mode is selected, the most important input data for the *Thermal Powertrain* subsystem are:

- Current gear: the one coming from the *Vehicle command* subsystem
- Torque requested for the vehicle motion: often recalled as *propulsion torque* inside the model
- Rear wheels speed: kinematically linked to the engine speed so that the ICE blocks can determine with accuracy the current working point
- Load shift torque demand: related to the rear EM, as it will be clarified later on

3.7.2 Modes inner structure

As it already happened when two mirrored blocks had to be described, the analysis will go through just one of them, with the necessary dedicated analyses in case of relevant differences among the two. As an example, fig. 32 shows the inner structure of the *Charge Sustaining* case.

The *Charge Sustaining* case is again subdivided into two minor subsystems, chosen on the basis of the current gear engaged. The first subsystem simulates the *ICE idle* running, while the second one is dedicated to all other in-gear running situations, where the engine both propels the car and recharges the battery. It is worth noticing that in the idle subsystem the EM layout is different from the one adopted for propulsion and regenerative braking, and so is its mechanical connection to the ICE: for this reason, an *efficiency correction* coefficient is adopted to take into account that (see fig. 32).

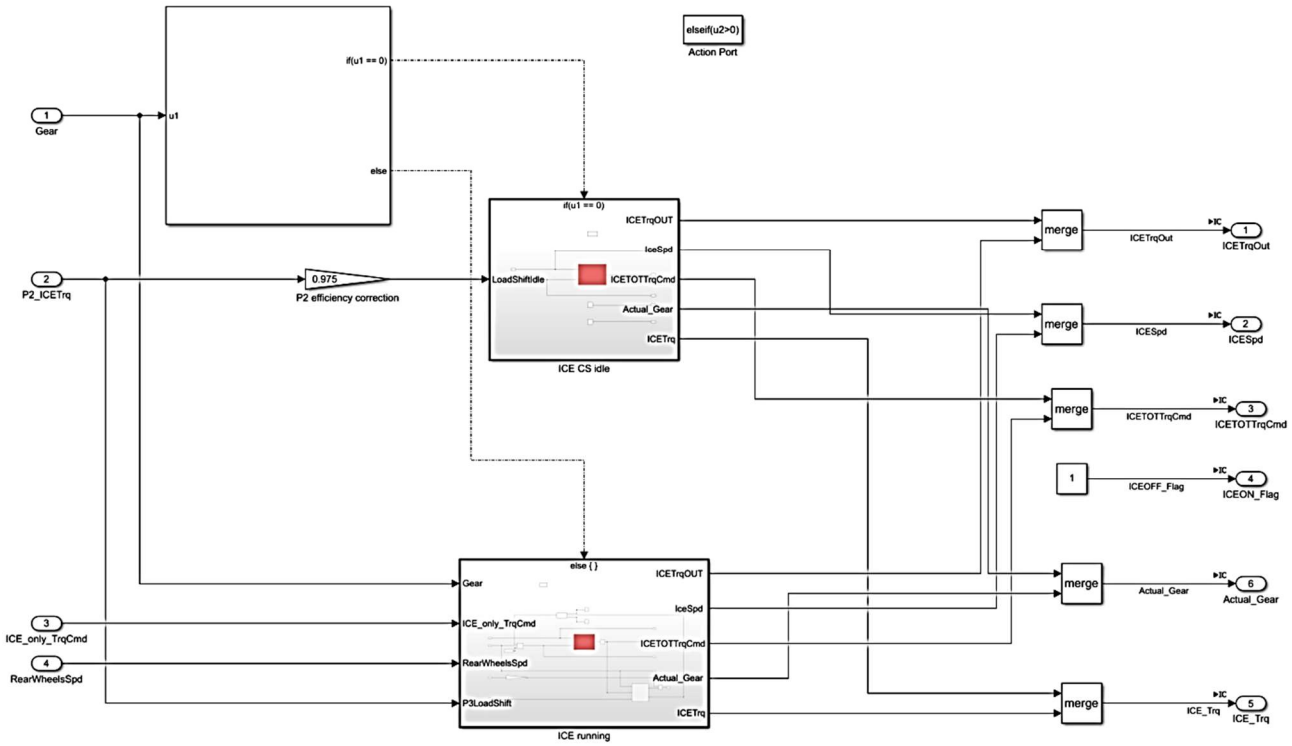

Fig. 32 CS Mode inner structure

Among the several outputs that belong to the CS Mode subsystem, it is interesting to notice for the first time the *ICETrqOut* value, that corresponds to output port 1, at the top-right corner in fig. 32: such output is the actual value applied by the ICE through the gearbox gears on the rear axle.

3.7.3 ICE running case

Next important step into this part consists in entering the ICE running case, which includes the Internal Combustion Engine maps and the dual-clutch transmission gears, as reported in fig. 33.

The *Hybrid* and *Charge Sustaining ICE running* blocks have a couple of differences: the engine speed when idling, and the load shift torque value. While the former can be set as a strategy parameter in the CS mode, and is fixed at the standard minimum value in Hybrid mode, the latter can be significantly different (depending on the SOC targets) between the two modes. Having decided to keep a slight load shift even in Hybrid mode, when no charging would be required in theory, is again a strategic decision that will be explained in the dedicated chapter.

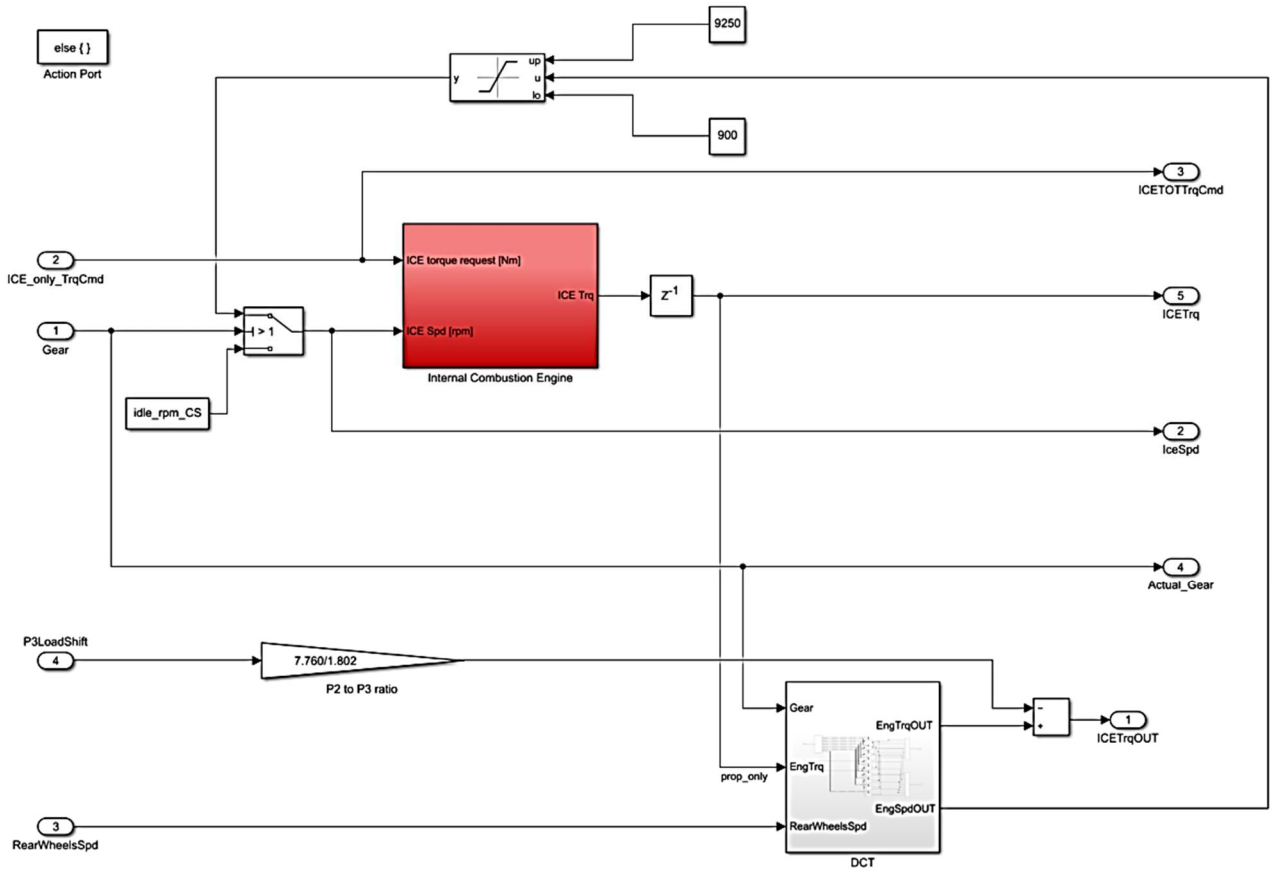

Fig. 33 ICE running blocks

Apart from the aforementioned variances, the structure is shared among the two modes an mainly consists in the *Internal Combustion Engine* block (depicted in red in fig. 33) and the *DCT* block. A *saturation* block is placed between the gearbox and the engine to keep the engine speed inside the design boundaries, and a *switch* block simulates the clutch when the idle gear is selected, by outputting the idle speed (that is set via the Matlab parameter *idle_rpm_CS*).

The DCT block contains all the various gear cases and computes the output torque and speed applied to the rear axle by the internal combustion engine. Such torque is also conflicting with the one applied by the rear EM when a load shift torque is required: in mechanical terms, the output torque from the gearbox has to counterbalance the one that the electric motor actuates, which is a resistive and negative torque.

3.7.4 ICE in idle

When considering the idle cases, the two modes behave in a rather different way. In Charge Sustaining mode, the engine is charging the battery with a torque requirement and a working point tuned by strategy-related parameters, visible in fig. 34.

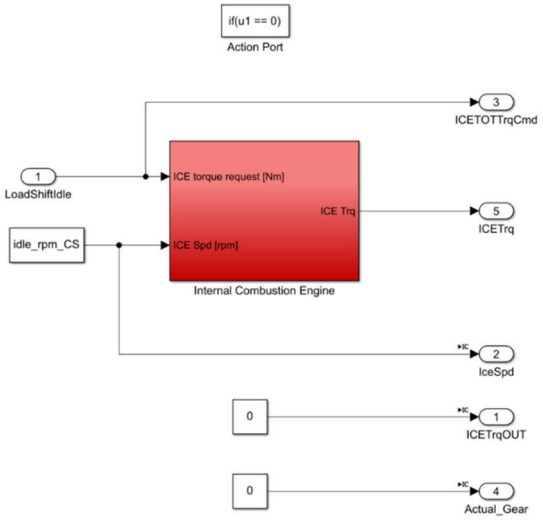

Fig. 34 ICE in idle during CS mode

In Hybrid mode, the same situation, with the vehicle standing still and no propulsion required, is performed with the ICE turned off. The corresponding block outputs again zero torque to the wheels, but also overall zero torque output (meaning that fuel consumption is also null).

3.7.5 Internal Combustion Engine

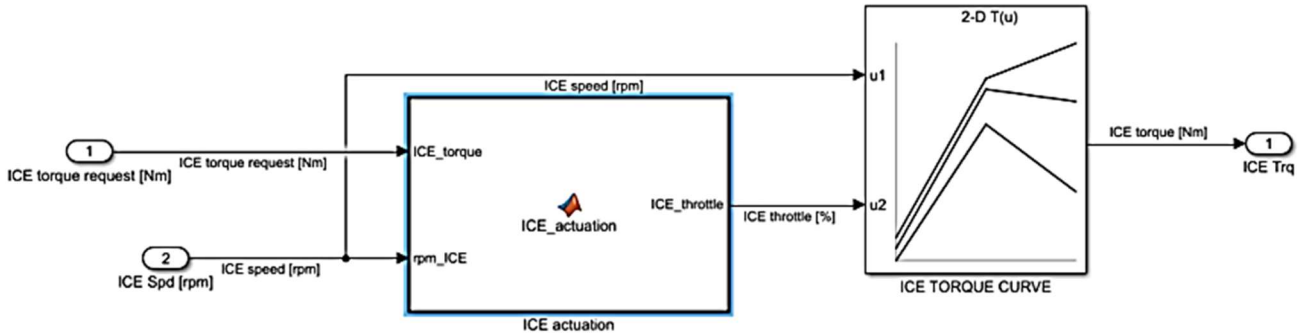

Fig. 35 Internal Combustion Engine blocks

A throttle input directly linked to the accelerator pedal was never employed: on the contrary, the pedal position was interpreted as a torque request and then sent to the actuators, namely EMs and ICE. Because of that, the *ICE actuation* Matlab function block outputs the throttle opening percentage on the basis of the torque request and the current engine speed entering. As it happened for other

specific powertrain components, these two blocs came entirely from other departments and underwent little or no modifications during the project.

With the throttle opening percentage recently obtained, the engine map (*ICE TORQUE CURVE* in fig. 35) reads again the current engine speed and outputs the torque that can satisfy the acceleration command.

3.7.6 Fuel consumption

A crucial block that was briefly mentioned earlier on is the one that measures the fuel consumption of the internal combustion engine. This minor subsystem collects the engine speed and overall torque output from the *Hybrid mode* and *CS mode* subsystems (see fig. 36 and fig. 31), and computes a series of energy related data.

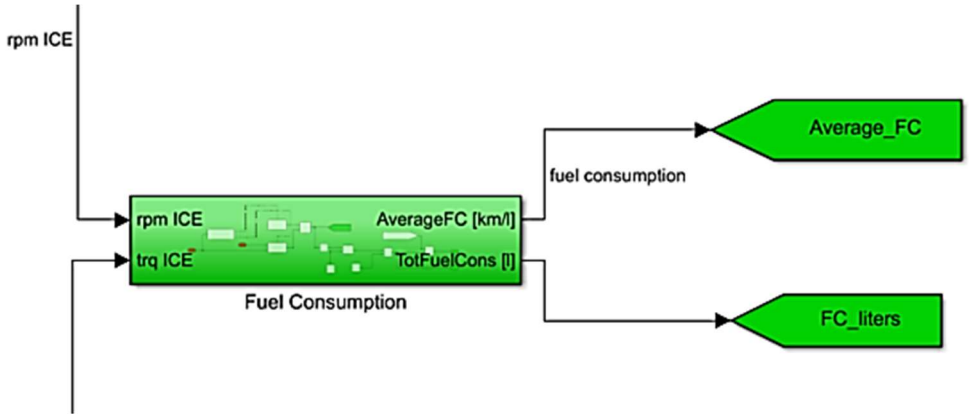

Fig. 36 Fuel consumption block

The two most important values obtained by this block for the aim of the project are the average fuel consumption and the total amount of fuel consumed, measured in liters. They are obtained integrating the hourly fuel consumption over the cycle time (see fig. 37).

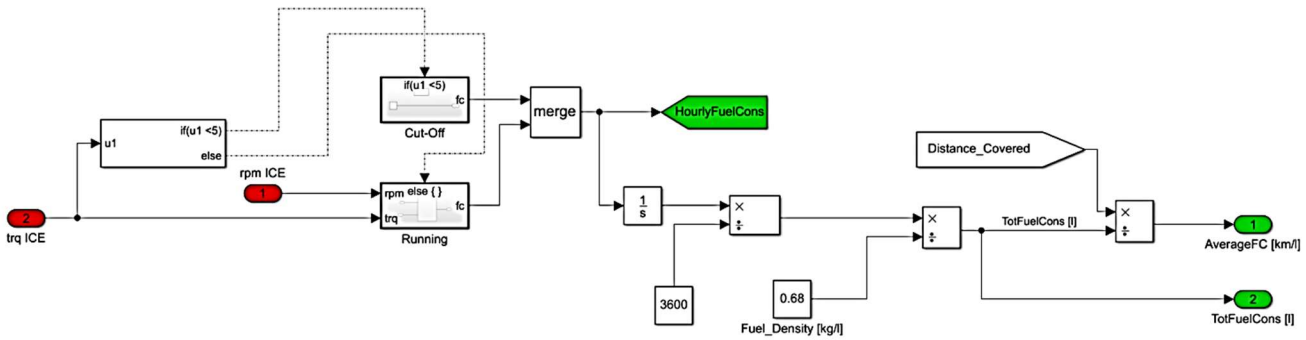

Fig. 37 Fuel consumption inner structure

The hourly fuel consumption is either zero, in case of zero-torque operations from the engine, or greater than zero, depending on the speed and torque outputs coming from the ICE blocks. The value is calculated by interpolating data coming from a 2-D lookup table (ICE speed and torque being the inputs).

The final amount of fuel consumed, having the fuel density and the overall cycle time, is then obtained via a straightforward mathematical operation, as well as the average fuel consumption calculation.

3.9 Electric Powertrain

The electric powertrain mounted onto the vehicle is mainly composed by two electric propulsion units, one for each axle, and the battery. As it is visible from input/output ports in fig. 38, this subsystem processes the vehicle cinematic conditions and acceleration demand, in order to output the correct torque values on the wheels. Even though it was already clarified in the *Model Overall Structure* section, it is worth repeating again that the subsystem mask is just a graphical support which does not represent the real components adopted on the physical prototype.

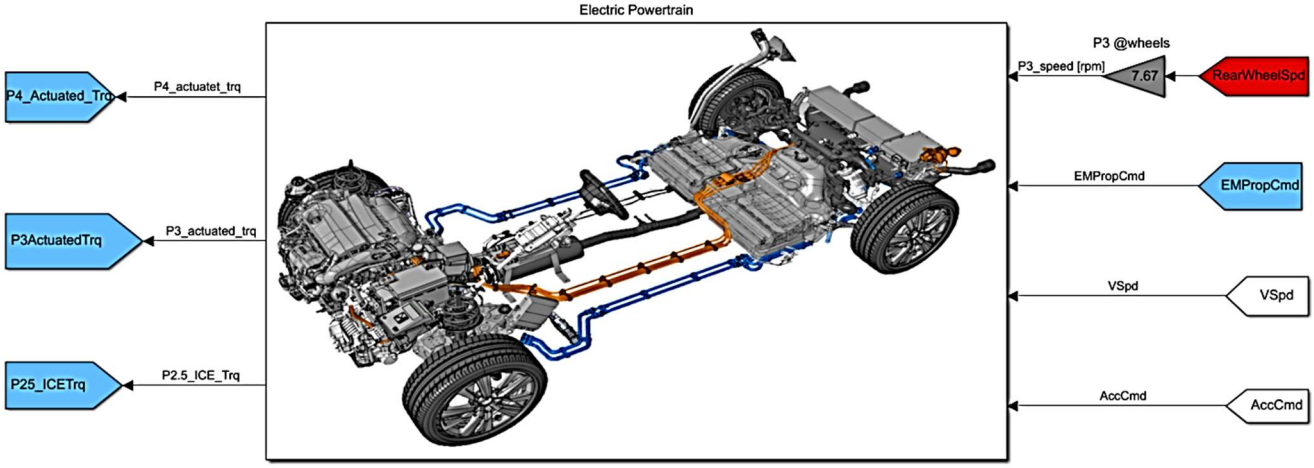

Fig. 38 Electric Powertrain subsystem mask and ports

3.8.1 Overall structure

The overall structure of the *Electric Powertrain* subsystem is reported in fig. 39.

The three most important components simulated in this subsystem are depicted in blue, and emphasised by reference letters in red. Those letters respectively indicate:

a) **Front electric motor**: set in P4 layout and commonly recalled as P4 EM
b) **Rear electric motor**: set in P2/P3 layout, also defined as P2.5 EM since it can switch between the two layouts depending on the driving conditions
c) **Battery**

Among the white blocks in fig. 39, most of them are functional blocks: they are fundamental to monitor and correctly manage data transfer between the electric motors and the energy storage system. Such blocks were progressively added and tuned as the model grew in complexity and accuracy, in order to better cope with transients and limit conditions. Some examples regarding the most important of them will be given later on.

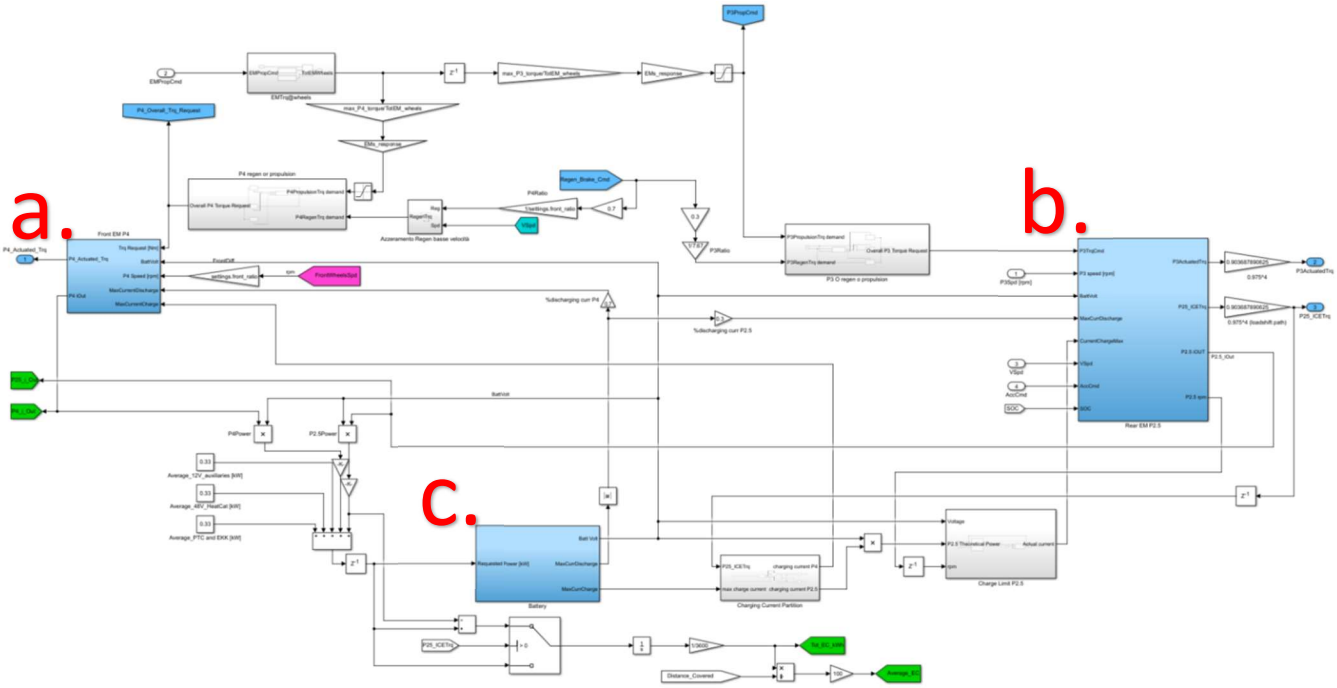

Fig. 39 Electric Powertrain subsystem inner structure

In order to "zoom in" and better understand what composes such subsystem, it is better to proceed in a schematic way and follow the input-output path of the subsystem.

3.8.2 EMs command

The torque command values coming from the dedicated subsystem are processed by the group of blocks on the top end of fig. 39. In particular, those controlling the P4 motor are represented in fig. 40. The *EMTrq@wheels* block is responsible for converting the generalized EMs torque command coming from the dedicated subsystem into a precise value computed at each wheel axle. As this block serves for both EMs, its output is then partitioned into two contributes, each weighted on the basis of the maximum torque output of the two actuators. An *EM_response* gain is installed to fasten up the EMs reaction time.

Being an electric motor able to satisfy both propulsion and braking torque requests, the block *P4 regen or propulsion* is meant to deal with the two different inputs and correctly manage current and torque positive/negative signs.

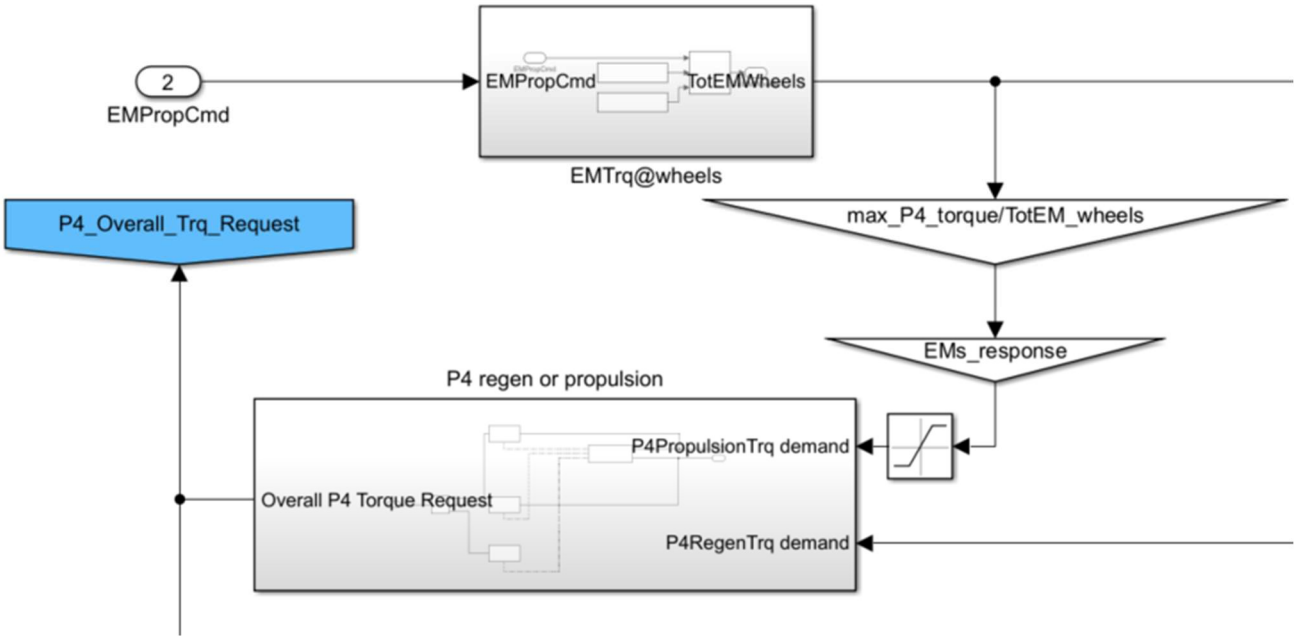

Fig. 40 P4 control blocks

The P2.5 electric motor, the one mounted on the rear axle, is controlled by a similar group of blocks, being it able both to boost the propulsion thrust and to apply a braking torque when utilized in P3 layout.

3.8.3 Current control

What is fundamental for the P.25 electric motor is the current management, as its double layout and thus double working principle makes it more complex to control than the front EM. The blocks *Charging Current Partition* and *Charge Limit P2.5* (see fig. 41) were designed for this reason.

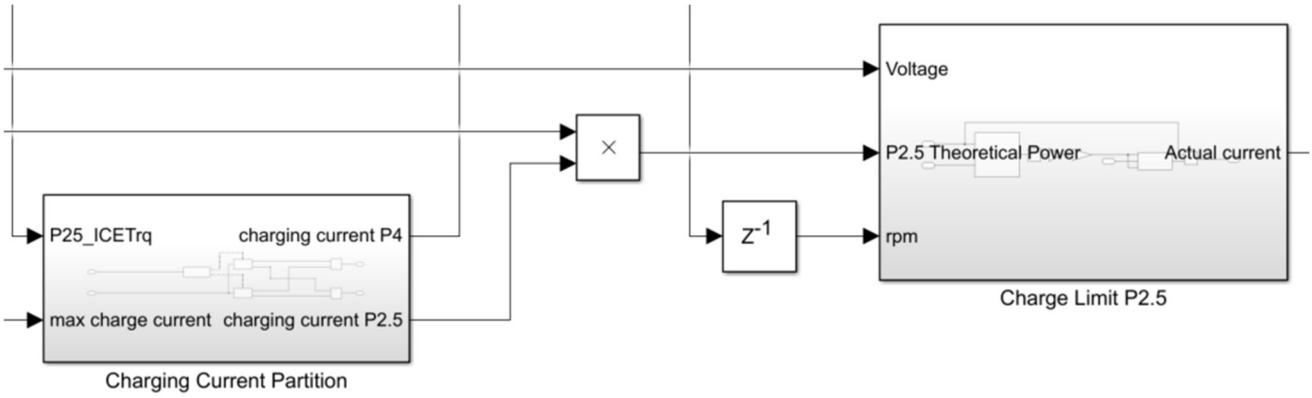

Fig. 41 P4 control blocks

The *Charging Current Partition* block starts from one important data, that is the maximum current that the battery can accept. Such value is mainly influenced by SOC and internal temperature, and decreases abruptly especially at SOC limit values, i.e. over 95 % of State Of Charge. Once the maximum current is known, the second input data, that is load shift torque required by the rear EM, determines whether the battery is being recharged by forced load shift or by regenerative braking. This differentiation is crucial: when applying regenerative braking, the major part of the charging current comes from the front EM, being it more powerful, and so its allowable charging current must be correspondingly higher than that of the rear EM. On the contrary, when load shift torque is required, the vehicle is not braking and thus the charging current from the front EM is zero, while the one from the rear EM is very high. Thus, a completely different partition must be applied to avoid limiting the recharging potential of the two actuators during the aforementioned phases.

The *Charge Limit block*, whose inner structure is shown in fig. 42, is designed to bound the charging power from the P2.5 EM inside the maximum values accepted by its inverter.

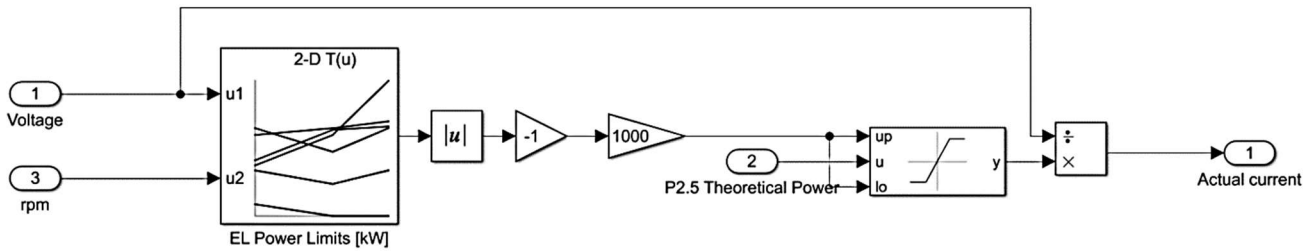

Fig. 42 Charge Limit P2.5 block inner structure

The *EL Power Limits* block is a 2-D lookup table that was designed during the project starting from manufacturer's data. It outputs the maximum kW that the EM can tolerate at the given working conditions (voltage and speed).

3.8.4 Regenerative braking command

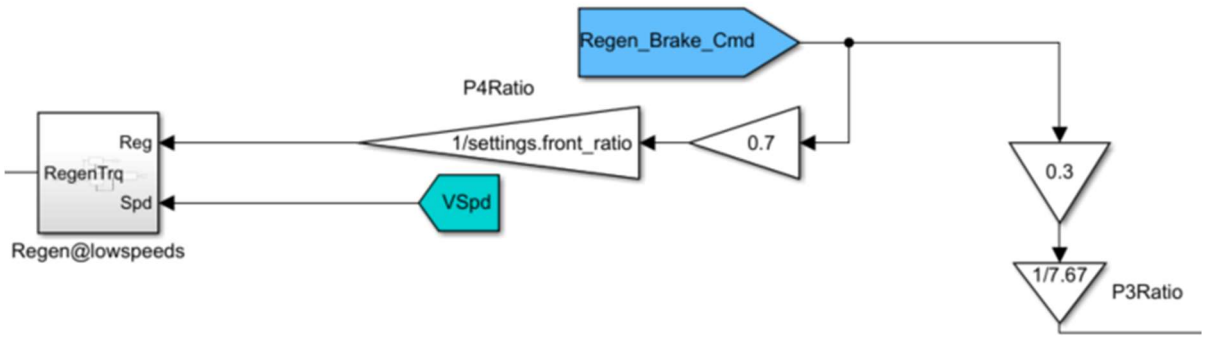

Fig. 43 Regenerative braking command blocks

The regenerative braking command (see fig. 43) comes from the *Brakes* subsystem, which will be examined in the next chapter. It is assigned to the two axles on the basis of their torque availability: being it a mechanical value, i.e. that takes into account the final ratio on the axles, it is first converted into the respective torque assignments by dividing by each final gear ratio.

3.8.5 P4 unit: the front axle EM

The front axle EM is a powerful unit, that following in-depth tests on various driving cycles, is able to run the car by itself and follow most of the various torque requests occurring during the considered driving cycles. As fig. 44 indicates, it is mechanically linked to the front wheels by a fixed gear ratio.

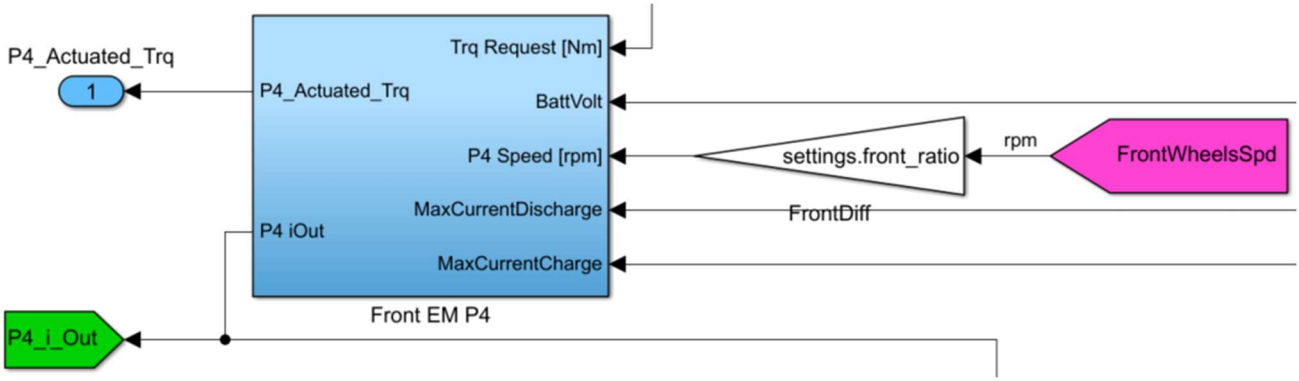

Fig. 44 Front EM input and output ports

The inner structure of the P4 subsystem is mainly composed by the experimental maps and the functional blocks that manage input and output values: the low-speed driving and transients proved to be challenging in terms of current and torque regulations, therefore a large number of those control blocks were designed. As it would be impossible for this part of the model to show the real blocks layout, it is more practical to schematize in a step-by-step procedure its structure and data-flow.

Inner working principles:

1. **Current and torque values are obtained**: torque request and EM rotor speed enter the subsystem: they are immediately associated to a first, possible output torque and current (either positive or negative, depending on the torque request) thanks to the working map obtained from bench tests. Functional blocks to prevent excessive speed, and control low speed behaviour, are implemented. A differentiation between generator and motor working efficiency is implemented too

2. **Battery boundaries are considered**: the battery charging and discharging current limits are considered, and, if necessary, they limit the current value obtained at the first step

3. **Final current and torque values are computed**: with the new current value obtained, a specific Matlab function enters again the motor maps and outputs a new torque value corresponding to the boundaries, as fig. 45 shows

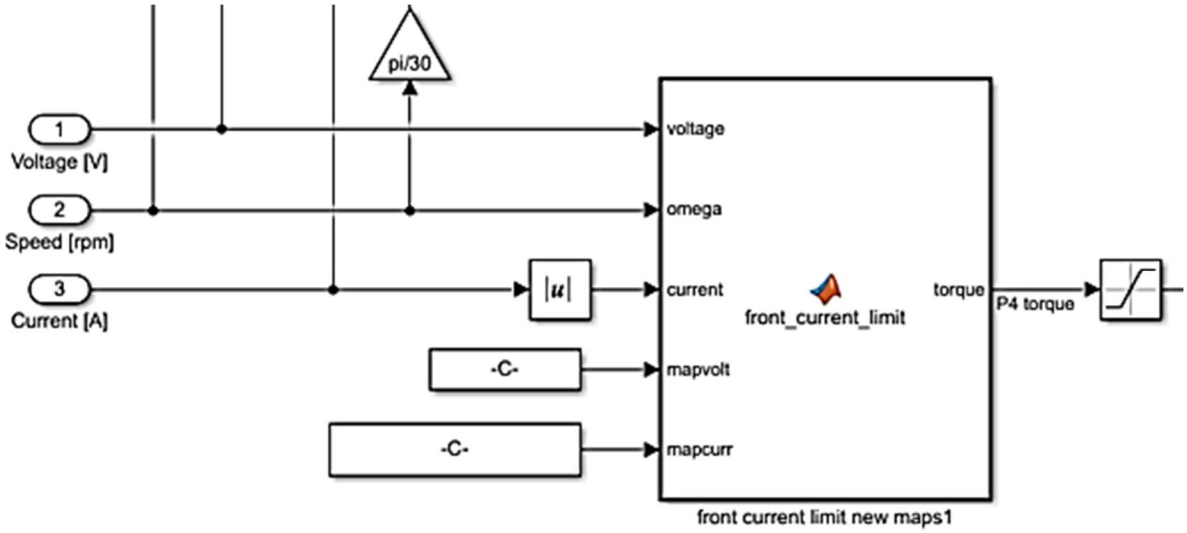

Fig. 45 Front EM second torque control

It is important to say that the efficiency is once again taken into account whenever the motor is running in generator mode.

As soon as the torque output value is defined and corrected, the *Peak Power Limit* block in fig. 46 controls for the last time the torque and checks that the peak value which the P4 EM can reach is sustained for a limited period of time: if the torque request remains too high for too long, a dedicated flag sends a warning message and this block limits the torque output until peak values are not required anymore.

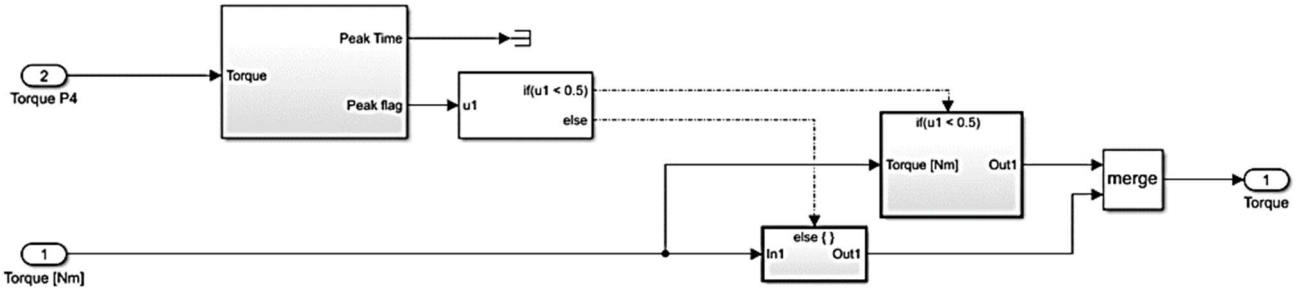

Fig. 46 Peak Power Limit block

3.8.6 P2.5 unit: the rear EM

The rear electric motor fulfils three main roles:

- **Propulsion**, acting as a boost when asked to support the front motor and, in case, the ICE
- **Regenerative braking**, in cooperation with the front EM
- **Load shift recharging**, during charge sustaining phases

Several input data are required to satisfy the performance and efficiency missions assigned: as it is reported in fig. 47, vehicle status data, as well as kinematic and command values are processed by the Rear EM P2.5 subsystem.

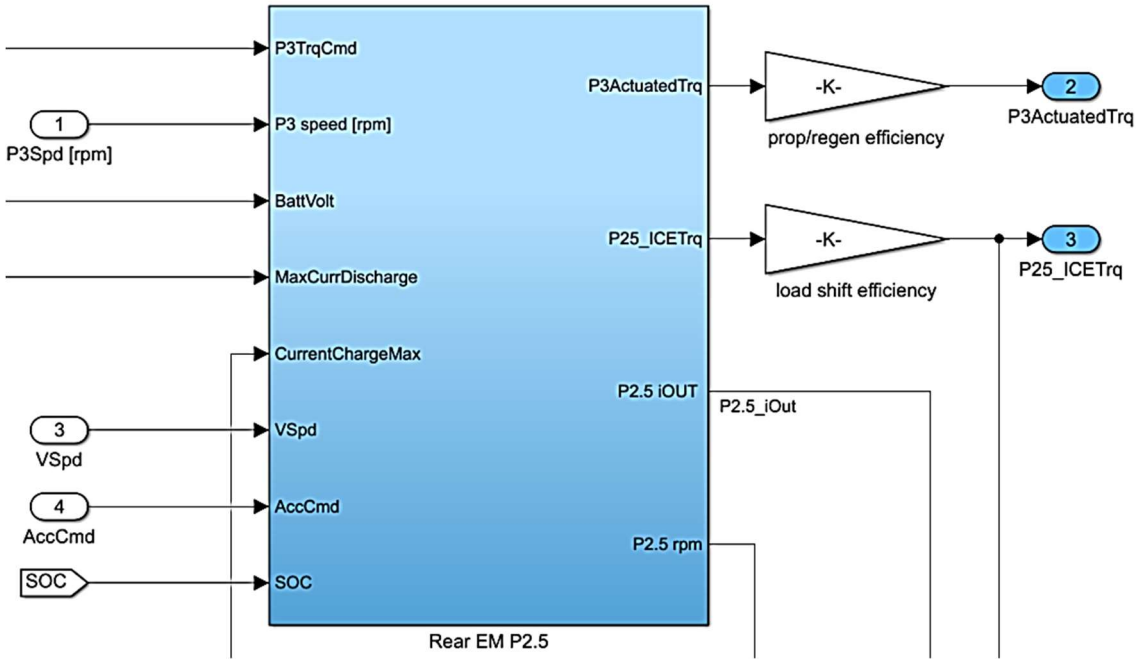

Fig. 47 Rear EM subsystem mask and ports

As it is clear when modelling electric motors, core input values are also those regarding battery data, namely charging/discharging current available, battery voltage and obviously, State of Charge.

Differently from the front EM, the rear unit can also demand torque to the ICE to recharge the battery, instead of applying pure propulsion or braking torque: this means that the subsystem structure had to become more complex.

Therefore, the subsystem is immediately divided into two parts, one dedicated to the *No propulsion* phases, and one to the *Hybrid* running. As it happened for the case of the P4 EM, it will not be possible to describe the entire structure and show all the minor subsystems: still, an overview of the most important groups will be provided and significant steps will be listed.

3.8.7 P2.5: no propulsion case

The *No propulsion* subsystem is composed by four different parts, that can be grouped as:

- **layout control** blocks
- **current definition** blocks
- **torque definition** blocks
- **torque actuation** blocks

The blocks responsible for the layout control are collected in fig. 48. The rules that decide how to use the P2.5 EM will be recalled later: what is now important is to define how this electric motor is simulated.

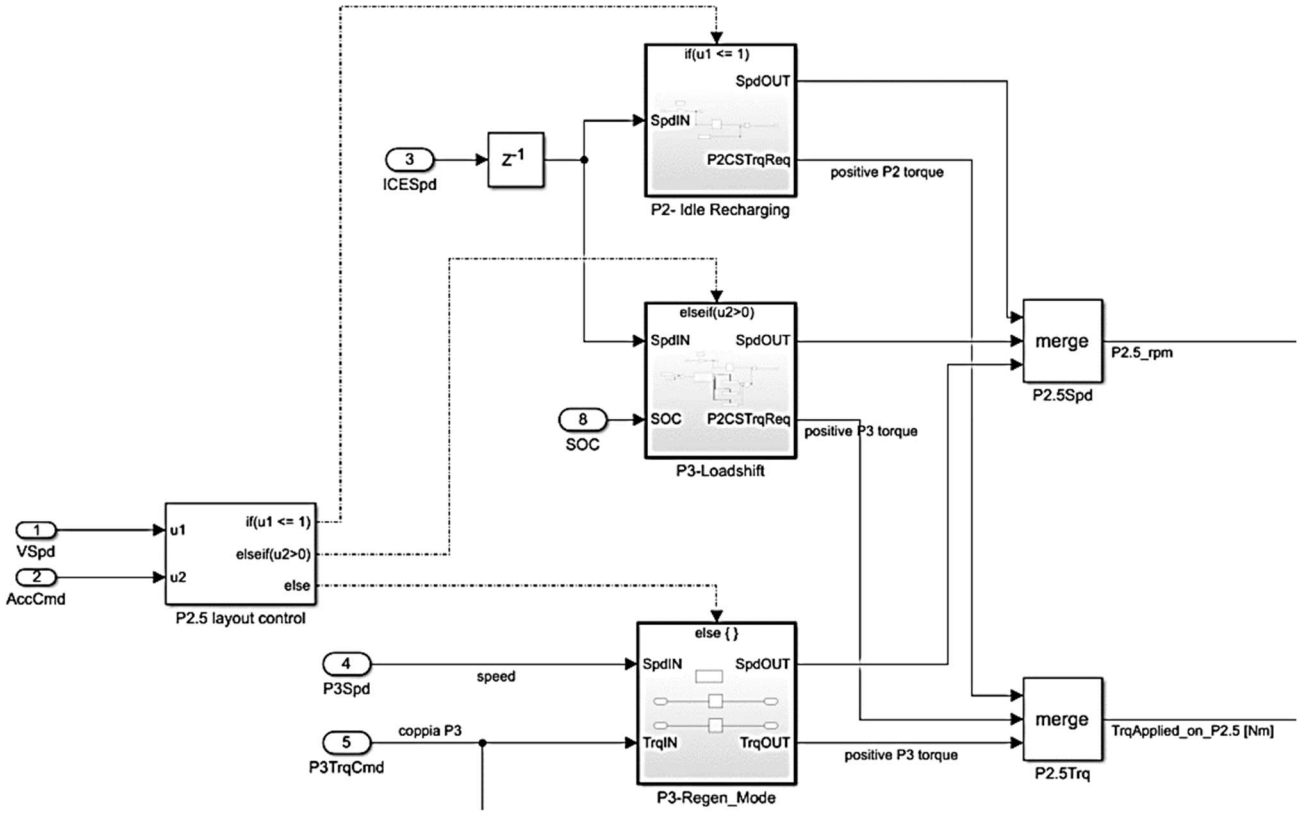

Fig. 48 P2.5 layout control in No propulsion phases

Depending on vehicle speed and acceleration command, the P2 or the P3 layouts are chosen: the choice of the correct block is fundamental to assure the correct gear ratio and motor speed. The sign of the torque applied instead is removed and applied later on with a dedicated block that recognises the driver's demand. Each of the three if action block depicted in fig. 48 (*P2-idle recharging, P3-loadshift and P3-Regen_Mode*) contains the motor map that is able to output a temporary value of torque at those conditions.

The provisional torque value obtained is then examined by the current definition blocks. Such part is composed by a three step control, visible in fig. 49. The first control is done inside the P2.5 Current Table, which includes another motor map, working in the opposite way with respect to the formerly cited one: a current output is determined on the basis of the motor speed, voltage and torque request. Similarly to what is applied on the P4 motor, the peak power is available for a limited amount of time (10 seconds, in this case) and a specific block is there to monitor possible steps out of that limit. The second control is done by decreasing the current values down to the battery limits, that are subjected to the charge partition rules mentioned in the *Current Control* paragraph. Third and last control is done by the *Inverter Efficiency* 2-D lookup table, which again decreases the absolute current value to take into account the unavoidable losses inside the inverter.

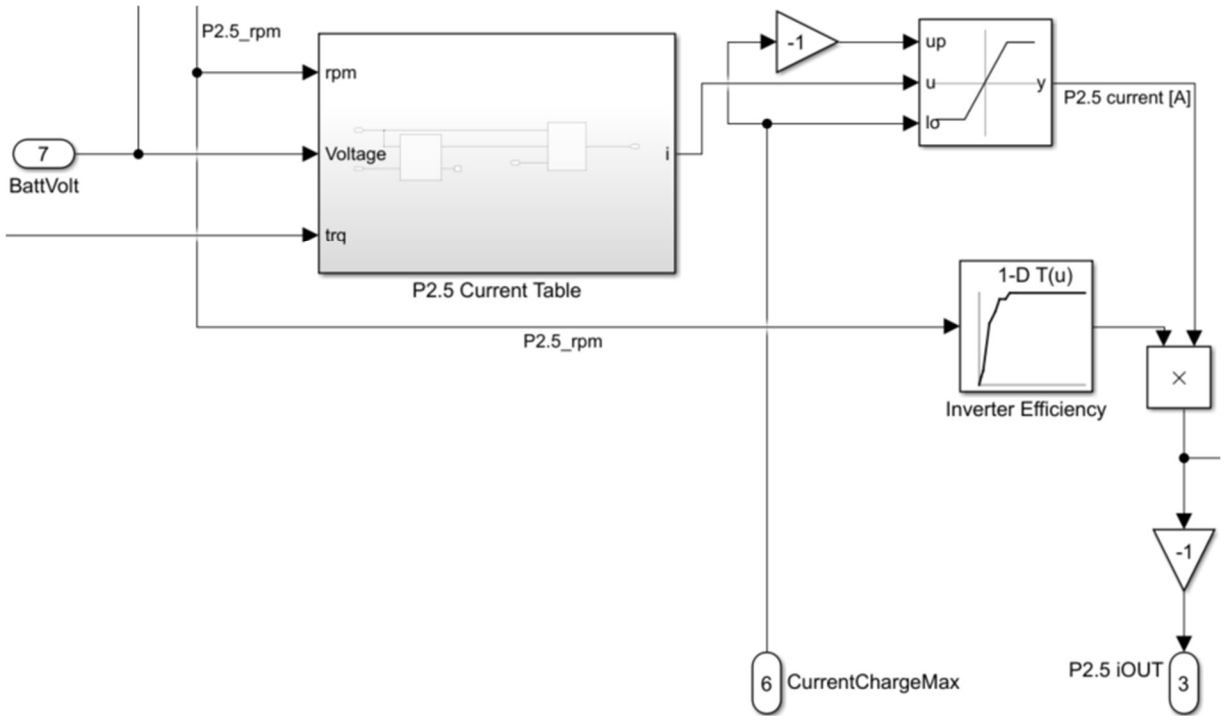

Fig. 49 P2.5 current definition blocks in No propulsion phases

Torque definition blocks are those responsible to define the final value of the torque actuated by the rear EM. Such task is accomplished by a two-parts group of blocks, composed by a *Matlab function (EM current limit* in fig. 50*)* and an *if case* (*Torque Sign control* in fig. 50) group.

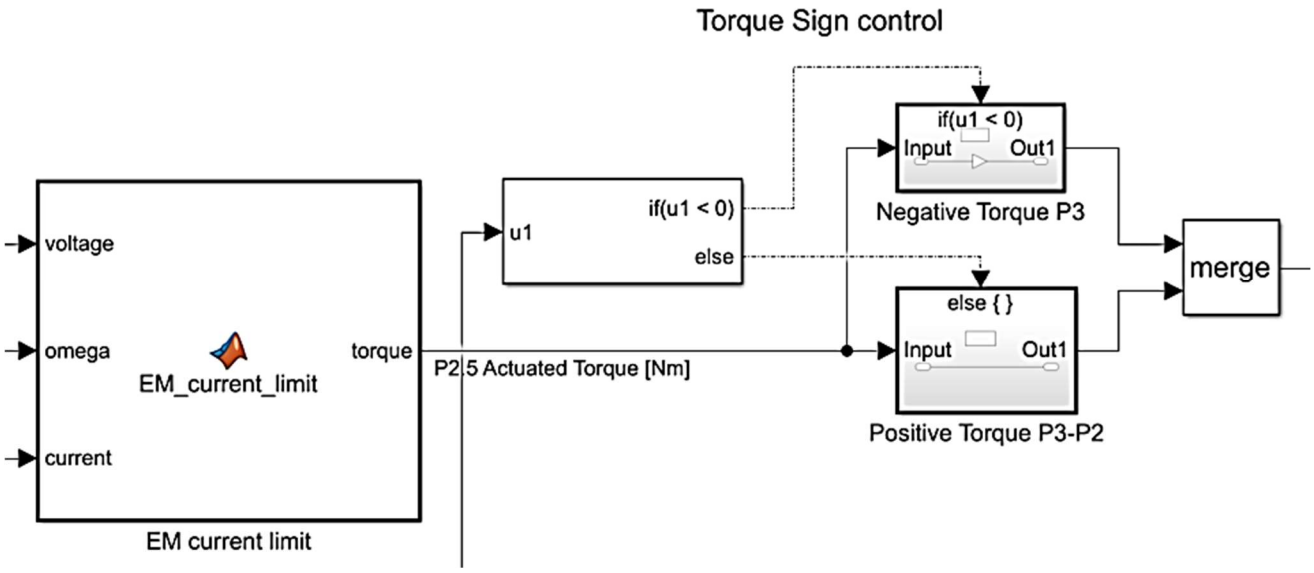

Fig. 50 P2.5 torque definition blocks in No propulsion phases

The EM current limit function checks once more the combination of voltage, rotor speed and current to output the final *P2.5 Actuated Torque* value. An extract of the Matlab code utilized follows:

```
voltage_vector=BST1_rear.voltage;

omega_vector=BST1_rear.rpm_interpolated;

[~,voltage_index]=min(abs(voltage_vector-voltage));
[~,omega_index]=min(abs(omega_vector-omega));

current_vector=squeeze(BST1_rear.current_interpolated(omega_index,:
,voltage_index));
[~,current_index]=min(abs(current-current_vector));

torque_vector=BST1_rear.torque_interpolated;
torque=torque_vector(1,current_index);
```

The function identifies the current value that is the closer to the actual motor working point, that is computed via interpolated rpm and voltage data. Once this value is known, the output is sent to the *Torque Sign control* group that adjusts the sign, depending whether it is load shift or braking torque.

As the last step of the No propulsion case, the torque actuation blocks assign the output torque to the correct mechanical paths, that are the P2 or the P3 layouts.

3.8.8 P2.5: Hybrid Mode

The inner structure of the *Hybrid Mode* subsystem is simpler than that of the *No Propulsion* one. This subsystem simulates the P3 unit working as a motor or as a generator, in acceleration and braking phases respectively. Being the layout fixed, the inner structure can be divided into two major groups:

- **current definition** blocks
- **torque actuation** blocks

The current definition process starts, as fig. 51 depicts, with the P2.5 Current Table block. In parallel to it, the current sign is defined. Next to these two blocks, as it happened in the No Propulsion case the battery current limits are considered, as well as the current absolute value reduction due to inverter losses. All these blocks were already mentioned, and they employ the same values of the previously described ones.

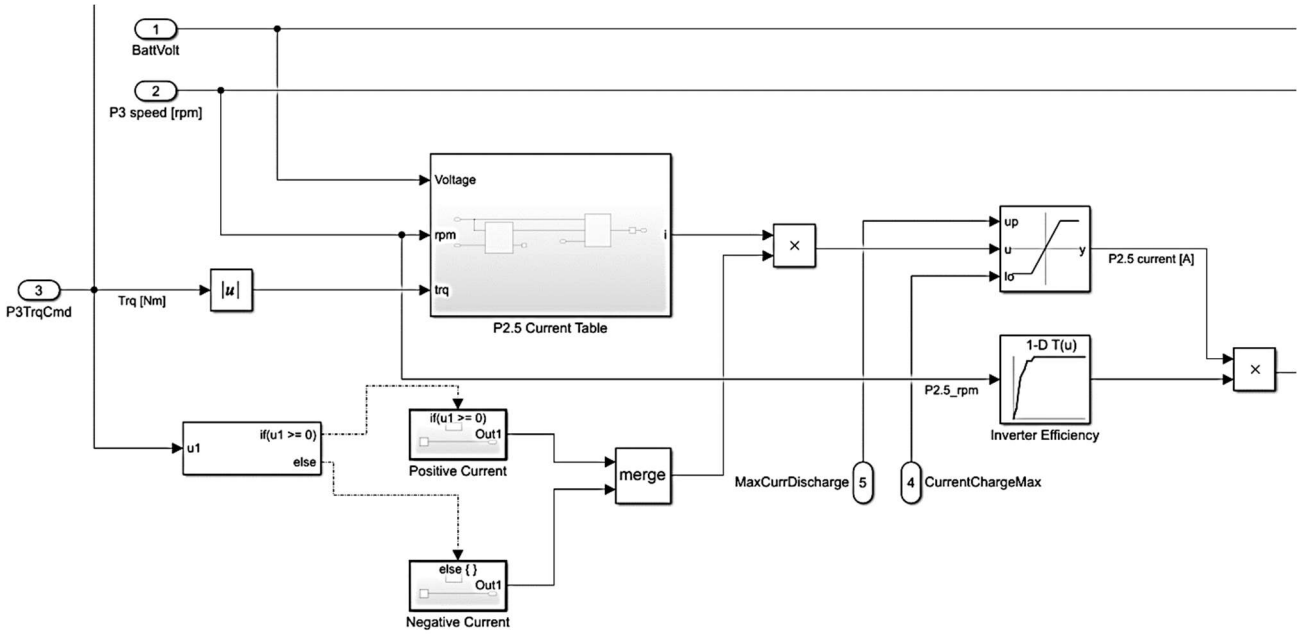

Fig. 51 P2.5 current definition blocks in Hybrid Mode subsystem

The second major group of blocks is the one related to torque actuation. This group is represented in fig. 52 and features two important blocks. The *EM current limit* Matlab function block, and the current sign control blocks.

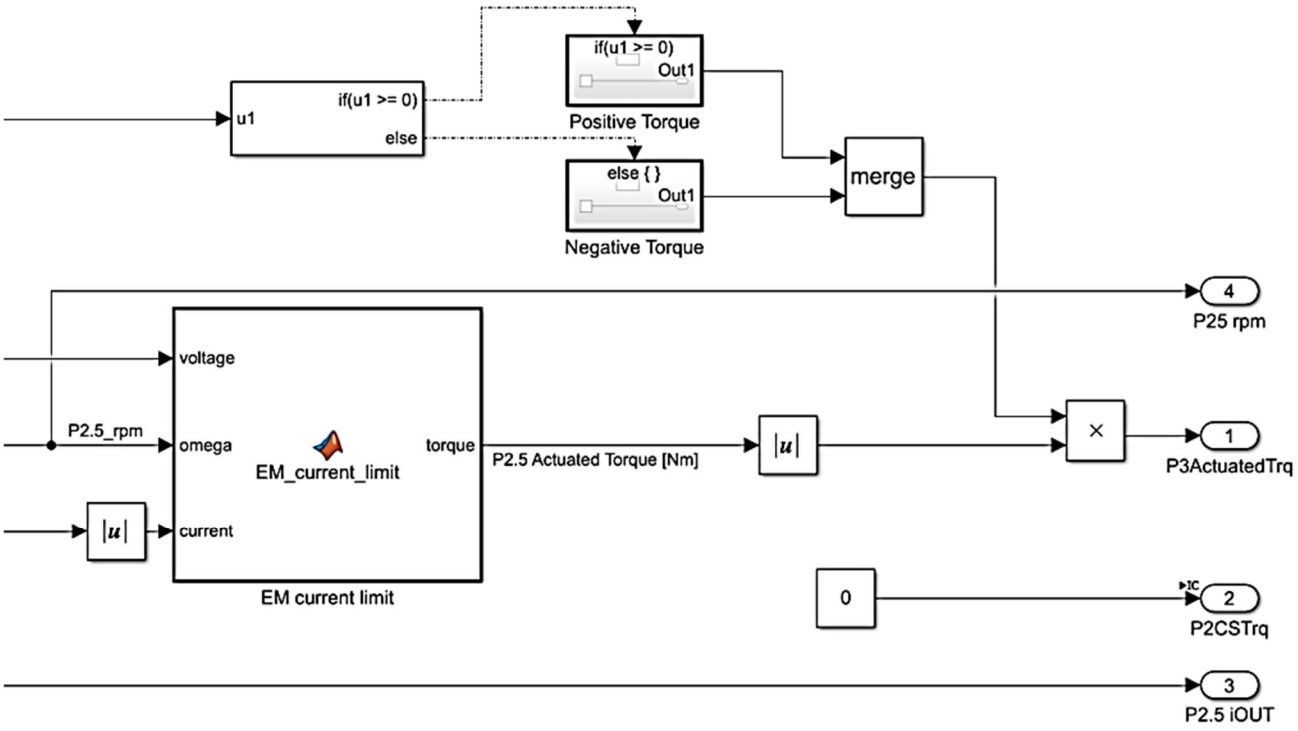

Fig. 52 P2.5 torque actuation blocks in Hybrid Mode subsystem

As it happened for the previous block group, the EM current limit Matlab function and many minor blocks were kept the same.

3.8.9 Battery

The Battery subsystem mask and ports are shown in figure 53. The most important input parameter that is demanded by the battery to the vehicle is the *requested power*, while the relevant values that are needed by the electric units are the *charge* and *discharge currents*, and the *voltage* at which the electric powertrain is operating. As a design characteristic, the voltage can vary between four levels.

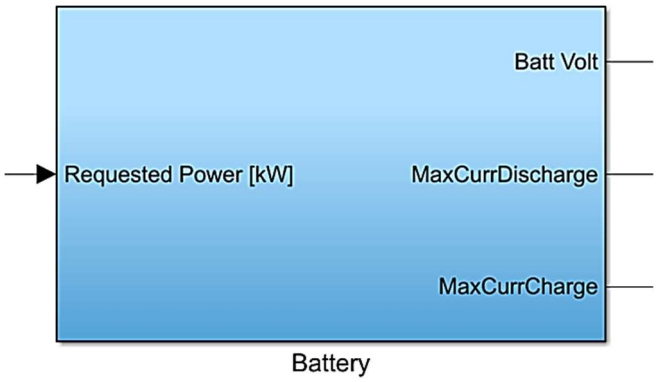

Fig. 53 Battery subsystem mask and ports

The battery was modelled as a black-box concept: its virtual model was provided as a complete and validated system, and it was not tuneable or open for further modifications. As a black-box model, it runs only via a specific set of input parameters, which is composed as it follows:

- **Minimum SOC allowed**: the lower this value, the higher the DoD granted to the strategy. This parameter was set in a conservative way, to preserve the SoH and to slow down battery aging. As it is reported by Kabitz et al. (Kabitz, et al., 2013), the higher the Dod, the worse the effect on battery health
- **Maximum SOC allowed**: this value was not set to 100%, to diminish the Constant Voltage charging phase, which is the one responsible for most of the 'cyclable lithium loss' and 'metallic plating' phenomena (Cordoba-Arenas, Onori, Guezennec, & Rizzoni, 2014)
- **Peak time**: length measured in seconds of the peak performance phase, where the maximum discharge current is available
- **Battery max temperature**
- **Battery initial SOC:** imposed by the virtual driver at the beginning of the drive cycle
- **Battery start temperature:** kept to the external air temperature of 25°C
- **Battery coolant temperature:** kept to the external air temperature of 25°C
- **Battery coolant volume flow:** of little importance for what concerns the project

Some of the most significant outputs are reported in fig. 54. The battery block as standard supplied the maximum charge and discharge power that can be exerted by the electric powertrain: however, as it was described in the previous paragraphs, the EMs require specific operating boundaries in terms of currents.

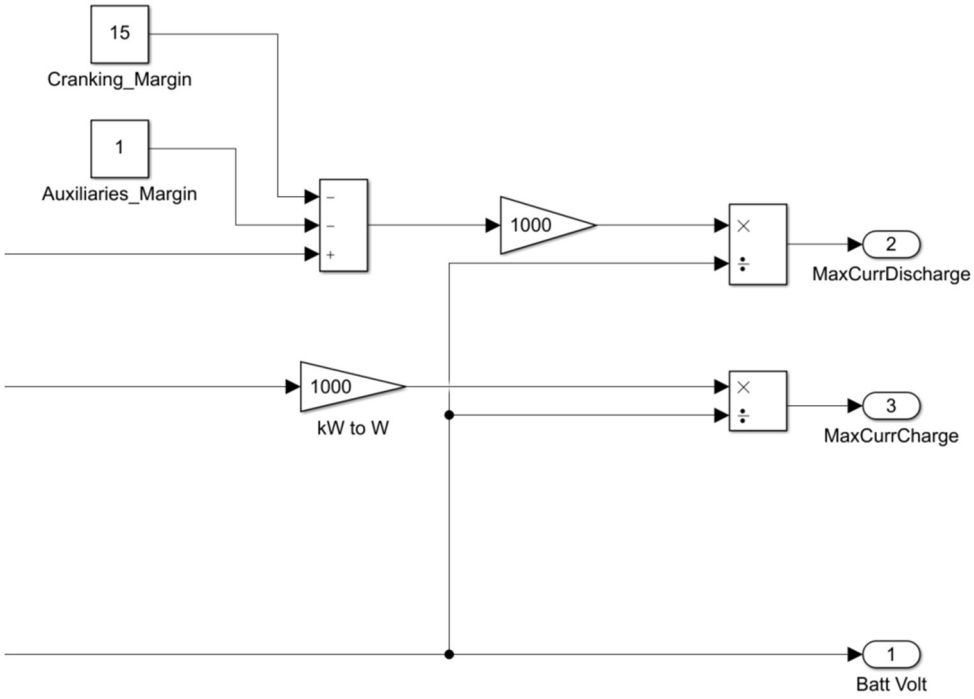

Fig. 54 Battery subsystem relevant output ports

It is important to note that the maximum discharge current to be sent to the EMs had to be first decreased by two rather different power requests.

The first one is the power required for the cranking phase of the ICE: such phase lasts for a very short time, and demands an almost impulsive torque to be applied from the rear EM, connected in P2 layout for this purpose, to the ICE. When considering the energetic impact over the total energy consumption in every drive cycle examined, it proved to be not relevant (less than 0.1 kWh over long driving cycles): it was just necessary to assure that there was always a 'safe margin' for that mechanism. The second power demand instead is continuous: the power margin reserved for the auxiliary devices had to be maintained through the entire length of the various drive cycles, and this severe energy demand had an impact on the optimization strategy too.

3.8.10 Energy consumption

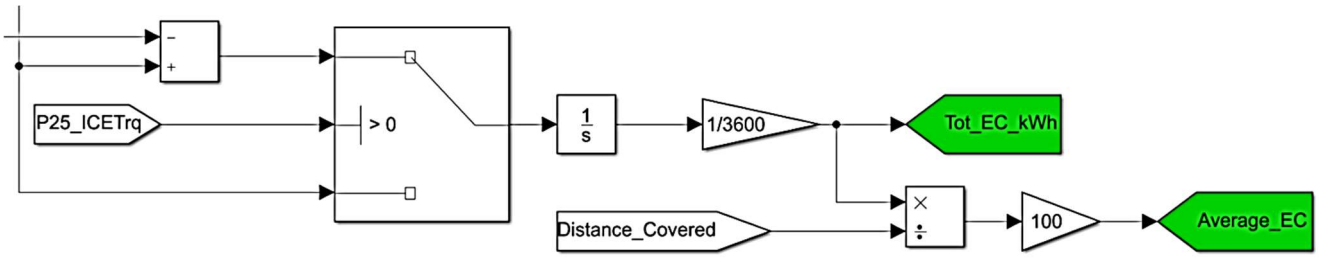

Fig. 55 Energy consumption blocks

Fig. 55 shows how energy consumption is computed: the requested power entering the battery is integrated over time, taking into account both charging and discharging currents. The overall amount is also processed together with the distance covered by the vehicle to show the average electric energy consumption when running. The switch block at the centre of fig. 55 is designed to prevent counting the recharging energy that does not come from the EMs regenerative braking but from charge sustaining phases. Charging currents entering the load shift phases are rather high, and are supplied by the ICE (and clearly obtained worsening fuel consumption): such currents are produced when the rear EM is applying a load shift torque on the ICE. Decoupling this energy from the overall balance is mandatory to avoid mistakes in the total energetic consumption of the two powertrains combined.

3.10 Brakes

The *Brakes* subsystem is the one responsible for converting the braking command into regenerative braking and friction braking torque command (see fig. 56 input and output ports).

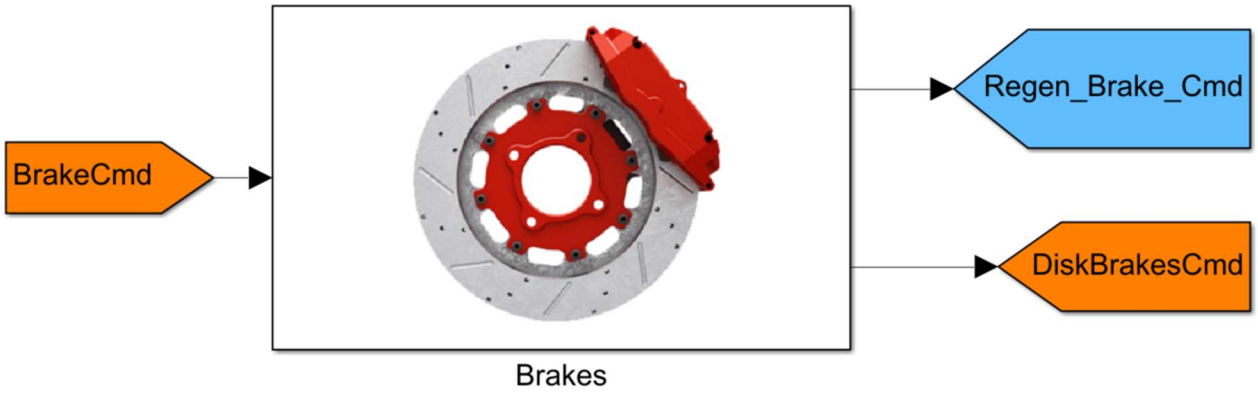

Fig. 56 Brakes subsystem mask and ports

In order to process the braking command coming from the *Vehicle Command* subsystem, as it happened for the actuator, a signal-into-torque conversion was applied. In particular, the total amount of available braking torque was computed, by assigning to the two braking systems an estimated amount of torque available. So respectively, the friction brakes were assigned a total torque $\alpha_{friction}$, the regenerative brakes a total torque β_{regen}. While the total torque α came from empirical data and could have been more precise with extensive tests and experimental assessments from the manufacturer's, the total regenerative torque available was considered as the maximum torque that the EMs could exert on the two axles. So, the total braking torque γ_{total} is the result of:

$$\gamma_{total} = \alpha_{friction} + \beta_{regen}$$

where:

- $\alpha_{friction}$ represents around the 83% of the total braking torque
- β_{regen} represents the remaining 17% of the total braking torque

It is interesting to notice that this percentage partition allows to directly associate the 0-1 command coming from the braking pedal to the thresholds here reported: this association played an important role in the mode choice logic.

The braking action is organized in three different modes, that are chosen depending on the intensity of the braking command, the current vehicle speed and the battery state of charge. As fig. 57 reports, these three modes are:

- **Strong Braking – depleting**
- **Gentle Braking – depleting**
- **No regen**

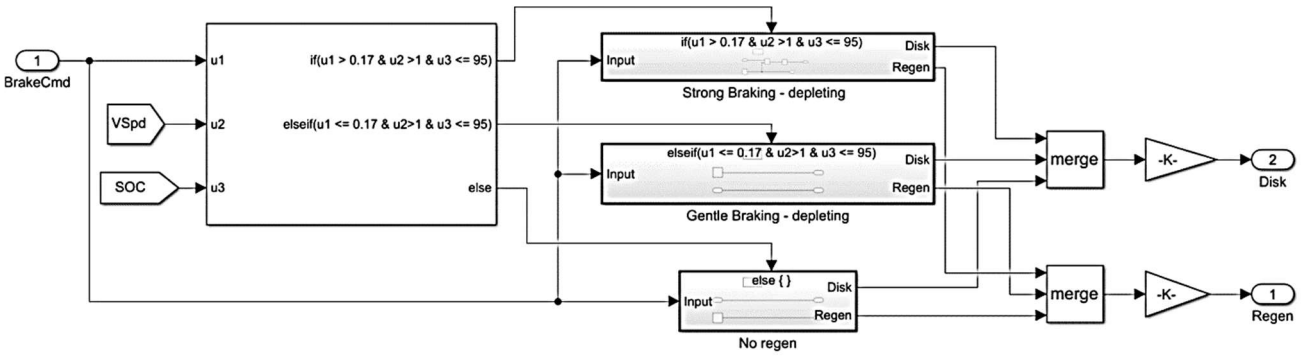

Fig. 57 Brakes subsystem three-modes structure

Strong Braking – depleting mode is selected when braking command request overcomes the possibilities of the regenerative braking systems, vehicle speed is different from zero and the SOC is lower than 95%. With this mode activated, friction brakes and EMs work together in parallel.

Gentle Braking – depleting mode is activated when regenerative braking system is adequate to slow down the vehicle: friction brakes are not involved and the maximum energy recuperation is possible, and therefore it is also the most energy-efficient mode of the three. Most of the driving cycles allow to remain in this mode when slowing down the car.

No regen is the mode that manages particular driving conditions, such as low or zero vehicle speeds, or fully charged battery : all the brake command is sent to the disk brakes that, unfortunately, dissipate the car kinetic energy. This happens because of the high SOC value: according to Peng et al. (2015), the regenerative braking should be avoided due to lower charge efficiency and to avoid possible over charging.

3.11 Modelling issues

During the first two months of model development, many parts of the vehicle were simulated utilizing the blocks from the *Powertrain Blockset* provided by Simulink:

- Dual-clutch gearbox
- Tires
- Front and rear differential
- Vehicle dynamics
- Driver commands

Apart from the Drive Cycle Source block, still utilized by Driver Command subsystem, none of them is still employed.

The *Powertrain Blockset* blocks were initially chosen because they were ready-to-work and complete blocks, that could help in speeding up the closing of the data loop and check for relevant bugs or modelling mistakes. Unfortunately, they proved to be quite unsuitable for the aim of the model and where slowly substituted by on-purpose designed ones: they all worked with a rigid, predefined set of blocks that needed several parameters to properly work, many of them very difficult to obtain. In addition, being their structure not adaptable, it became difficult to implement inner controls and strategy-related blocks that after a few months became the core part of the project.

As the last reason, the model simulation speed increased dramatically when removing those blocks, and designing instead the model own subsystems.

A second relevant issue came from the nature of the car itself: given that the real, drivable vehicle was missing, unlike other similar energetic studies, the continuous updating procedure that most of the components underwent during the months of work forced to add blocks, change parameters and train again the strategy before repeating and collecting all tests data one more time. This unavoidably extended the course of the project, but it was necessary to maintain the required similarity and alignment in terms of hardware components to the model used by the R&D department (the series hybrid that will serve as a reference in the results and conclusion chapters).

4. Energy management strategy

First, a brief introduction to what were the reasons why the strategy was selected, and which was the technical background and external environment that characterized that choice. Then, the strategy is gradually examined in details, starting from the literature archetypes that inspired it and then entering into the details of every parameter.

4.1 Strategy framework

The aim of the project was to realize an optimization strategy working without a priori knowledge of the driving mission. This target made it possible to focus on real-time strategies, which react step-by-step to the external inputs, such as resistant forces and reference speed.

Since the very beginning of the project, several boundaries helped in better defining such strategy:

- High accuracy in following the reference speed trace
- All motors have to work inside their speed and torque design limits, without any possibility to change them: as it was anticipated before, aim of the project is not component dimensioning or sizing
- Gearbox shifting schedule fixed, and developed by an external department: this means the engine operating point line cannot be chosen by a possible algorithm-based strategy
- Battery SOC must respect minimum and maximum values suggested by manufacturer to maintain the State of Health (SoH) over time, which is heavily affected by excessive DoD (Bolun, Oudalo, Ulbig, Andersson, & Kirschen, 2018)
- Capability to take into account new parameters and variables (as it happened during the course of the project, like SOC targets and running modes)
- Computation of polluting emissions not considered: still, it is clear that CO_2 emissions are reduced by adopting an energy-optimization strategy, being them almost directly proportional to the fuel consumption; this does not hold for the other pollutants
- Car driveability and safety to be preserved: car disk brakes were implemented, even if completely out of the strategy environment; it is also worth mentioning that several blocks were installed in order to lower the amount of gearshifts or changes of paces, even though they were required to reach the best consumption values possible
- Simulation machine not capable of high level performances

Due to the abovementioned project constraints and in particular to the lack of gear shift control, a numerical approach (such as that of *Dynamic Programming*) was considered not suitable (Li & Gorges, 2019) and the focus was posed onto fuzzy-logic approaches instead. The flexibility of a *rule-based* approach was eventually preferred: as Finesso et al. report (2016), it requires a relatively low computational effort, and the rules identification via the adoption of machine learning techniques can noticeably increase controller robustness and accuracy.

However, according to Enang and Bannister (2017), '*despite widespread utilisation, rule-based HEV control methods, still present some significant challenges. Typically, in a rule-based HEV control strategy, a huge amount of time and investment in qualified work force is required to develop the strategy, owing to the long rules definition and calibration process'*. The strategy development during the course of this project faced the same challenge: how the calibration process was addressed will be discussed in the following section.

4.2 Offline Calibration Process and Training: Sensitivity Analyzer

The Simulink Sensitivity Analyzer played a fundamental role in the development of the entire strategy. The rule-based concept relies on a set of conditions and algorithms that need to be 'trained' in order to maximize the overall efficiency improvements. This training part was performed with the help of this tool: what was needed in this training phase was a method to find, among all the possible strategy parameters the one that produce the best overall energy consumption, and this software proved to be really effective. Clearly, the Sensitivity Analyzer is also able to perform many more tasks than those that were utilized during this project, but for sake of simplicity only its application for this optimization case will be described.

An overview of the Sensitivity Analysis follows. It can be fractioned into a multi-step procedure:

- **Parameter(s) selection**
- **Random Values generation**
- **Requirement selection**
- **Evaluation**
- **Results comparison**

Parameter(s) selection: this first phase mainly consists in choosing the parameter that has to be tuned. For example, the amount of torque that the rear EM has to require to the ICE during load shift phases can vary between 0% and 100%, that means that it can totally avoid loading the engine (0% case, and coefficient 0 in the virtual model) or require all the torque available (100% case, and coefficient 1 in the virtual model).

Random Values generation: now that the parameter under analysis is chosen, it is time to create the set of experiments to find the best value. The variation range is chosen, varying between a minimum and a maximum value, and the number of samples to be tested is also defined. Following the previous example, the random values can go from 0.1 to 1 (see fig. 58); moreover, 20 samples are taken following the uniform distribution[3] along this range, to obtain a more clear and complete overview of how varying this parameter the simulation results are affected. This step puts already in evidence one big advantage of this tool: it can execute multiple tests over the same model, evaluating

[3] Other distributions like the Normal, Poisson and Weibull ones were available too, but they were less suitable for the purpose of the undergoing analyses

uniformly and precisely the impact of the specified parameter variation, without using only engineering knowledge or theoretical considerations.

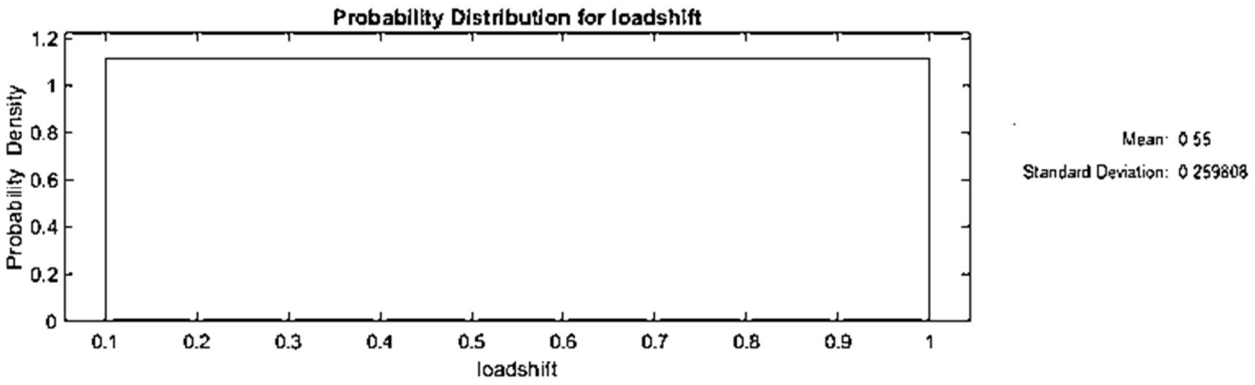

Fig. 58 Random Values ready for testing at the beginning of a sensitivity analysis

Requirement Selection: this step consists in finding the target that has to be reached. Coming to the project case, the target was always the same, i.e. reducing the energy consumption. To obtain that, the variable that has to be minimized must be identified by the software. For example, this happens by choosing the *tot kWh* signal inside the *Vehicle Dashboard* subsystem, as fig. 59 shows. Once this variable is selected, the software must be set with the indication *minimize*: many more actions could be engaged, such as maximize, position the signal with respect to a specific bound, match or track another signal, or even create a custom requirement.

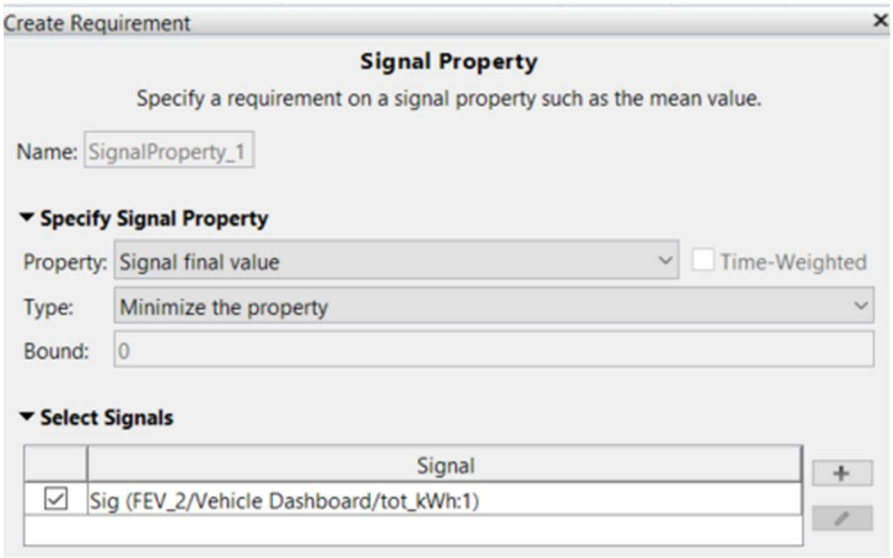

Fig. 59 Requirement selection during Sensitivity Analysis

Evaluation: then, the parameter evaluation process starts. The computer is asked to simulate time and time again the entire model over the chosen driving mission, until all the combinations prepared

during the previous steps are examined. This step turned out to be very demanding for the computing machine, up to a point where it became unavoidable to upgrade the RAM and also assure proper ventilation to the inner components.

In addition, a very long time is required to perform an evaluation: this time is influenced not only by the computing power, but also by the driving cycle chosen for the evaluation. While US06 driving cycle lasts for only 600 seconds, all the other cycles utilized in the calibration process are longer, starting from at least 1800 seconds. It is important to notice that during the evaluation phase, no modifications can be made to both the Simulink Model and the Matlab code: otherwise, the evaluation fails and all results are compromised. This process can last for more than 6-7 hours.

Fig. 60 shows how the results are progressively collected during the evaluation: the graph on the left side shows the energy consumption results from every single parameter choice, while the graph on the right shows how these results are distributed.

To improve the accuracy and the optimization process, the evaluation can be repeated over different driving cycles and with different initial conditions (in general, the most important one is the initial battery SOC). For instance, when tuning the load shift strategy, the initial SOC must be kept lower than for other cases, so that to maximize the *Charge Sustaining* phases and better highlight the impact of that particular parameter.

It is important to note that theoretically, it could have been possible to directly implement all in once the entire set of the strategy parameters and evaluate the best combination possible with those values. However, the amount of samples required would have drastically slowed down the project progresses. It was simpler to determine the variations and to implement them by analysing the singular impact.

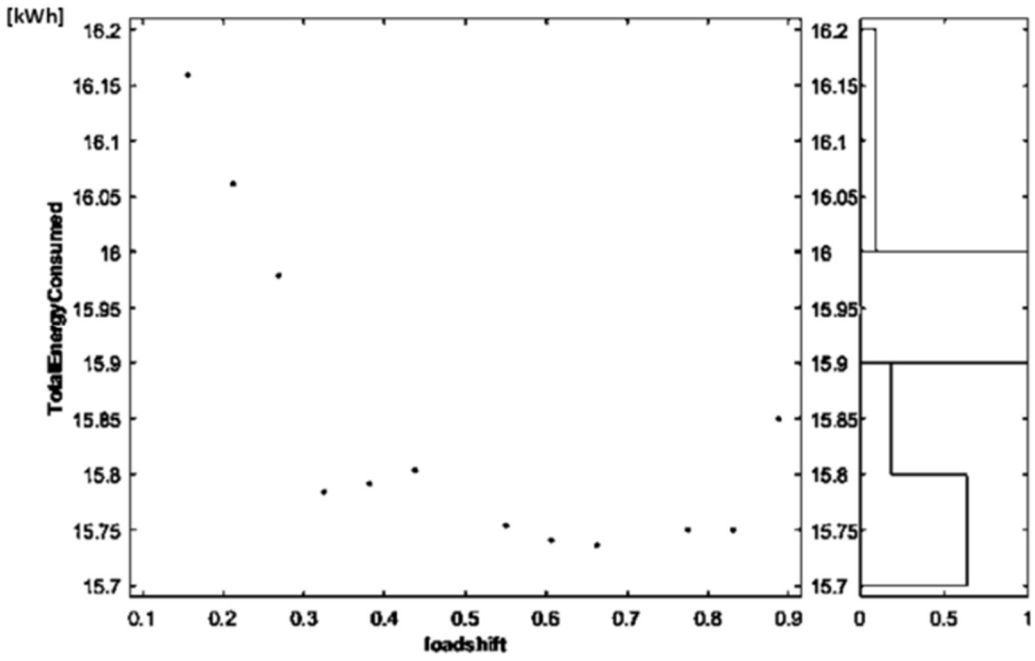

Fig. 60 Data are being collected during Sensitivity Analysis

Results comparison: once that all the samples have been tested, the results are collected graphically and numerically and the best combination is immediately found. The example of fig. 61 immediately shows that on the US06 driving cycle (chosen for this analysis) the fuel consumption is optimized in 0.6 - 0.8 range for the *load shift*.

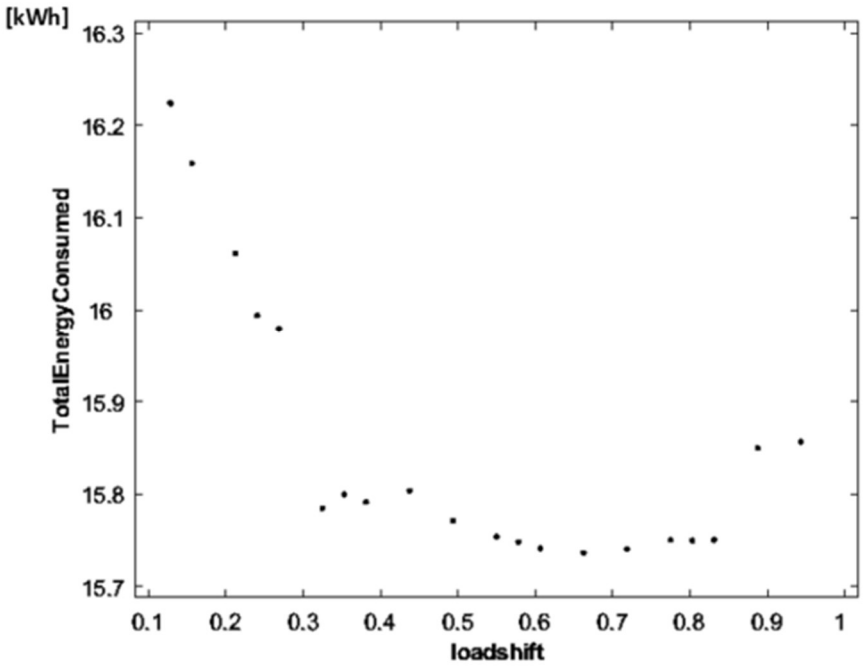

Fig. 61 Sensitivity Analysis: final results

4.3 Powertrain configuration choice

An important decision to be taken at the beginning of the project consisted in deciding which powertrain configuration to choose: the question was whether to embrace the series hybrid configuration, or the parallel one. Vehicle layout constraints made it impossible to consider the power-split option.

Such question was answered employing three different approaches: the first one consisted in examining how the other car brands approached the hybrid supercar new segment; the second was aimed to understand how the Lamborghini car under analysis was arranged; as the third and last approach, it was necessary to go through an extensive literature research and data examination over series and parallel configurations. In particular, the two last approaches were strongly merged together, using the third one as a tool to better conduct the second step analysis.

4.3.1 Considerations over state-of-the-art vehicles and literature research

A state of the art analysis of the most recent hybrid supercars, as reported in chapter 2, showed how car makers were clearly oriented towards the parallel configuration, especially considering the better performance and improved driving pleasure that the direct mechanical linkage between ICE and wheels could provide over the series one. However, being those priorities not the one driving this project, this first indication was not considered adequate to justify this choice. Having the target to design a driving algorithm able to maximize the efficiency, driving pleasure and performance was to be assigned to other specific driving modes available for the driver.

A more extensive analysis of the vehicle technical characteristics, as well as an investigation of literature examples and early studies definitively solved the dilemma: the work of Karbowski et al. showed that the parallel configuration had a ‘ better fuel consumption in charge sustaining mode than the series and the power-split ’ (2009). When considering the architecture of the PHEV under exam, the presence of a unique traditional battery instead of several supercapacitors, negatively affects the overall energetic efficiency. The electric energy storage system plays a vital role especially when series configuration is applied, as it ‘ *is affected by the electrical component performances* ’ more than the parallel one. In particular, *‘ two main problems arise: short lifetime and high losses in charging and discharging phase ’*. The high power cycling is much more suitable to supercapacitors, as they feature high-power discharge and higher efficiency when compared to batteries (Lanzarotto, Marchesoni, Passalacqua, Pini Prato, & Repetto, 2018). Unfortunately, such devices were not installed on the project car.

4.3.2 Considerations over project boundaries

In addition, some considerations were made about the internal combustion engine in particular. It is clear that, considering the niche segment the project car belongs to, such engine is an high-performance unit. Even though no engine maps and values could be reported in this thesis for confidentiality reasons, a clear tendency towards high rpm, high power regions of this unit has to be underlined, as well as the fact that its overall power and torque output is superior to those of the two electric units combined. These propulsion roles are inverted with respect to the ones usually designed for the series HEV configuration, as a team of English researchers underline, ‘*which is powered primarily by the electric motor and secondarily by the ICE ’* (Enang & Bannister, 2017) . They proceed by reporting that:

‘ *Internal combustion engines used in series HEVs are generally small compared to those used in conventional vehicles and only account for less than 50% of the maximum power needed to propel the vehicle. Several automotive companies e.g. Mitsubishi, Volvo and BMW, have explored the possibility of series HEV development. Despite this in-depth research, commercial application of the series HEV development is still very limited to heavy duty vehicles. Although series HEVs tend to have highly efficient engine operation, this benefit is quickly outweighed by the fact that they often require very powerful and expensive batteries, with a high energy density to operate.* ‘

A common drawback that generally favours the series architecture is the increased mechanical complexity of the parallel configuration: the possibility to adopt a smaller engine, that does not need to be connected to the wheels, allows for the elimination of the gearbox, thus having weight savings

and more freedom in designing and placing the engine compartment, in addition to being also simpler for what concerns energy management (Zhuang, et al., 2020).

However, these drawback was clearly not considerable at the beginning of this project: the engine size and torque map, as well as the presence of the gearbox and all the gearing mechanisms, did not allow to exploit the theoretical series advantages, or at least investigate them.

As the last point, it is important to state once again that the only driving criterion for this research was the energetic efficiency. When considering the emission of pollutants instead, the series hybrid proves to be a strong competitor to the parallel hybrid: this is due to the fact that the engine describes far less *cranking* phases than its opposite solution, and then it operates at almost steady-state conditions, with beneficial effects in terms of inner engine temperatures, friction losses and exhaust gasses chemical composition.

Having clear in mind the energetic optimization target, the parallel configuration was chosen.

4.4 Working Principle: Two-Layer control and State Machine strategy (multi-mode strategy)

According to Millo and Rolando (Millo & Rolando, 2011), the presence of different power sources in a parallel-hybrid vehicle makes it necessary to develop a two-layer powertrain control system:

- the first layer, which they define *supervisory controller*, ‘ decides when the […] power split algorithm should be applied and when, instead, a special behaviour (e.g. pure electric drive) should be forced due to specific situations’
- the second layer instead, details the required *power split* to satisfy the power demand

When applying this concept to the vehicle under investigation, this two-layer structure was increased in complexity, even though the basic principle remained the same. As it will be shown in the *Operating Modes* section, the vehicle follows the so-called *State Machine* strategy, also known as multi-mode strategy. This strategy, following the definition provided by Tran et al. (2019), ‘ *works on a specific operation or state of the vehicle using a flow chart or decision tree of the stable conditions related to the previous conditions and present input values* ’ and it ‘ *dictates the operating modes, for example, the engine mode (ICE propelling the vehicle), boosting mode (both ICE and EM propelling the vehicle), and charging mode (ICE propelling the vehicle and charging the battery). The transition between the operating modes is decided based on the change in driver demand, a change in the vehicle operating conditions, and system/subsystem faults* ’.

The multi-mode strategy implemented into the simulated car in particular declines the power split algorithm into two main modes, that are *Hybrid* and *Charge Sustaining* Mode. In particular, when Hybrid Mode is on, the EMs satisfy the whole power request, provided that the total amount required remains under the maximum EMs torque limits imposed by initial design constraints. Once that this threshold is crossed, the thermal engine adds its own torque by turning on and being connected via the gearbox to the wheels (see fig. 62) and the power split case is active.

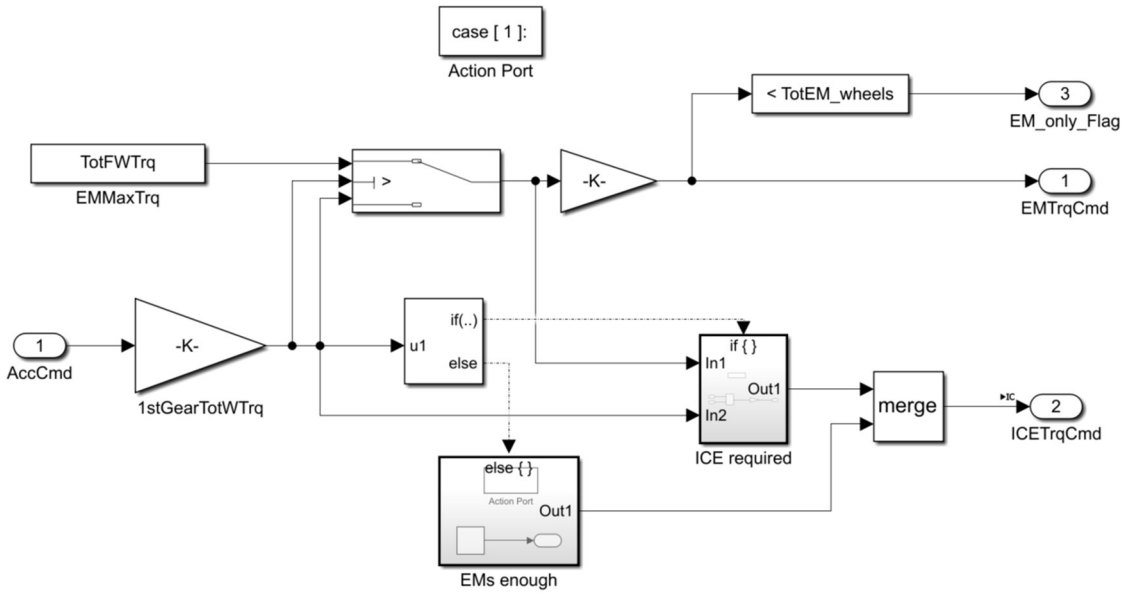

Fig. 62 Power split algorithm in Hybrid Mode

It is clear that this particular algorithm, that prioritizes the EMs intervention over the ICE one, is done due to two reasons. The first reason is that the electric powertrain, given its technical capabilities, is fully able of propelling the car and satisfy every possible power requests during all examined driving cycles scenarios, and using it just as a boost would not employ its potential. Second reason, being this project targeted towards efficiency, the longer the ICE is turned off, the lower the fuel consumption. On the contrary, other sportier operating modes available on the car, that focus on driving pleasure and performance, invert on purpose the aforementioned algorithm decision making process: the ICE is the main actuator, always turned on and delivering power, and the EMs enter into action in *boost* mode to enhance the overall longitudinal acceleration. When SOC targets allow for it, this initial and important power split rule helps lowering down the energy consumption of the vehicle, given that the electric powertrain is significantly better in terms of efficiency when compared to the thermal one: as an example, at the end of the project it was interesting to compare the electric-only vs thermal-only powertrain consumption over the US06 driving cycle: experimental results showed that the same car, over the same mission, utilized over 4 times less energy (measured in kWh) running using the electric powertrain with respect to the case using only thermal one.

When entering the *Charge Sustaining* mode instead, the supervisory controller simply demands power to the thermal powertrain only: the electric units are not allowed to discharge the battery, and therefore they only work in regenerative braking phases (or in load shift, for the case of the P2.5 unit). This straightforward powertrain management allows for an immediate and direct *power split* layer too.

4.5 Two major Operating Modes

Being a PHEV, the car was designed to operate into the two traditional operating modes for such hybrids: *Charge-Depleting* (CD) and *Charge-Sustaining* (CS). As it is defined in principles by Arenas et al. (2014), the vehicle discharges the battery in CD phases by employing the electric units in propulsion, both in parallel with the ICE engine or in pure electric-only driving. When the car is operated that way, the battery energy is decreased. On the contrary, when *CS* mode is chosen, no pure electric mode is allowed and the ICE is constantly switched on in *Hybrid* mode. The battery state-of-charge is kept between two predefined minimum and maximum values, chosen by the virtual driver.

The necessity to cope with the complex powertrain layout of this particular car, together with the need of making an efficiency-optimization strategy adaptable to many different driving conditions, made this double-only operating mode not flexible enough. The core of the strategy does not rely on those two modes and the simple power split differences between the two; instead, it is based on the set of rules that manage the powertrain and that will be described in details in the following section. Still, the two-modes division is useful to clarify how these rules are approached depending on the mode the vehicle is running in.

4.5.1 Hybrid Mode: working principles

As it was briefly anticipated previously, the *Hybrid* mode is the standard operating mode at the vehicle start, provided that the battery is fully charged or the SOC is high enough to satisfy the driver demand. The *Driver Command* and *Torque Command* subsystems act together as the aforementioned *supervisory controller*: based on the vehicle kinematic conditions, as well as driver goals and battery conditions, they establish which power split to apply, and therefore whether to enter the pure e-driving or the parallel hybrid one.

In particular it is clear from research studies on electric motor efficiencies that:

‘*the electric system loss significantly increases as the power increases. Hence, there is a threshold at which it is beneficial to turn on the engine to provide the main power for the propulsion power demand while using the motor to supplement the power demand. ’* (Zhang, Chunting Mi, & Zhang, 2011)

Utilizing the most efficient areas of the propulsion units is a clear target of this strategy: however, this principle should not go against another important statement, that Zhang et al. also provide:

‘ However, it is important to ensure that the available battery energy is consumed at the end of the drive cycle; otherwise, the battery is underutilized ’

Ending the driving cycle with a relevant amount of energy stored in battery (i.e. high SOC) means *wasting* that energy and increasing the CO2 monitored emissions, as well as fuel consumption. Therefore, the strategy can recognize both the necessities and reaches a compromise that proved to be effective over several driving missions. In particular, the car running in hybrid mode is authorized to deeply discharge the battery, and to employ the ICE only to support strong power demands, as long as the SOC remains above a specific threshold. After that, the car enters a specific mode, that

Kriegler defines (2019) as Mixed Vehicle Mode (MVM): the electric propulsion is chosen when power requests and speeds are low enough, and the two powertrains alternatively propel the vehicle. Note that, in case of low SOC (but still above the minimum one required by the driver) the ICE is additionally loaded of a small recharging torque from the rear EM to supply the electric power directed to the auxiliaries, thus preventing battery discharge.

4.5.2 Charge Sustaining mode: working principles

While the *charge depleting* phase is extensively adopted in *Hybrid* mode, determining a deep battery discharge, the *Charge Sustaining* mode adopts the thermal powertrain as the only propulsion system to maintain the SOC above the threshold required by the driver. This mode is particularly useful when the driving mission is too long to be entirely covered by a unique charge depleting phase: this is the case of the homologation procedures, that specifically requires a *charge depleting* phase followed by a charge sustaining-only cycle. But the same problem occurs for the longest driving cycles available, that are the Real Driving Emission cycles: in particular, the RDE speed profiles examined during this project were performed over more than 30 km long routes, that was beyond the electric-only range of the car. As Zhang et al. note, ' *if the SOC is high and the travel distance is short, the vehicle should run in CD mode. On the other hand, when the SOC is low or the travel distance is long, the vehicle should run in the CS mode* ' (2018).

It should be mentioned also the possibility that the driver might require his car to maintain the battery SOC, and run only via the thermal powertrain: this was implemented and tested by setting the initial SOC equal to the maximum SOC available.

During *charge sustaining* phases, the ICE does not only drive the car, but it is asked to recharge the battery. This recharge process can happen in many ways:

- When the car is at zero speed, and the engaged gear is the neutral one, the ICE runs at a strategy-related speed and runs the rear EM as a generator, and connected via the P2 layout
- During driving phases, if the SOC is much lower than the one required by the driver, the ICE is heavily loaded by the rear EM, this time mechanically linked in P3 layout
- During driving phases, as the current SOC becomes closer to the target SOC, the load shift torque is progressively reduced up to a minimum value that, as it happened for *Hybrid* mode, prevents battery discharge due to auxiliaries consumption

4.6 Strategy rules

This section examines how the car powertrain reacts to the driver inputs that include:

- acceleration command
- braking command
- operating mode chosen

and how it responds to the internal car inputs too:

- battery SOC
- vehicle speed
- gear engaged
- torque actuated

It does so thanks to a set of sub-strategies: each of them will be described in the following paragraphs.

4.6.1 EMs deactivation

This part of the strategy is responsible for excluding the electric motors from their propulsion duty when the vehicle is constantly operating at high speeds, and thus with a rather high average torque request. Instead, using those situations to charge the battery can preserve the battery usage as Brouk et al. observe (2015), and make it available for low-speed driving conditions where the EMs are more suitable. This was done by setting a couple of specific parameters via Matlab command: *ICE_only_speed* and *soc_long_route*.

ICE_only_speed is the speed value at which the deactivation takes place, while *soc_long_route* is the SOC threshold below which such phenomenon is authorized.

Both values were set reaching a compromise between few contrasting points:

- The lower the speed threshold is set, the higher the probability to waste battery energy by ending up the cycle with high SOC percentage
- Similarly, the SOC threshold, following several tests results, represents the value at which most of the missions end, and a high value would result in wasted energy
- An high speed threshold makes the EMs work in a high-speed, high-power region, when the battery energy is almost finished: for sake of efficiency, these rapid-discharge working points should be avoided
- Too low SOC threshold would imply a greater Depth of Discharge value, that is harmful for the battery health

Fig. 63 reports one of the tests that were performed over the WLTP drive cycle to tune the speed threshold. As it will be the case for most of the minor strategies that will be examined in the following paragraphs, the total impact of this variation alone over the complete energy consumption of the car is not numerically high, but when considering each small contribution as a whole the combined effect of all these rules is much more relevant. In addition, during the early stages of strategy development,

the variation range was much higher, and so the results range was: this last graph expresses a more focused range, aimed at finding the best value.

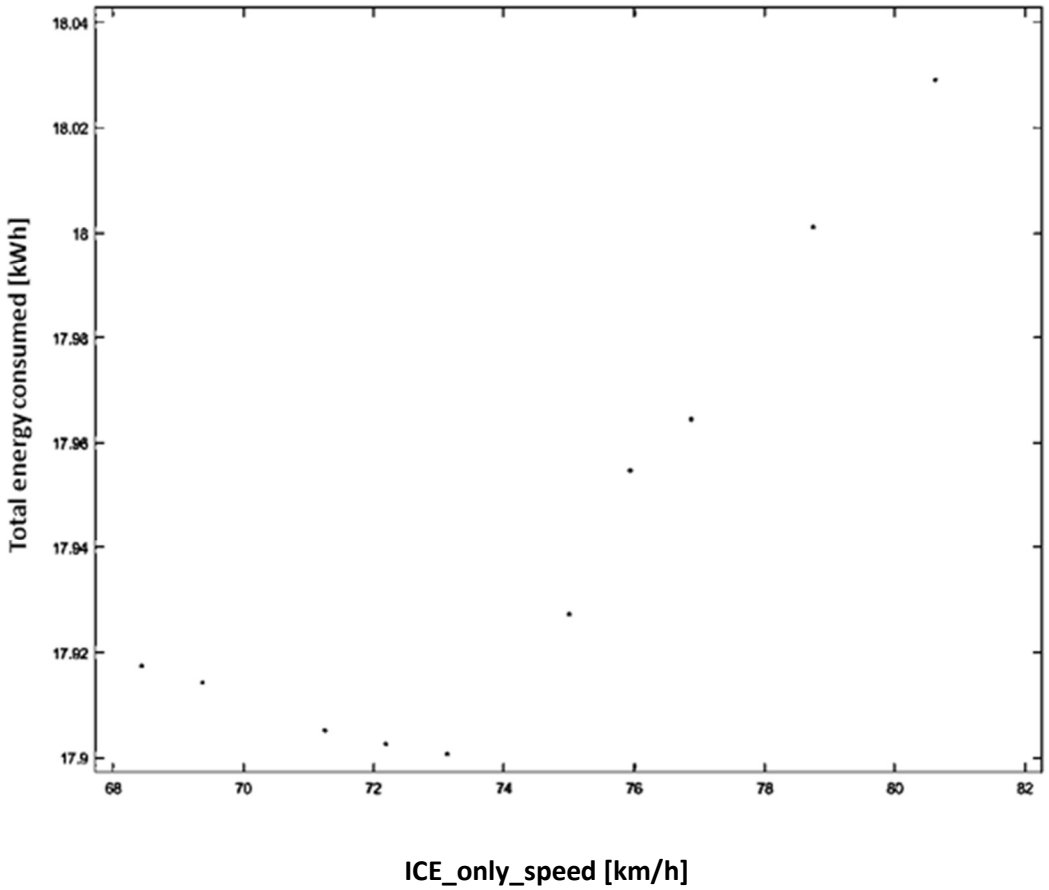

Fig. 63 Speed threshold selection for EMs deactivation strategy

Similarly, the SOC threshold was set to 25% after a few *Sensitivity Analyses*, done starting from variable initial SOC (but always in the high range) and performed over US06 and WLTP cycles. In particular, the results from WLTP were more useful, thanks to its length and much more irregular speed profile. Fig. 64 depicts how this value can dramatically impact the overall energy consumption, and therefore how important it is to tune it properly. It is also important to mention that the speed threshold impact is heavily dependent on the SOC threshold value: the lower the SOC threshold is set, the lower the impact of the speed threshold variation, especially on US06 and WLTP homologation cycles. Having a more powerful machine available, possibly adopting parallel-computing, an extensive testing session over much longer RDE cycles could optimize those values further more. However, the main focus was put on US06 and WLTP as benchmark testing procedures for EU and US homologation tests, and so calibration was done with particular attention to them.

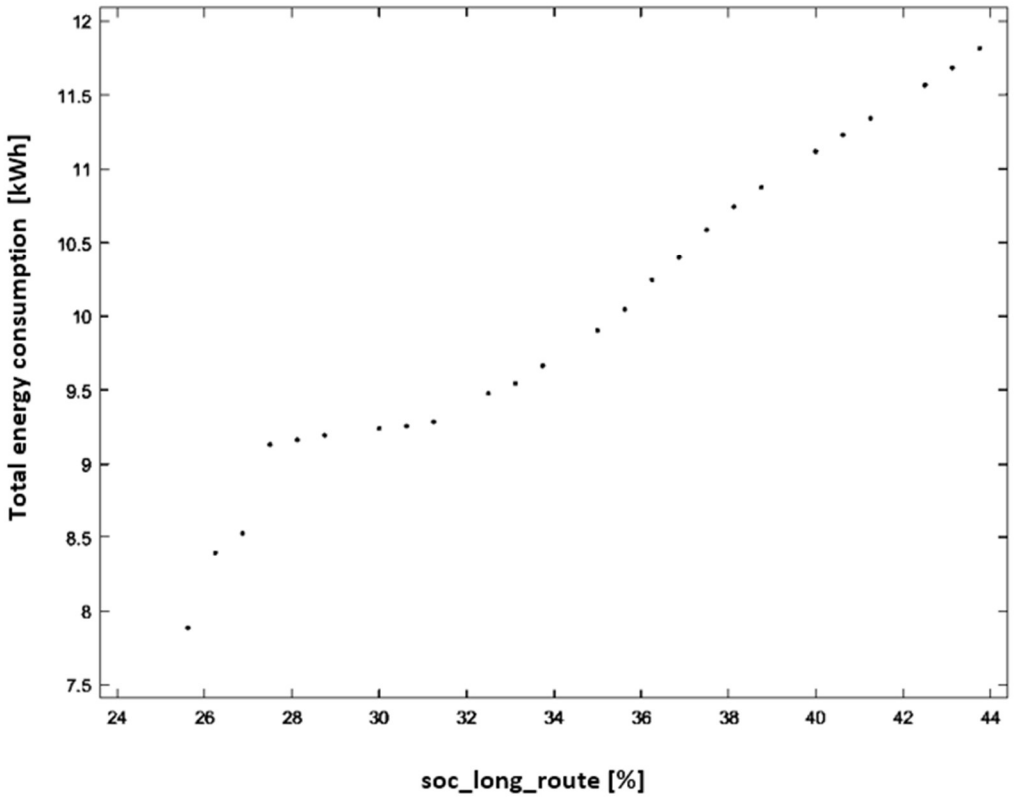

Fig. 64 SOC threshold selection for EMs deactivation strategy

It is clear that this EMs deactivation strategy does not impact high SOC driving scenarios, where the energy stored in the battery is sufficient to drive through the route only turning the engine on during the very last kilometres of driving. Those scenarios, typical of the Hybrid mode and in particular of the *charge depleting* phases, cannot be optimized, since there is no doubt about the powertrain to be employed: it was clear from every consumption test on the car, but also according to Meng and Currier ' *Due to the high efficiency of the electrical power train, the use of internal combustion engine has no positive impact on energy consumption* ' (2016).

4.6.2 Default Charge Sustaining targets

Another important sub-strategy is the one behind the *Charge Sustaining* targets, namely the minimum SOC that is authorized before the *Charge Sustaining* phase is triggered, and the maximum SOC above which charging is terminated.

The minimum SOC value of 20% was defined through a compromise similar to that of the SOC threshold for EMs deactivation: too low values led to harmful *Depth of Discharge*, but they allowed to employ the full energy storage potential from the battery. On the contrary, too high values did not allow for long charge depleting phases that are in general greatly beneficial for the vehicle energetic optimization. As a common approach with the other strategy rules, extensive testing was performed over different driving conditions, but in addition the final value had to be aligned with the other value

employed by R&D department researchers, in order to avoid incongruities when comparing the SOC profiles over driving cycles.

For what concerns the maximum SOC value, its tuning is heavily dependent on the driving mission. Sensitivity Analyses over WLTP and, less interestingly, US06 cycles put in evidence that the load shift phase (and so the maximum SOC) had to be low, to avoid the already mentioned waste of battery energy. On the other side, the combination with the EMs deactivation strategy made it logic to extend the SOC maximum target slightly over the SOC threshold, to maintain a small energetic margin for the electric powertrain in case the car needs to run in low-speed scenarios. In addition, a wide enough SOC range helps smoothing the fluctuation frequency between *charge sustaining* phases and *charge depleting* phases. Following up all these considerations, a value of 30% SOC was chosen.

4.6.3 Electric All-Wheel Drive

A rather interesting test was performed to investigate whether it was convenient or not to utilize the rear electric motor, much smaller and less powerful than the front unit, to propel the vehicle and not only as a generator in load shift or braking. The test was performed over the US06 cycle, comparing three different options:

- **Front EM only**
- **All-wheel drive at low speeds, front EM only at high speeds**
- **All wheel drive at all speeds**

In particular, the intermediate solution was realized by deactivating the rear EM via a *switch* block when the vehicle speed crossed the same threshold value adopted for the EMs deactivation strategy, namely *ICE_only_speed*.

The tuning results indicated that the last option, the electric AWD, proved to be the most efficient, as fig. 65 reports. The chart clearly shows how the average energetic consumption decreases as the two electric units are allowed to combine their torques throughout the entire driving cycle.

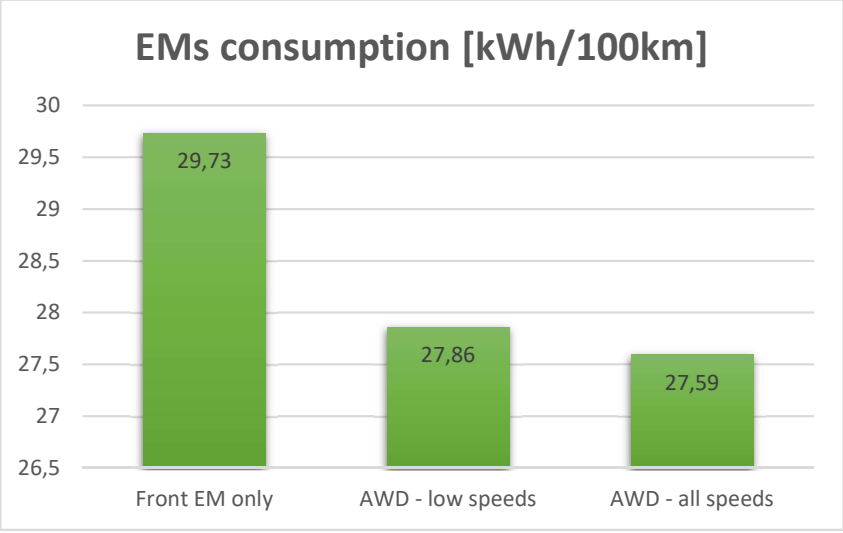

Fig. 65 Electric AWD investigation test results

It is important to notice that this particular test was conducted over the US06 cycle: it is a very demanding cycle, characterized by sudden acceleration and braking phases, and with an average speed higher than that of the WLTP. This cycle was chosen to highlight the differences between the two possible AWD solutions, that would have had much closer results over a slower speed profile, unavoidably.

4.6.4 Idling phases

This part of the strategy focuses on optimizing the powertrain behaviour when the car is idling in neutral gear, standing still. All the drive cycles tested during the project have frequent idling phases, so the problem had to be addressed.

In particular, the research focused on the choice of the idling speed of the ICE – P2.5 generator group: as it was briefly mentioned before, when the idle gear is engaged the rear EM is connected mechanically to the engine with the P2 layout. This means that the gearing mechanism is integrated to the gearbox and is not directly connected to the wheels. The same layout is also employed for the cranking phase, even though such phase was not relevant for energetic computations.

The speed choice was made on the basis of a dedicated series of *Sensitivity Analyses*, both on US06 and WLTP cycles. Again, the most reliable results came from the analyses done on the second speed profile, as idling phases lasted longer and were more frequent[4]. This speed parameter, as the model became better and better, was deeply revised.

At first, initial results indicated as the best idle speed the 2000 rpm region. However, the latest updates including new current maps, inverter efficiencies and mechanical efficiencies turned out to have a huge impact on this optimum value, as fig. 66 shows.

The simulation results showed an overall trend towards energy consumption decrease, as the engine speed was decreasing too. Therefore, the final value was set to the minimum engine rpm, that is 900 rpm.

[4] See Appendix for a comparison between the two speed profiles.

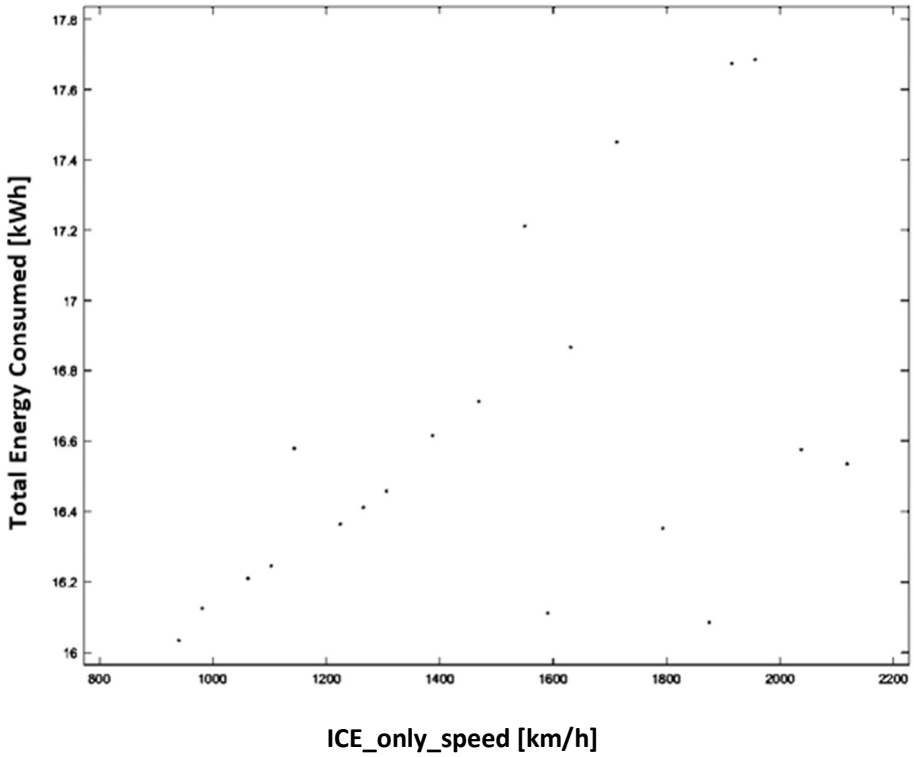

Fig. 66 Idle speed tuning tests

It is important to notice that in normal operating conditions, i.e. Hybrid Mode, the engine is always turned off when the idle gear is engaged, both in low-speed braking (apart from high speed decelerations in 6th, 7th and 8th gear) and in motionless phases. This was a straightforward approach to enhance fuel consumption when no torque was needed, and improve energy recuperation while regenerative braking by decoupling the negative torque actuated by the engine during decelerations (Tufano, De Bellis, & Malfi, 2018)

4.6.5 Fractioned load shift strategy

Load shift phases are necessary when external charging is not available and either:

- the battery SOC must be maintained above its minimum value
- the driver wants to maintain a certain amount of energy inside the battery
- the driver wants to charge the battery while driving

The dedicated strategy proposed during the project is aimed to reach the three possible targets, while keeping the fuel consumption as low as possible. This was done by designing a *SOC-based load shift* phase, that changes the charging pace depending on how close the target and current SOC are. The idea for this strategy came from to the one adopted by Kum et al. (2010) , where *' a new variable, Energy-to-Distance Ratio (EDR) is introduced to quantify the level of SOC with respect to the remaining distance '*. In that case, the researchers were focusing on the physical remaining distance along the test cycle; in this case instead, the concept of distance is specifically referring to the numerical

difference between the two SOC levels. The way this is conceived and implemented into the vehicle model is shown in figure 67.

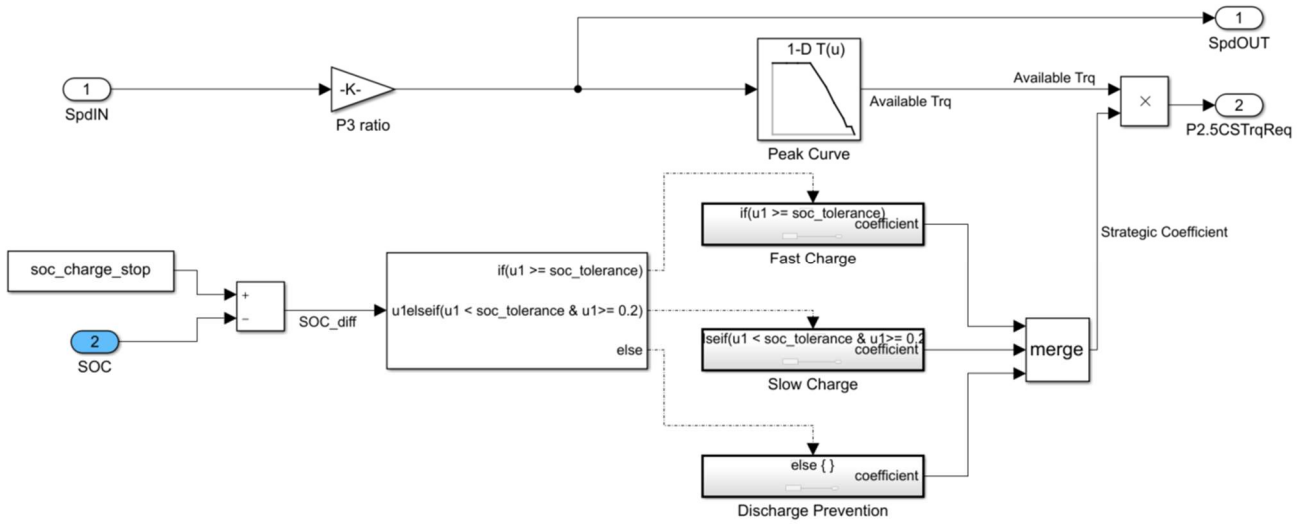

Fig. 67 Load shift strategy

The overall load shift torque that the rear EM demands to the thermal engine is the P2.5CSTrqReq output port at the top-right corner of fig. 67. Such torque is computed as:

*EM available torque * Strategic Coefficient = Load shift torque [Nm]*

The available torque is the maximum value the rear EM can output given the speed conditions: it is the direct output of its speed-torque map provided by the supplier.

The *Strategic Coefficient* instead varies with respect to how close to the SOC target the current one is: this is computed as the algebraic difference between the two values, and analysed (the *SOC_diff* signal at the input port of the *switch* block) to determine the charge intensity.

The charge intensity of the *load shift* phase is fractioned into three steps:

- **Fast charge**
- **Slow charge**
- **Discharge Prevention**

Fast charge: current SOC outside the tolerance

Fast charge phases are adopted when the difference between the two SOC levels is greater than the strategic parameter *soc_tolerance*. The charge rate is the maximum possible, in order to quickly approach the target and utilize the engine within its best efficiency areas: it was clear from the analyses of the engine maps that low-torque regions were not favourable in terms of fuel economy, and it was decided to make the most of its available torque while it was already running for propulsion duties. This approach was also consistent to the studies of Banwait et al. (2009), as well as to the results of Zhang et al. (2010).

High torques are demanded to the engine, and consequently high charging currents are reached: as it was previously mentioned in the *Thermal Powertrain* section, the role of the *Current Control* blocks became fundamental as the current limits applied to the rear had to be stretched out to manage such values and avoid limitations to the charging procedure.

Slow charge: current SOC inside the tolerance

The vehicle enters *slow charge* phases when the current SOC is no more far from the target, and it is inside the tolerance region. The gap to be closed is smaller (less than 0.5 difference between the two values) and the charging pace is therefore decreased. This intermediate phase was introduced with the additional target of having a smoother, more regular transition between the *fast charge* and the *discharge prevention* phases in terms of torque and SOC fluctuations.

Discharge Prevention: target SOC reached

This last mode is particular important, and deserved an extensive tuning session to be optimized. Since the SOC target is reached, the aim of this phase is not to increase further more the battery energy: this would lead to wasted energy, or even worse, to out-of-the-scope final SOC values that do not satisfy the driver requirements. Instead, this *discharge prevention* phase is aimed to maintain the SOC value despite the battery energy consumption caused by the auxiliaries: such consumption is constantly affecting the energy balance of the vehicle and can decrease the SOC level significantly even during the thermal-only propulsion phases.

An example of how this last phase works is shown in fig. 68.

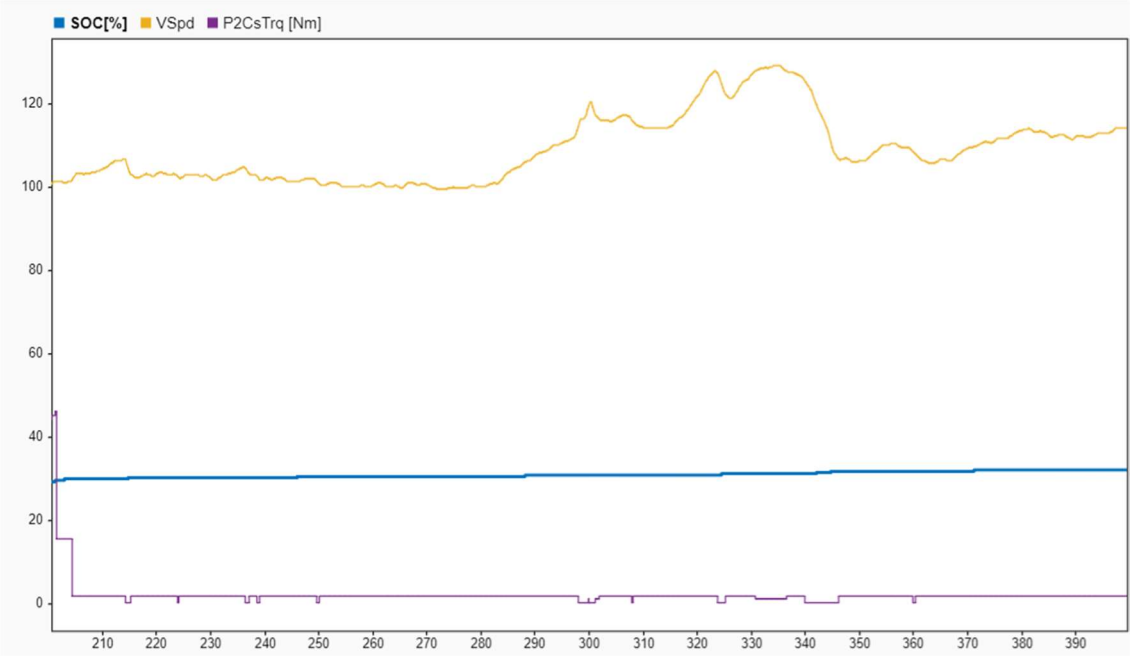

Fig. 68 Speed, SOC and P2.5 torque profiles during *discharge prevention* phase

The graph indicates the vehicle speed, the battery state of charge and the rear EM output torque. Such torque was tuned up to be the 3% of the maximum torque the P2.5 unit could produce, as it was the precise value that could maintain the SOC stable. Note that the EM applied torque on the engine is noticeably higher than the one visible on the graph: the purple value still has to be filtered by the

dedicated gearing mechanism that connects the rear EM to the ICE. This means that the total torque demand to the engine in *Discharge Prevention* phases can reach up to 20-30 Nm. Much higher torques are required for the *fast charge* and *slow charge* phases.

All the *Strategic Coefficients*, as well as the *soc_tolerance*, were tuned by dedicated analyses, that were repeated multiple times due to the technical updates of electric and mechanical components.

An interesting example of the impact of the discharge prevention mode over the consumption results is provided below:

Discharge Prevention	**[km/l]**	**[kWh/100km]**	**Fuel [kWh]**	**Electric [kWh]**	**tot [kWh]**
No	11.33	11.33	18.48	2.636	21.116
Yes	12.39	9.595	16.89	2.232	19.122

These results were measured over the WLTP cycle, with an initial SOC of 60%. Half of the strategy was not optimized or implemented yet, and many technical modifications had to be done still. Anyway, this was to put in evidence that a partial version of this fractioned load shift strategy proved to save up to 10% energy with respect to the normal one, just by employing more efficiently the same powertrain.

5. Results

This chapter reports the energy consumption results derived from the progressive model and strategy tuning.

The first three sections of the *results* chapter are organized on the basis of the *running phase* adopted. The r*unning phase* criterion distinguishes between three possible conditions the vehicle is running in:

- **Charge depleting (CD) tests**
- **Charge sustaining (CS) tests**
- **Homologation tests: charge depleting + charge sustaining**

Single charge depleting and *charge sustaining* tests were extensively performed on the shortest cycles only, namely US06 and WLTP. Such tests were conceived to monitor the impact of the sub strategies over specific driving conditions, something that could not be possible to determine with accuracy over the longer RDE missions. The charge sustaining results will also show more detailed information about the vehicle speed, SOC, and ICE status, so that an example of the car approach to those phases is provided.

Note that it would have been clearly impossible to force a depleting-only RDE cycle, due to its length way beyond the electric range of the car. The *homologation tests* were instead performed over the European cycles, which are the doubled WLTP cycle and the two RDE ones. This entire series of tests was run periodically to monitor the progresses of the strategy.

After going through the mentioned steps divided per testing conditions, the fourth and the fifth section of this chapter provide a comparison between energy consumption results respectively distinguishing between hybridization degree and powertrain configuration chosen. In particular, the fourth section divides by:

- **mild hybrid**
- **full hybrid**
- **plug-in hybrid**

hybridization degrees, while the fifth shows the results of the:

- **thermal-only**
- **parallel hybrid** (project car)
- **series hybrid**

powertrain architectures, measured over each driving cycle.

In particular, the thermal-only version was designed so that to employ exclusively the internal combustion engine as propulsion unit. The series hybrid architecture (whose consumption results will be shown too) comes from an inner development project of the Lamborghini R&D department.

Clearly, being the project car still in the development phase by many different departments, several minor technical updates occurred regularly, almost on a weekly basis, forcing the making of new tests and strategy adjustments.

5.1 Parallel Hybrid - Charge depleting tests

Charge depleting results are those collected to examine the behaviour of the vehicle when mostly driven by the electric powertrain. This means that all the tests put together in this section were obtained starting with 95% initial state of charge. Those cycles were particularly useful to evaluate the impact of the previously mentioned sub strategies regarding *EMs deactivation* and the choice of the electric all-wheel drive. The strategy impact over the results is the lowest, therefore also the numbers of tests was lower with respect to other typologies.

5.1.1 US06 results

The US06 cycle is the shortest among those utilized during the project. For this reason, it is also the only one that could be driven entirely in electric mode, without turning on the internal combustion engine. This means that the minor changes during development visible in fig. 69 were entirely due to technical updates to vehicle components. The only relevant result that was achieved, more due to the way the virtual model was designed, consisted in avoiding the ICE to enter during the few strong accelerations that are implemented in this cycle. The earlier versions of the *Torque Command* subsystem had the minor drawback of making the ICE excessively reactive to the accelerator pedal request: this caused the overall energy consumption to be dramatically worsened, as the ICE was turned on and contributed to the propulsion even though the EMSs available torque was more adequate to fulfil the driver requests. The higher energy consumption results of the latest version are due to the ICE contribution absence in the latest stages of the development.

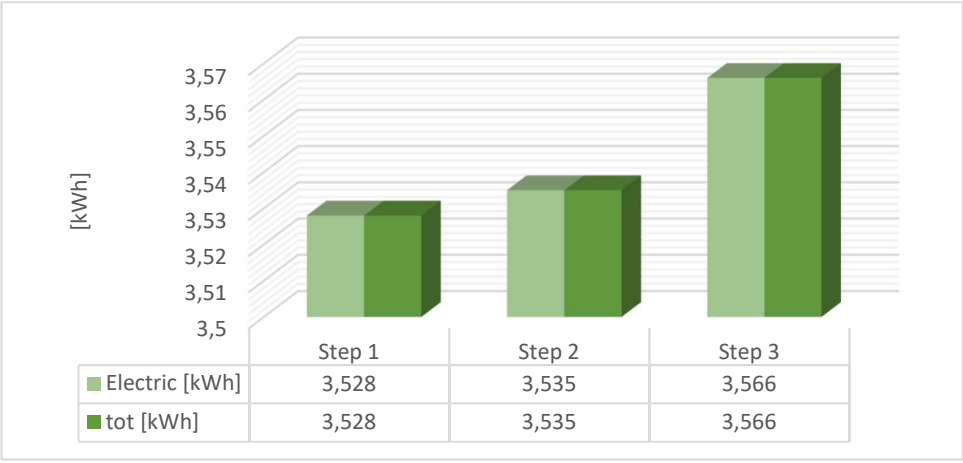

Fig. 69 Energy consumption trends over US06 CD phases

5.1.2 WLTP results

The WLTP cycle, differently from the US06 one, requires the thermal powertrain to support the electric one. Still, for the greatest part of the mission the vehicle is driven in electric-only mode, so again variations between the model evolution steps in fig. 70 are not as relevant as they will be for the case of longer cycles that will be reported in the following sections.

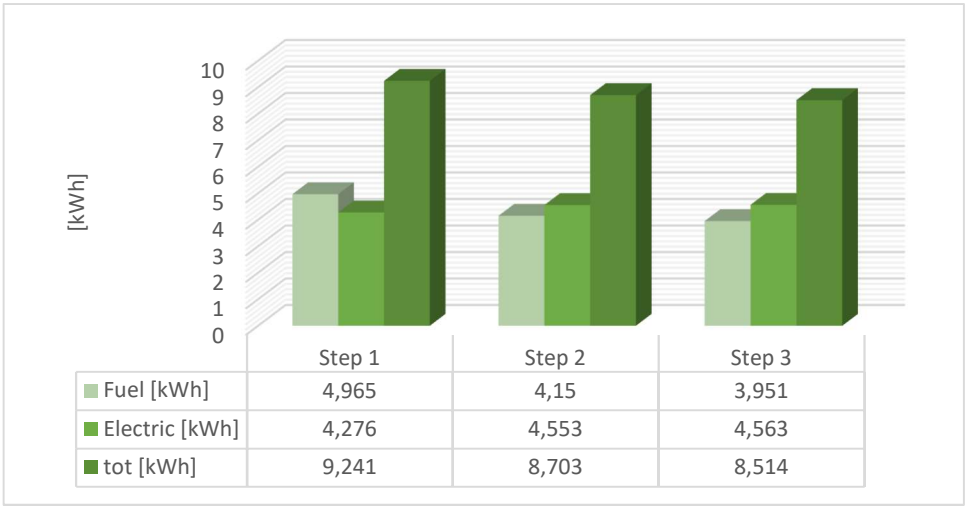

	Step 1	Step 2	Step 3
Fuel [kWh]	4,965	4,15	3,951
Electric [kWh]	4,276	4,553	4,563
tot [kWh]	9,241	8,703	8,514

Fig. 70 Energy consumption trends over WLTP CD phases

The strategy improvements helped in exploiting more the electric powertrain and in reducing the ICE usage: therefore an improvement of 7.67% of the overall energy consumption was achieved.

5.2 Parallel Hybrid - Charge sustaining tests

These tests were performed by adopting the following initial conditions:

- Initial SOC: 50%
- Minimum SOC target[5]: 48%
- Maximum SOC target: 50%

Such parameters where chosen to mainly monitor the progresses of the load shift strategy, both in idle and in running mode, without the influence of the charge depleting phases nor the EMs deactivation strategy, that is applied at lower SOC values.

Differently from the case of the charge depleting tests, the charge sustaining phase is heavily influenced by how the powertrain management strategy works. This implies that while only slight improvements were noticed over the depleting phases, the following results show a far more noticeable positive trend in efficiency. Differently to what happened for the depleting phases analysis, the charge sustaining cases will also include an overview of the vehicle status data over the each cycle, so that to better understand how the strategy combines the electric and the thermal powertrains.

5.2.1 US06 results

The positive impact of strategy tuning is clearly visible in the decreasing trend shown in fig. 71, that reports the energy consumption of the car along the US06 cycle.

It is particularly important to note how increased the contribution of the electric powertrain was, when compared to the initial phases that had the ICE running almost continuously.

The earlier results in fig. 71 were gathered after a noticeable hardware update that involved most of the components of the vehicle. A major step down in energy consumption was achieved with the secondo version, which introduced the *discharge prevention* mode, as well as an improved EMs deactivation implementation. May results were realized thanks to the progressive load shift strategy, and a dedicated current control system to manage the charge/discharge rates of the two EMs. The last version, indicated in fig. 71 as the June one, shows the impact of the new gearshift control algorithm as well as the introduction of new mechanical efficiencies.

The efficiency improvements led to 24.1% decrease in overall consumption.

[5] SOC targets are those that trigger the charge sustaining mode: when the SOC becomes higher than the maximum target required, the vehicle enters *hybrid mode* that authorizes the *charge depleting* phase temporarily.

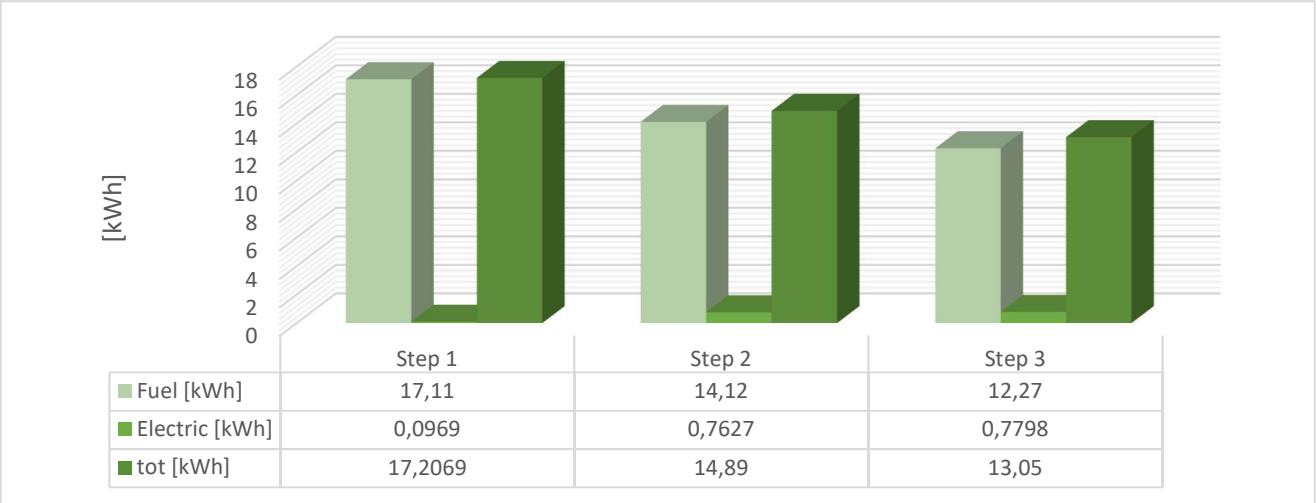

	Step 1	Step 2	Step 3
Fuel [kWh]	17,11	14,12	12,27
Electric [kWh]	0,0969	0,7627	0,7798
tot [kWh]	17,2069	14,89	13,05

Fig. 71 Energy consumption trends over US06 CS phases

The savings in ICE usage are visible in fig. 72, which shows the vehicle status information collected during the US06 cycle.

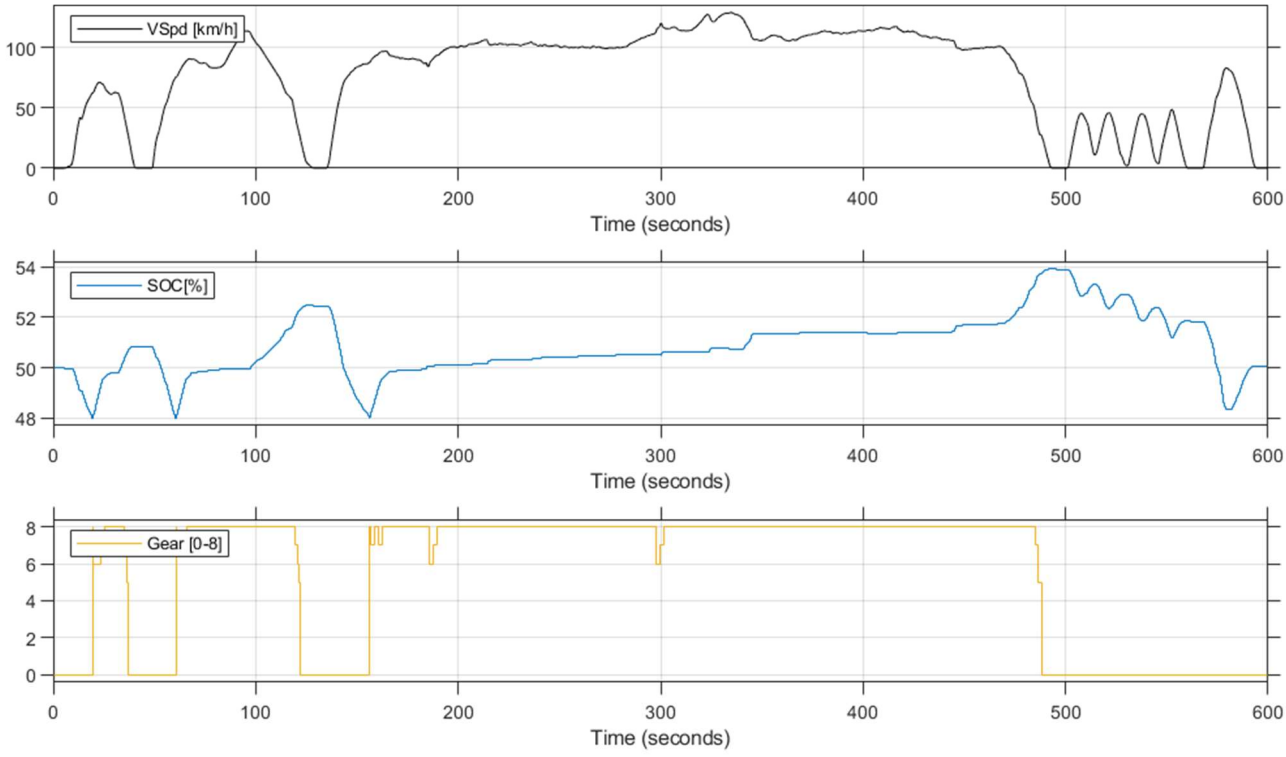

Fig. 72 Vehicle status information over latest US06 CS phase

The top-end graph represents the vehicle actual speed during the US06 test, measured in km/h. The chart below indicates how the battery State-of-Charge varied during the test, while the yellow and orange signals in the charts below show the engaged gear and the engine speed respectively.

When looking to the 0-130 seconds range in all graphs, it is visible how the electric powertrain is authorized to drive the car, once the regenerative braking and the load shift charging achieve a SOC level above the desired target. In that situation, the engaged gear and the ICE speed often remain null, which means that the thermal powertrain is turned off and is disconnected from the wheels. Instead, the ICE is asked to drive the car in the intermediate part of the driving mission, where the average speed is high and brakes are not employed. This phase is also exploited to slightly increment the battery SOC by increasing the torque demand to the ICE via load shift: the energy cumulated in the battery is stored and immediately employed in the last part of the cycle, which is much more suitable to the electric powertrain for its lower average speed and the frequent decelerations. This last depleting part allows to exploit all the remaining battery energy that would be “wasted” and conclude the cycle with an SOC matching the target with accuracy.

5.2.2 WLTP results

The benefits of the new strategy were numerically much more evident in the case of the WLTP driving cycle, shown in fig. 73. The lower average speed favours the electric powertrain, which can operate only at the lower speeds and better contribute to the propulsion mission, substituting the ICE more frequently than for the case of the US06.

Considering the WLTP charge sustaining phases, the car kWh consumption improved by more than 39% between Step 1 and 3 variants, as the strategy was progressively optimized and the model updated. The technical reasons behind this progress were already reported for the US06 test case.

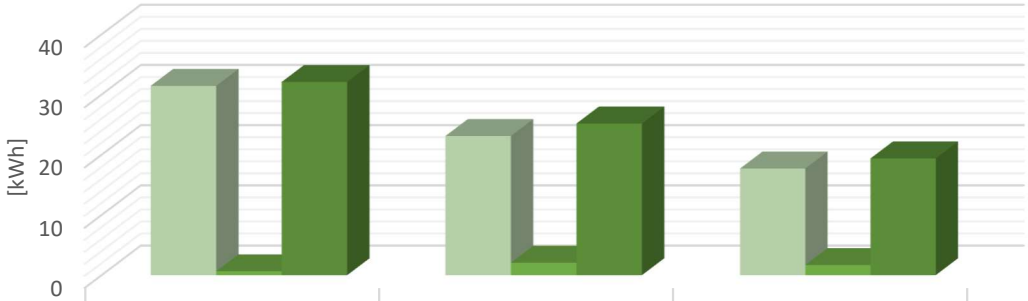

	Step 1	Step 2	Step 3
Fuel [kWh]	31,45	23,12	17,71
Electric [kWh]	0,6507	2,07	1,675
tot [kWh]	32,1007	25,19	19,39

Fig. 73 Energy consumption trends over WLTP CS phases

Fig. 74 provides with the vehicle status information collected during the WLTP charge sustaining phase. Such signals, whose values are updated to the latest June version, are much more irregular than those in the US06 cycle for two reasons.

First reason, the vehicle velocity requirements are more gentle, i.e. the average speed and acceleration requests are lower: thus, the electric motors are able to work for longer time periods.

Second reason, the speed profile is more irregular, and more realistic too: gearshifts are more frequent, and consequently, the engine speed profile is smoother too.

This suitable conditions pay well when entering charge sustaining phases: the electric motors can contribute substantially to the torque demand over the time period.

Earlier strategies that were tried and discarded adopted different SOC targets or charge rates, in an attempt to differently exploit the thermal-only phases. The best combination found is the one represented in fig. 74.

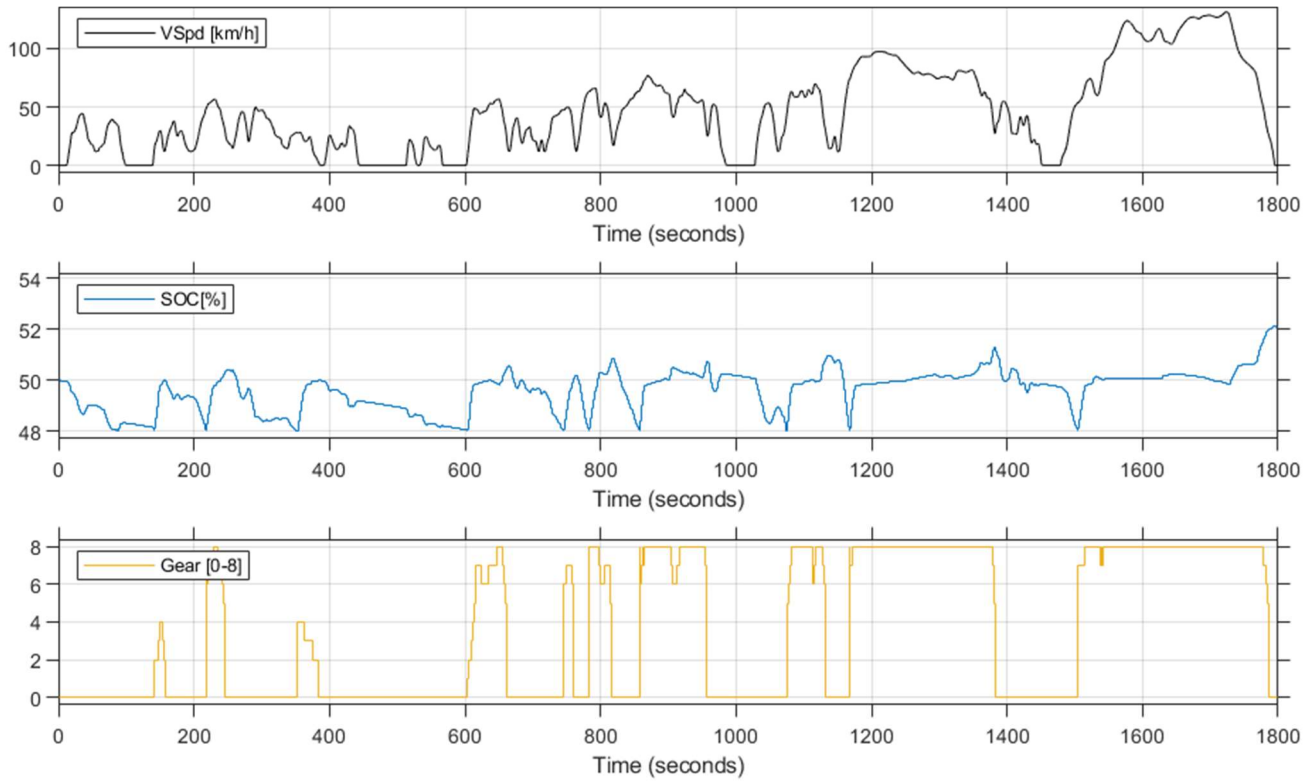

Fig. 74 Vehicle status information over latest WLTP CS phase

5.3 Parallel Hybrid - Homologation tests: charge depleting and sustaining combined

The last section of this chapter reports the most important results collected, that are those which summarize the impact of the strategy over the longest driving cycles. Thanks to the wide range of speeds and SOC levels, it is possible to put in evidence the overall impact of all the strategies mentioned before, which are all determinant in progressively lowering down the kWh count. The reference homologation tests used were the WLTP Class 03, repeated twice; the Real Driving Emission cycle measured in an Italian downtown and surroundings (later recalled as RDE B); the Real Driving Emission cycle recorded in a German city and its countryside (RDE A). Due to the presence of a long initial charge depleting phase, as expected the improvements are not as significant as in the case of charge sustaining tests only.

5.2.3 WLTP homologation test

The European homologation test was simulated extensively, as reported in fig. 75. It was the main reference for the evaluation of the strategy impact over energetic consumption.

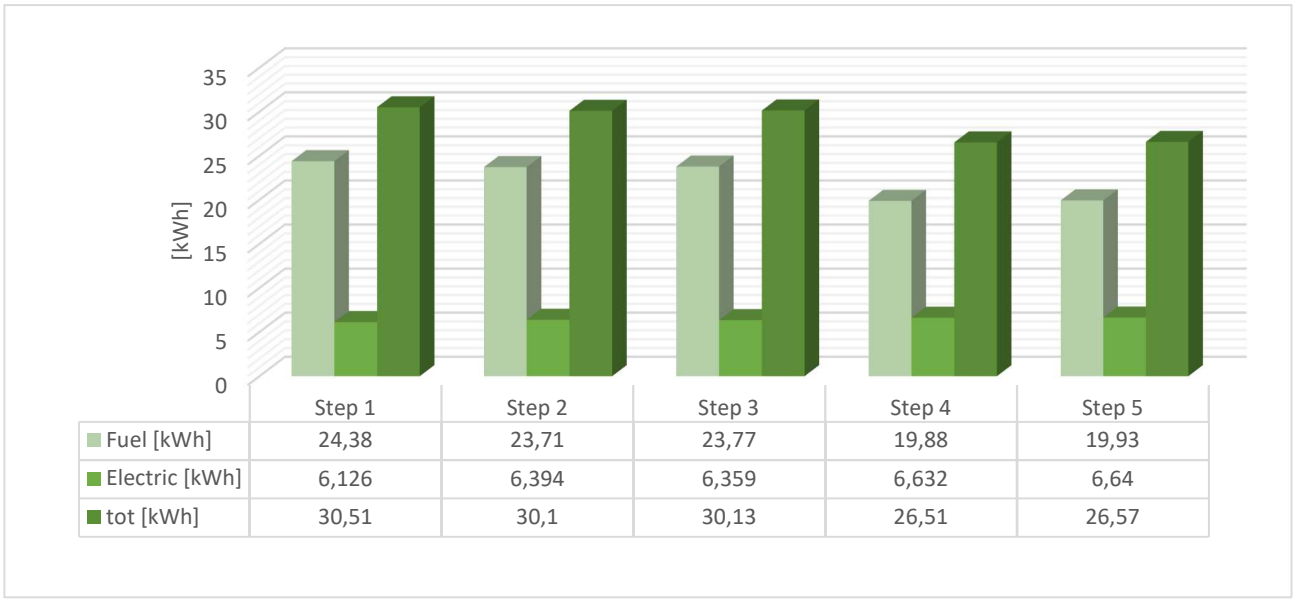

	Step 1	Step 2	Step 3	Step 4	Step 5
Fuel [kWh]	24,38	23,71	23,77	19,88	19,93
Electric [kWh]	6,126	6,394	6,359	6,632	6,64
tot [kWh]	30,51	30,1	30,13	26,51	26,57

Fig. 75 Energy consumption trends over WLTP homologation test

The tendency, yet again, was to employ the electric motors at lower speeds by extensively exploiting the *EMs deactivation strategy*, and charging the battery at high speeds via *load shift*. Such strategies were fundamental to operate both the electric powertrain and the thermal one at their best working points, that are respectively partial load, low-to-medium speeds for the former, and high loads, high

speeds for the latter[6]. The strategy improvements led to a 12.91% of further decrease in energy consumption compared to the initial versions results visible in fig. 75.

5.2.4 RDE A homologation test

The RDE A drive cycle is the longest among those utilized during the project. The initial urban part is mostly covered by the electric powertrain the electric powertrain, while the high speed sub-urban and highway velocity profiles, that can quickly discharge the battery, are managed by an alternating combination of the two.

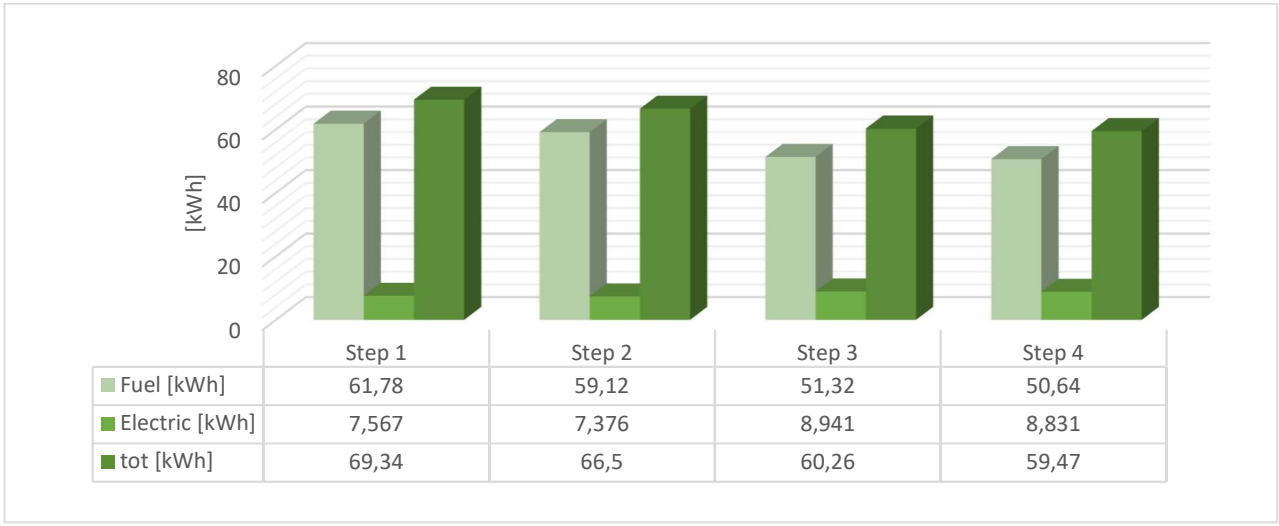

	Step 1	Step 2	Step 3	Step 4
Fuel [kWh]	61,78	59,12	51,32	50,64
Electric [kWh]	7,567	7,376	8,941	8,831
tot [kWh]	69,34	66,5	60,26	59,47

Fig. 76 Energy consumption trends over RDE A homologation test

As fig. 76 shows, A results were improved by 14.2% between April and May. The shift from thermal to electric powertrain is rather noticeable when looking at the partial kWh consumption progresses over the weeks.

5.2.5 RDE B homologation test

The RDE B driving cycle is more energy-demanding than the A one. Again, the initial urban phase is mostly covered by charge depleting, while the second half of the cycle employs the parallel combination of the two powertrains, with a remarkable preference towards the thermal unit. Unfortunately, the driving cycle suddenly ends at high speed, without an intermediate lower-speed phase before stopping, or even a progressive braking. Such phase is generally covered by turning off

[6] Engine and motors maps could not be shown

the engine, and thus improving the energy consumption: on the contrary, this cycle forces to “waste” a non-negligible part of the energy cumulated in the battery, and terminate the cycle with a SOC slightly higher than the ideal one.

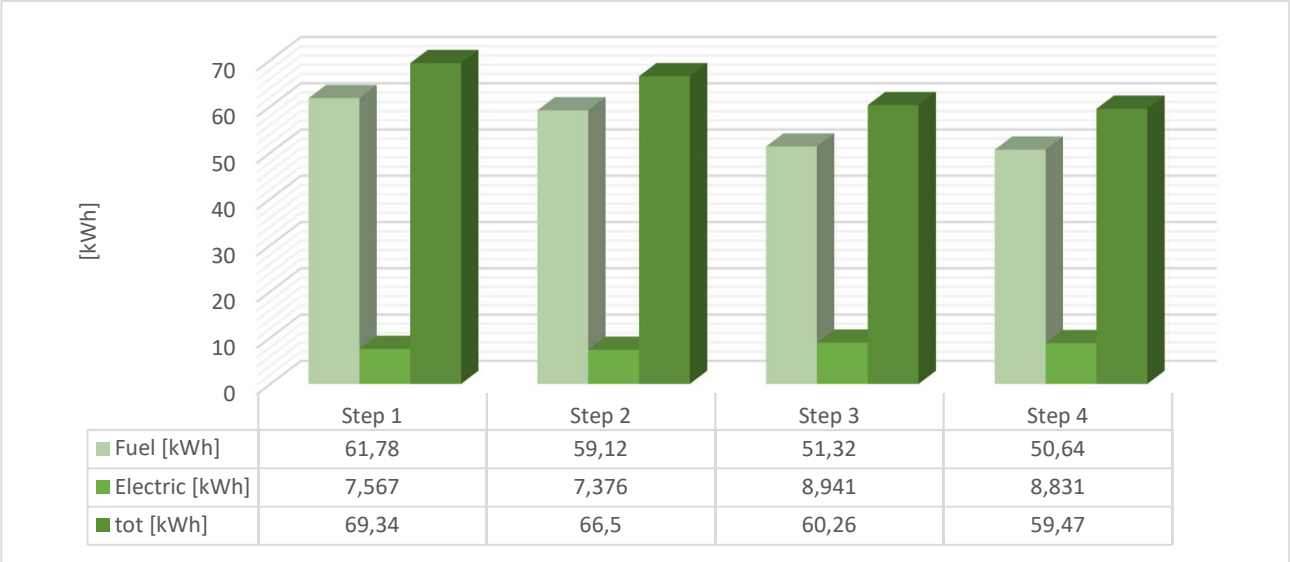

	Step 1	Step 2	Step 3	Step 4
Fuel [kWh]	61,78	59,12	51,32	50,64
Electric [kWh]	7,567	7,376	8,941	8,831
tot [kWh]	69,34	66,5	60,26	59,47

Fig. 77 Energy consumption trends over RDE A homologation test

Fig. 77 reports the progresses of the energetic consumption due to the improvements in the strategic powertrain management. The overall kWh count decreased by 9.56% over the earlier versions.

5.4 Hybridization degrees comparison

This section compares the consumption performances of the project car depending on the hybridization level implemented.

It is focused on comparing the energetic impact of having:

- **mild hybrid**
- **full hybrid**
- **plug-in hybrid**

powertrains over the WLTP Class 03 and US06 driving cycles. In addition, the WLTP case will show how torque outputs are managed over the same cycle as the powertrain phase changes.

The *mild hybrid* simulation was performed adopting an equivalent thermal powertrain[7] used on the project car, without the EMs propulsion assistance. The model works as a *Mild Hybrid* vehicle, which recuperates the energy wasted during braking phases to power the auxiliaries and the cranking phases. On the contrary, the *Full Hybrid* variant is the same model developed during the project, but without externally supplied energy from the grid in terms of SOC level. The model is forced to maintain the SOC level, as It is not allowed to discharge the battery beyond the 2% tolerance range of the initial SOC, so that to preserve the battery energy throughout the mission. The *plug-in hybrid* variant instead is authorized to deeply discharge the battery from all the energy cumulated when plugged to the grid: it starts from 95% SOC and it automatically chooses whether to employ the thermal or the electric units depending on the strategy rules.

5.4.1 WLTP results

It is interesting to put side by side the energy utilization along the same reference driving cycles: this allows to see how important it was to satisfy the torque request (that is shared by all three cases) with the most efficient actuator available at those conditions. This particular part of the project highlights how crucial it is to employ the energy stored in the battery from grid recharging, but also from regenerative braking, in propulsion mode.

The first test was based on the WLTP Class 3 cycle, single-run[8]. The results, reported in fig. 78, show a significant difference between the plug-in and the mild-hybrid, which respectively run in thermal only and charge depleting phases: this has to be mostly attributed to the long electric-only phase that allows the engine to remain turned off for most of the time.

[7] The vehicle mass was not changed, as no data were available to estimate with accuracy the weight difference when substituting the full hybrid with a mild-hybrid architecture. This means that the mentioned Mild-Hybrid version might have slightly higher consumption data when compared to a on-road, realistic model with defined technical characteristics.
[8] The homologation cycle based on WLTP Class 03 is composed by two cycles in sequence

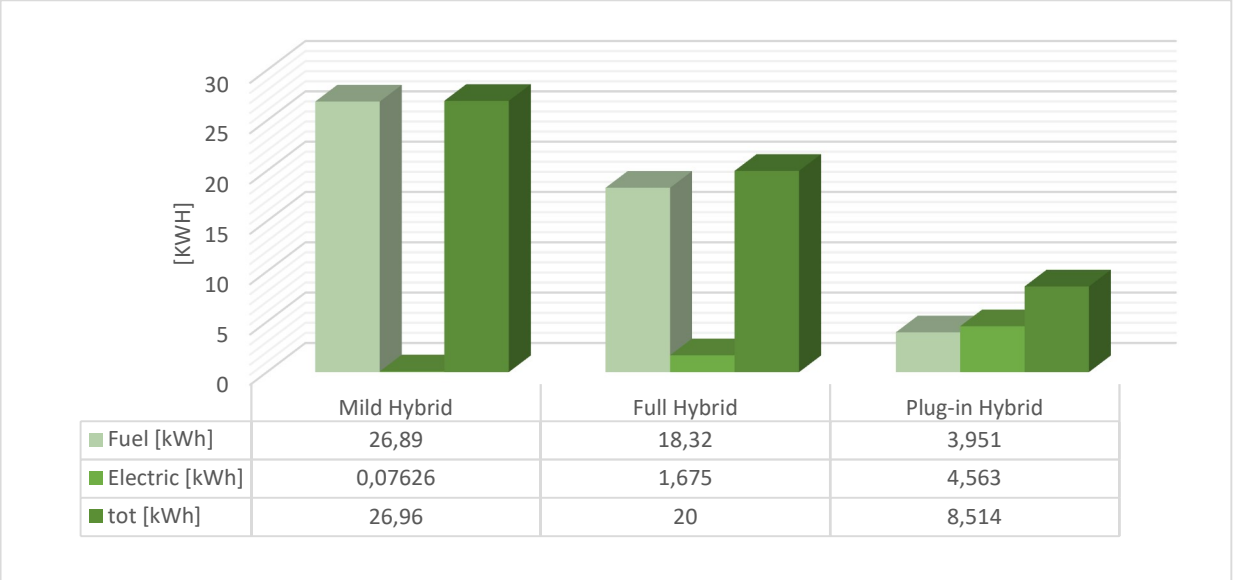

	Mild Hybrid	Full Hybrid	Plug-in Hybrid
Fuel [kWh]	26,89	18,32	3,951
Electric [kWh]	0,07626	1,675	4,563
tot [kWh]	26,96	20	8,514

Fig. 78 Consumption trends of the different hybridization degrees over WLTP cycle

The correlation between the electric powertrain intervention and the total amount of kWh consumed is rather clear. In particular, figure 79, 80 and 81 allow to compare how the different torque requests are satisfied depending on the actuator chosen by the strategy. Note that, for sake of confidentiality, it was not possible to show the exact torque values: the signal curves are reported through normalization of the y-axis values.

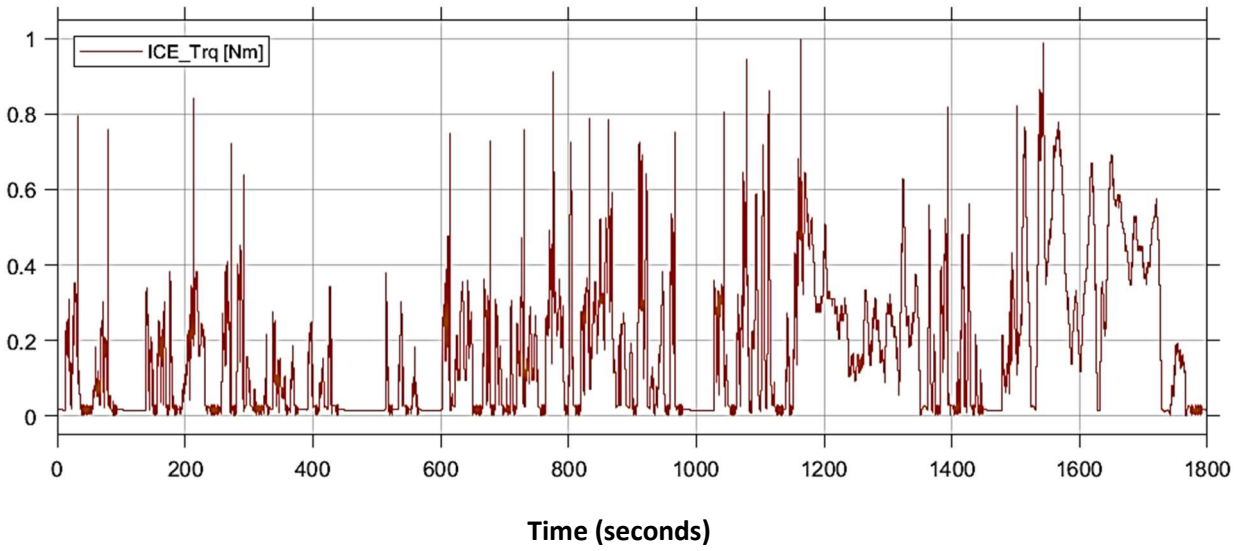

Fig. 79 Torque outputs over WLTP cycle for the mild hybrid variant

The chart in figure 79 represents the case where only the internal combustion engine is advocated, with a gear always engaged. This happens because the electric propulsion for such particular case is not allowed to manage propulsion tasks, so that the battery energy is not utilized. This is done by setting the electric motors to zero-torque output in propulsion (a low drain current is still present).

The engine is always on, and thus the energy consumption values are the highest possible, as reported previously in fig. 78.

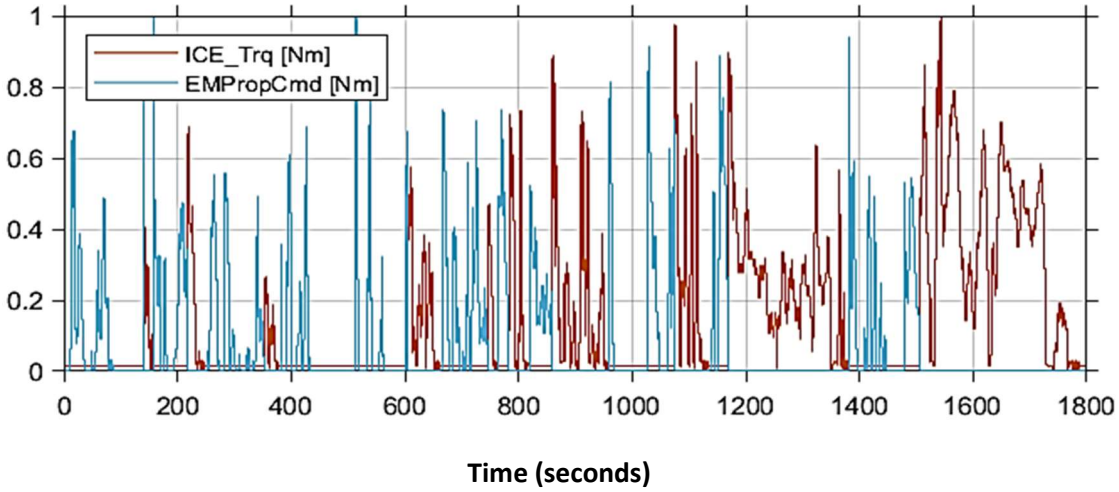

Fig. 80 Torque outputs over WLTP cycle for the full hybrid variant

Fig. 80 instead represents both the internal combustion engine and the electric motors torques. It is interesting to notice how the two powertrains are alternated, depending on the strategy decisions based on SOC values and all the other parameters examined in precedence. When the ICE is turned on, it both propels the vehicle and provides a rapid charge for the battery, that happens thanks to the rear EM used as a generator. When the SOC level is above the *charge sustaining* target and the power request is low enough, the ICE is turned off and a limited *charge depleting* phase is actuated. In addition, the battery energy can benefit from regenerative braking, that can significantly improve the energy consumption in an irregular cycle such as the WLTP Class 03, that shows recurrent braking phases. A slight ICE torque can be applied during idle phases, in order to keep the SOC value close to the level chosen at the beginning of the driving cycle.

The chart in fig. 81 shows the reason why the energy consumption results of the plug-in hybrid model differ that much with respect to the mild hybrid one. The energy stored in a fully charged battery allows the car to drive in pure electric mode for more than 91% of the cycle. The remaining part, as it was briefly clarified before, could have been covered with the electric storage energy still. However, the strategic approach that was designed and trained over all the various cycles cited forces the EMs deactivation and makes the ICE enter only during the very last part of the cycle, when the vehicle velocity is beyond the EMs deactivation threshold, and the SOC value is low enough to allow such decoupling. This is done to save the remaining battery energy for low speed duties that are likely to occur at the end of a high speed route.

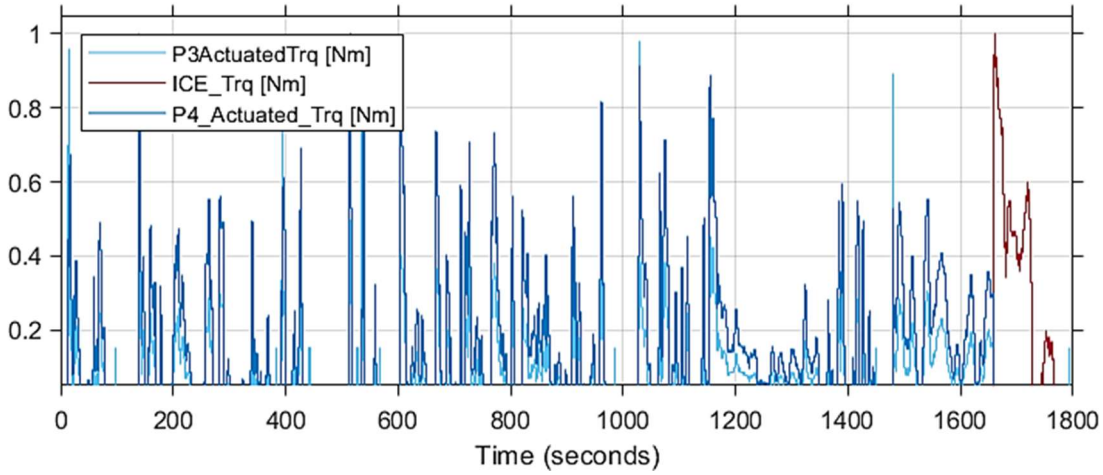

Fig. 81 Torque outputs over WLTP cycle for the plug-in hybrid variant

5.4.2 US06 results

The second test was performed over the US06 cycle, which challenges the car in a rather different way with respect to the WLTP Class 03. The average torque and speed requests are higher and therefore the energy consumption varies. Figure 82 reports the results obtained, which show the strong advantage of the PHEV especially when the driving mission is reduced in length. In that case, the mild hybrid reaches an interesting value, if compared to the full hybrid version. Still, it is worth noting that the mild hybrid version has an unrealistic regenerative braking capability for such hybridization level. This also determines a negative net energy balance over the US06 cycle, as the braking phases are able to recuperate more energy than the amount spent by the auxiliaries.

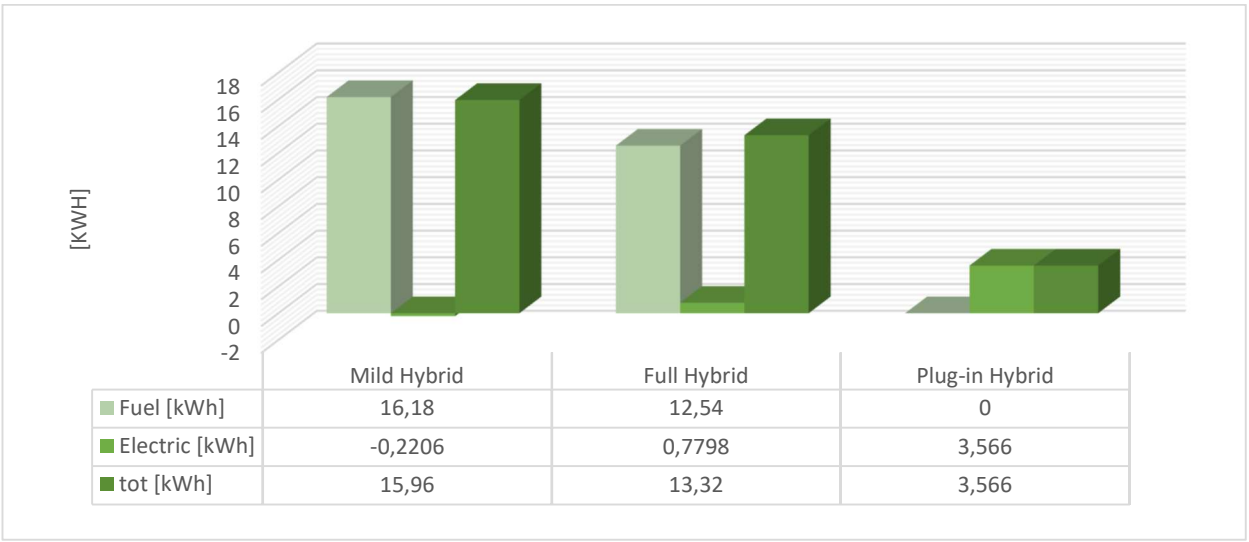

	Mild Hybrid	Full Hybrid	Plug-in Hybrid
Fuel [kWh]	16,18	12,54	0
Electric [kWh]	-0,2206	0,7798	3,566
tot [kWh]	15,96	13,32	3,566

Fig. 82 Consumption trends of the different hybridization degrees over US06 cycle

The mild hybrid results are not that far away from those of the full hybrid. When comparing the two charts in fig. 83 and 84, which indicate respectively the engine torque and, alternatively the engine

and motors torques, it is clear that most of the cycle is still driven by the thermal powertrain, and regenerative braking phases are less frequent than in the case of the WLTP cycle. This is why the results are rather similar.

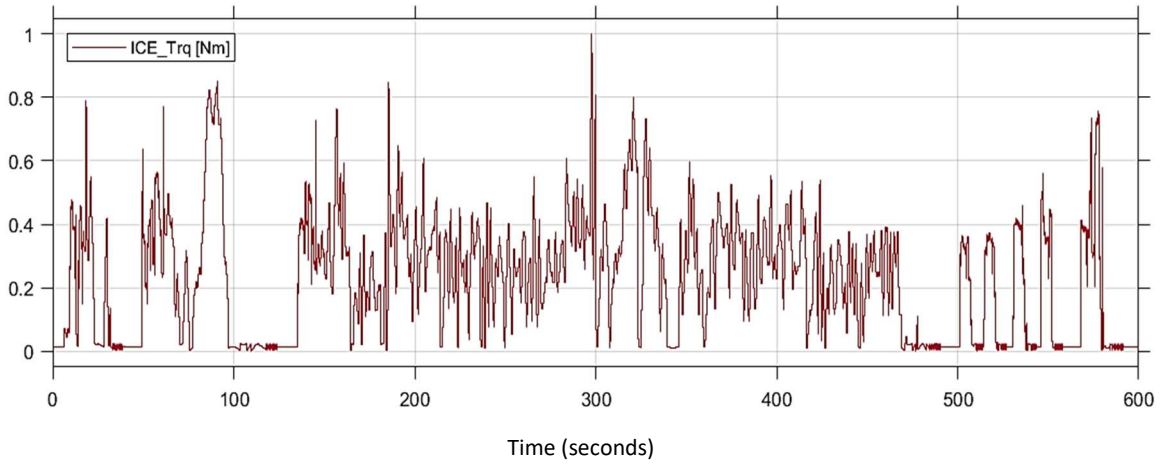

Fig. 83 Torque outputs over US06 cycle for the mild hybrid variant

The electric powertrain is able to drive the car in zero emission mode in the entire suburban part that concludes the cycle: the gradual braking phases that are one after the other performed allow to maintain an SOC level high enough to avoid another *charge sustaining* phase with the ICE on.

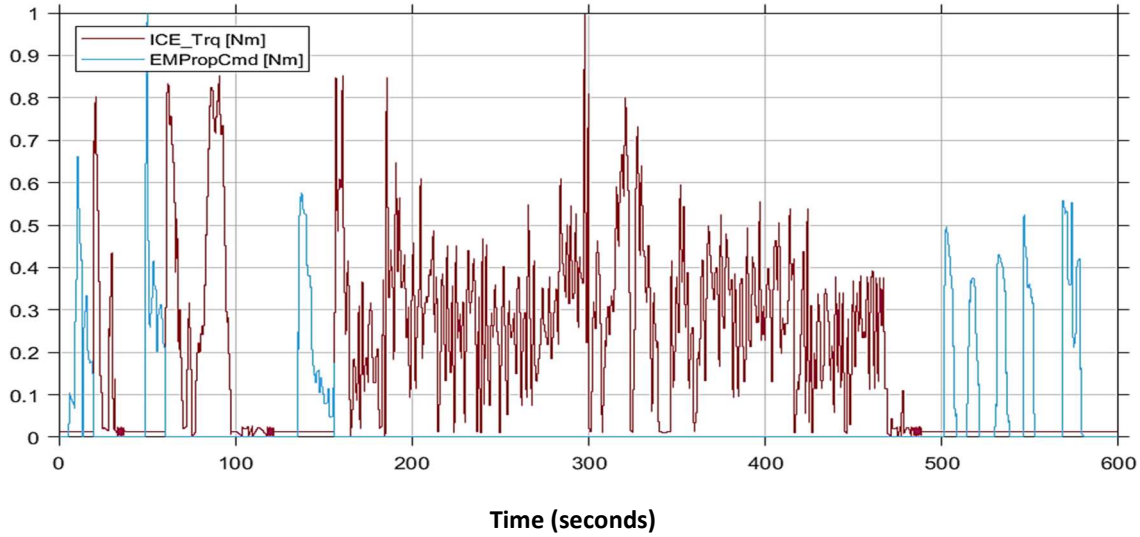

Fig. 84 Torque outputs over US06 cycle for the full hybrid variant

On the contrary, once that the vehicle becomes a PHEV, i.e. it is authorized to discharge the battery employing the grid energy, the short US06 cycle can be completed in electric only mode, and no fuel is burned by the internal combustion engine. The strategy was trained to allow this energy usage, as it is always better to discharge the battery first, and then utilize the lowest amount of fuel possible to maintain the SOC level. Fig. 85 shows how the front and rear EMs work together to propel the car entirely in electric mode. As it was stated again, the charts are normalized for confidentiality reasons, so values are not directly comparable between different curves.

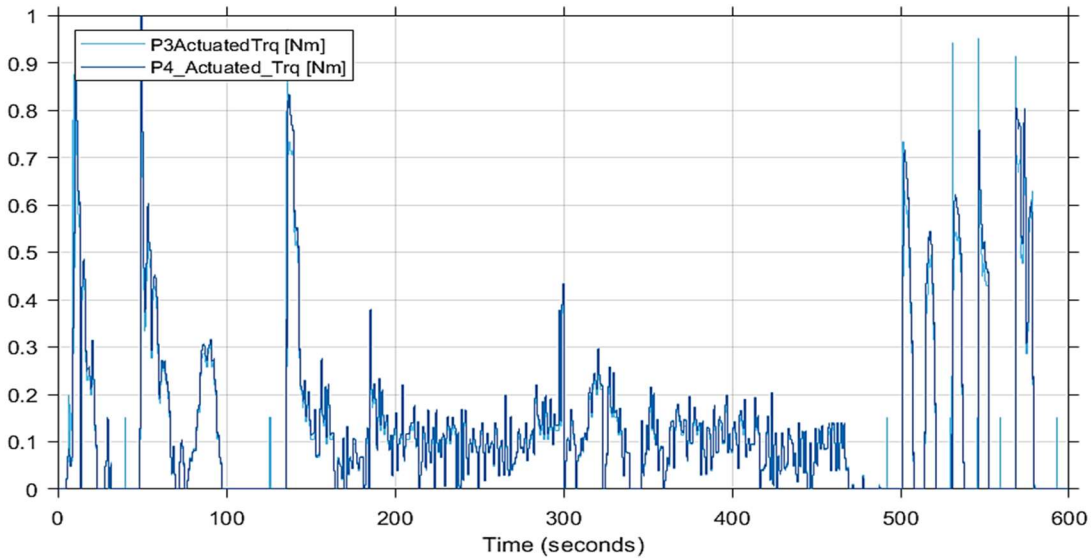

Fig. 85 Torque outputs over US06 cycle for the plug-in hybrid variant

5.5 Powertrain configurations comparison

This section shows how consumption performances of the project car varied depending on the architecture implemented. They were respectively:

- **mild hybrid**
- **series hybrid**
- **parallel hybrid**

While the first and the third architecture were designed and implemented together during the project, the series model was already implemented and optimized in its strategy for company internal investigations. Such virtual model utilizes the same engine, battery and motors but was designed in a rather different way, and employs a different energy management system (for example, only the front EM is used in propulsion). Therefore, comparison results can be considered correct, but not perfectly accurate, as modelling difference may have slightly influenced those values. The mild hybrid model is the same that was previously described and compared when investigating the influence of the hybridization degrees; similarly, the parallel hybrid version is the one that employs the grid energy and starts from 95% battery SOC: it employs the optimization strategy and can alternate *charge depleting* and *sustaining* phases depending on the mission requirements, as it was seen previously in the dedicated chapters. The mild hybrid will serve as a reference to compare the strategy of the series and the parallel hybrid architectures.

The three options were tested over three different European homologation cycles, namely WLTP Class 03, RDE A and RDE B. In all cases, the battery was always fully charged at the mission start, apart from the mild hybrid tests. Note that due to the different architectures employed, a direct comparison that included also the electric powertrain consumption was not possible. Therefore, the energy consumption will be based on the fuel consumed[9].

5.5.1 WLTP results

The WLTP comparison consisted in performing two WLTP Class 03 runs, so that to entirely discharge the battery and also perform a charge sustaining phase. It is very important to notice a first difference between the series and the parallel hybrid: while the former is tuned so that to completely discharge the battery first, and then to maintain the SOC value, the latter does not allow the complete discharge due to its discharge prevention mode that disconnects the EMs once the SOC is below a threshold. This implies that the first round, as it was already shown by charge depleting tests, was not entirely covered in electric mode. Both series and parallel hybrid mix the two powertrains during the second round.

[9] As stated before, both series and parallel model employed the same components and started with the same amount of energy stored into the battery

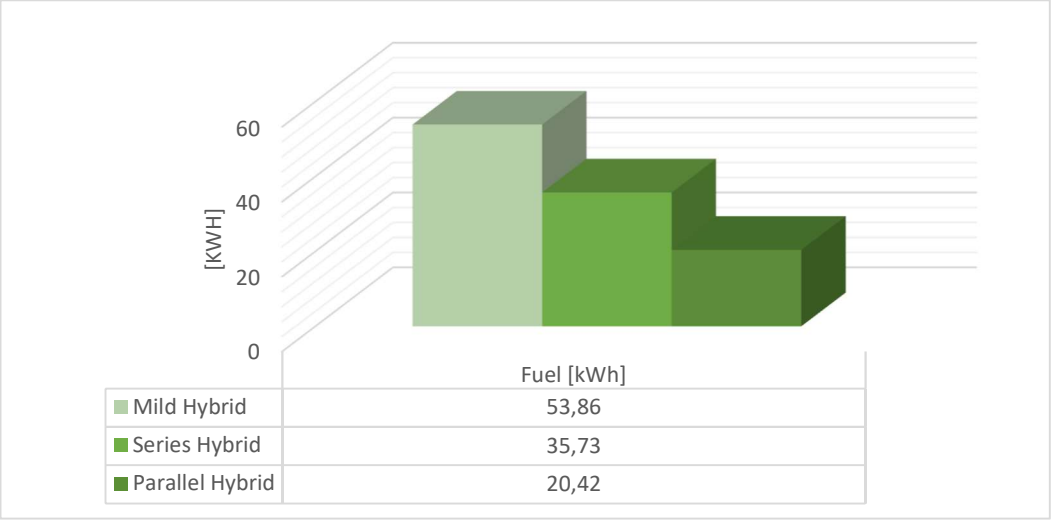

Fig. 86 Powertrain configurations comparison over WLTP cycle

The results of the three configurations are reported in fig. 86: due to the inferior length of the WLTP cycle and the relatively moderate average torque request, the series and the parallel hybrid can greatly benefit from the grid energy supply and exploit it in a long *charge depleting* phase that lowers down the overall kWh count. Still, despite the common depleting phase, the benefits of using the different efficiency areas and employ the ICE mainly for propulsion goes in favour of the parallel hybrid. Such architecture, with the final optimized rule-based strategy, reduces the energetic consumption by 62.1% when compared to the mild hybrid version, while the series hybrid one only cuts by 33.6% the fuel usage. When comparing the two full hybrids, an overall fuel consumption advantage of 42.8% goes in favour of the parallel one.

5.5.2 RDE A results

The second sequence of tests was performed over the RDE A speed profile. This cycle, whose profile is reported in the *Appendix*, is more energy demanding than WLTP: this strongly impacts over the series hybrid efficiency, as the motors are forced to work in a working region with strong discharge currents and high speeds. This worsened efficiency will be even more evident when considering the RDE B cycle.

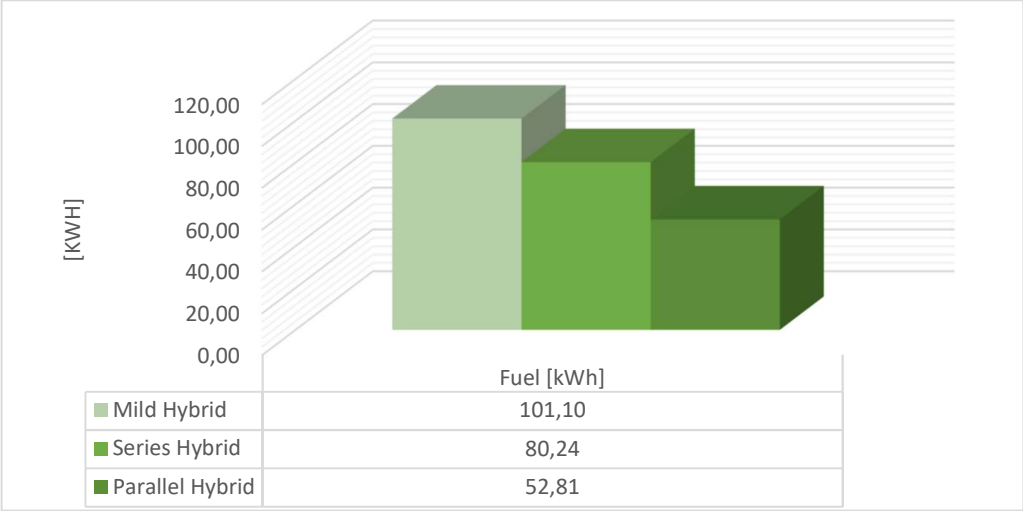

Fig. 87 Powertrain configurations comparison over RDE A cycle

It is clear from the results in fig. 87 that again, the two PHEV models can initially benefit from the grid energy to reduce the usage of fuel. The first part of the cycle could be covered by both in depleting phase; however, as the speed increased, the parallel model started alternating the two powertrains, while the series hybrid kept discharging the battery without taking into account speed or SOC levels. The numerical results of adopting this adaptive strategy are the following: while the series hybrid saves 20.6% fuel with respect to the mild one, the parallel strategy achieves a 47.8% reduction. This means that the parallel hybrid uses 34.2% less fuel than the series one.

5.5.3 RDE B results

The final comparison was performed over the RDE cycle registered in an Italian city and countryside, a rather demanding cycle in terms of average torque and speed requests, as it was already mentioned previously. Fig. 88 shows how the fuel consumption varies depending on the architecture chosen.

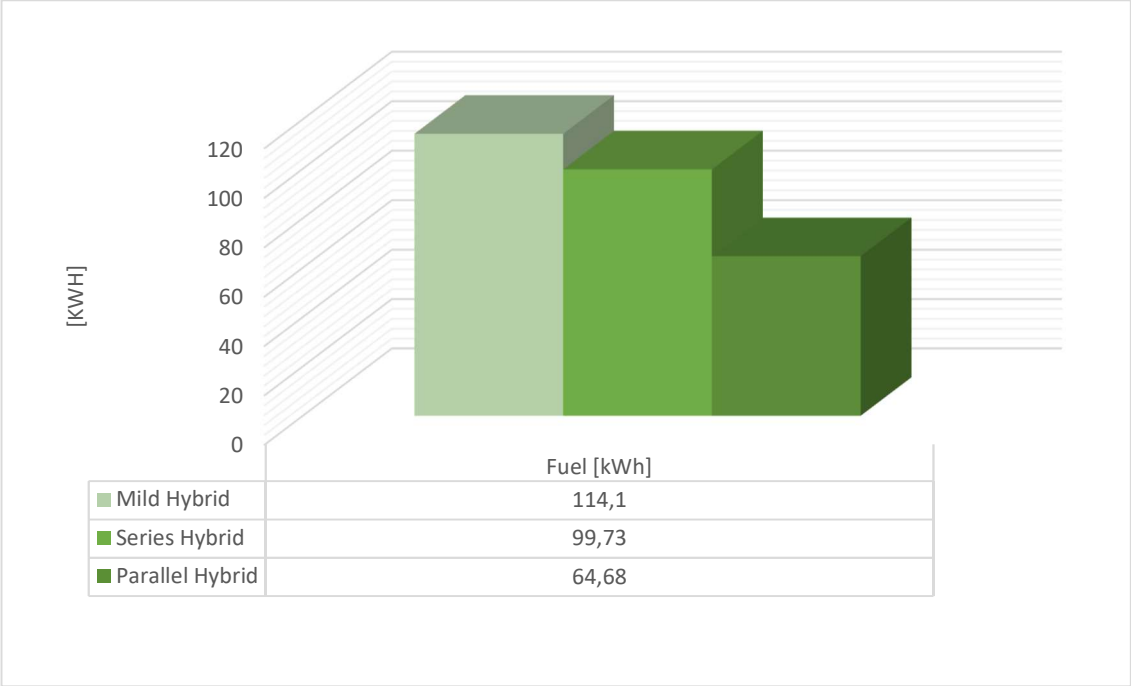

Fig. 88 Powertrain configurations comparison over RDE B cycle

Due to the high average speed, the energetic impact of the initial charge depleting phase shared by the two PHEVs is less relevant than in the previous cases. Still, it allows to reduce the fuel consumption by 12.6% in the case of the series hybrid. On the contrary, the parallel hybrid model recognises the high-speed, high-power-phases, that are instead employed to charge the batteries and in parallel drive the car through the ICE. The EMs are used only at specific conditions. This helps in further reducing the fuel consumption by 43.3% with respect to the mild hybrid, and by 35.1% with respect to the series one.

6. Conclusions and future work

The political and industrial context of the automotive sector is clearly moving towards electric mobility: this new trend has to be faced by supercar producer taking into account both customer expectations in terms of performance and drivability, as well as legal boundaries in terms of environment sustainability. The project was meant to define the energetic efficiency as the top priority target, improving the energy management strategy of the car high performance powertrain.

Therefore virtual model of the car was designed and tested until it reached the stability and accuracy necessary to provide reliable results. Such model was built to simulate longitudinal performances only, with a particular focus over powertrain systems and on their energetic consumption. It was built over experimental maps and realistic components, in order to align it as much as possible to the already existing one, which was earlier developed by Lamborghini.

Then, the data collection for the strategy design started. First, technical solutions and standards adopted by the state-of-the-art hybrid supercars from the main competitors, as well as those from Lamborghini itself, were examined and compared between each other, in order to obtain guidelines and suggestions for the strategy creation. In addition, the most important components mounted onto the vehicle, and their technical characteristics, were analysed to prepare the strategy tuning phase. A deep literature research followed, as the last and most important step. Academic studies over motors, engines, batteries and energy management systems were consulted and played an important role into the strategy creation.

A detailed description of the strategy was then reported. The way it operates, how the optimization processes were run, and how such strategy behaved over various working phases and driving cycle was extensively described. The strategy proved to be adaptive to different combinations of torque requests, speeds, battery state of charge and driver commands.

Several tests were carried out to demonstrate the major difference in term of improved fuel consumption when compared to the same virtual car, based on the series hybrid architecture. Findings show that the different powertrain combinations chosen in real time by the proposed rule-based strategy improved the fuel consumption of the parallel hybrid model, up to a point that, when tested, such approach proved to be considerably more efficient than the series hybrid, respectively by:

- 34.2% over the RDE A cycle
- 35.1% over the RDE B cycle
- 42.8% over the WLTP Class 03 cycle

Still, there is plenty of room for further development concerning the proposed strategy. The most important feature that would further improve the efficiency would certainly be the *a priori knowledge* of the route. With a real time strategy as a target, the knowledge of the route in advance was not acceptable and so, optimum results could not be achieved yet: as an example, the RDE B and the WLTP Class 03 cycles both end with a very high speed phase, that leaves a non-negligible amount of battery energy unused. Had the route be known in advance, the vehicle would have undergone a

complete *depleting phase* before entering the last high speed one, or at least, it would have stopped the *discharge prevention* phase during the last part of the cycle.

Another very important development point regards the vehicle emission reduction. The series hybrid model, features nearly *steady-state* working conditions of the internal combustion engine: once it is turned on, it remains at the same speed, decoupled from the wheels. Such architecture is not affected by multiple cranking phases as it happens for the parallel one: those phases, especially with cold engine, might affect the overall pollutant emissions. Therefore, it would be rather interesting to compare again the series and the parallel hybrid architectures, when taking into account CO_2, NOx, particulates and other pollutants. The relevant advantage in terms of fuel consumption of the parallel hybrid would logically have a positive impact on the CO_2 count too, but for what concerns the other chemicals, the problem has to be addressed still.

As the very last step of development, other priorities that were initially ignored might be now taken into account, in particular those regarding the braking system (to be coordinated in its management strategy with the safety department) and driver comfort in longitudinal accelerations (gearshift map and torque allocation). Further development over these additional points would make the model even closer to the reality.

7. Acknowledgments

Ringrazio il mio relatore, professor Stefano Malan: sin dal primo colloquio ha dimostrato saggezza, interesse e puntualità davvero preziose: più di tutte, ha sempre avuto tempo da dedicarmi. A Claudio Manzali, il mio responsabile in Lamborghini, un grande grazie per avermi accolto in azienda: ha capito le mie passioni ed esigenze, e mi ha affiancato con costanza e allegria nelle fasi di lavoro e non. L'attenzione nei miei confronti è stata quella che solo un ex-stagista, al mio stesso posto qualche anno fa, poteva avere. Ringrazio molto anche Enrico Sammarchi: i suoi consigli e il suo materiale per il modello sono stati indispensabili in questi mesi. Un grande grazie va ad Andrea Toso. Lui (e tutta la sua famiglia) mi sono stati da guida ed esempio dall'ultimo anno di liceo fino all'ingresso nel mondo del lavoro.

Questi anni di vita lontano da casa, e ancor più gli ultimi mesi di convivenza, mi hanno mostrato quanto devo essere grato ai miei genitori e ai miei fratelli: mamma Daniela e papà Lorenzo mi insegnano ogni giorno cosa vuol dire essere figlio ed essere uomo. Hanno accettato tutte le mie decisioni, anche quando per loro significava rinuncia e sacrificio. Marco e Giacomo mi arricchiscono ogni giorno, sono parte di me: la loro saggezza, la loro presenza, sono state un riferimento per i momenti belli e per quelli difficili. Hanno dato e danno un contributo unico e fondamentale a tutte le mie scelte.

Ringrazio la mia Tata: più che una nonna, è una saggia seconda mamma, che mi ha cresciuto e ha creduto nel mio futuro di ingegnere, dai giorni dei Lego a quelli al Politecnico. Voglio inoltre dedicare un grazie speciale a due cugini tra tutti, Camilla e Giovanni. La prima, perché passano gli anni, le città, i gruppi d'amici, ma lei resta per me un punto di riferimento per intelligenza e capacità di voler bene. Il secondo invece, perché oltre ad essere una specie di fratello è anche grazie a lui (forse non lo sa) che mi è nata la passione per l'ingegneria. Sono molto grato anche alla Zia Lucia e alla Zia Donatella, che mi hanno affiancato in alcune fasi delicate degli studi.

Ora gli amici di Parma. Emanuele, che come nessun altro mi è stato e sarà sempre vicino, il mio migliore amico del cui spessore umano e della cui presenza non potrei fare a meno. Francesco e Alessandro, amici autentici e generosi, con cui mi sento sempre a casa. Jacopo, Matteo e Michele, e tutta la nostra compagnia così aperta, così musicale e allegra, che mi ha accolto ad ogni ritorno a Parma. Davide e la Francesca, che nei momenti importanti di questi anni ci sono stati e da cui studi, lavoro e impegni non possono allontanarmi. Camilla, Carolina, Cecilia e Maria, ragazze che mi hanno scavato dentro e mi hanno lasciato diverso. Davide e Giorgio, che hanno rappresentato un modello da seguire in questi anni di studi. Un grazie affettuoso anche alla compagnia classe: gli anni di studio sono finiti, ci siamo sparsi per l'Italia ed Europa ma questo non ci ha divisi: ritrovarci e stare assieme è sempre stato molto importante per me. Filippo, Giacomo, Nicola e Alberto: i quasi vent'anni di lento declino da atleti a frequentatori di ristoranti sono stati più allegri con voi al mio fianco.

Ci sono state anche persone che ho conosciuto fuori Parma in questi anni, e che ringrazio di cuore per l'amicizia. Non posso che iniziare dai due Federico, a cui si sono aggiunti Riccardo e Marco: con me hanno vissuto la vita quotidiana a Torino, mi hanno dato forza e aiutato a superare esami e momenti duri. Poi chiaramente la compagnia degli Autoveicoli: Gianni, Umberto, Alberto e Francesca, che hanno studiato con me al Politecnico. Abbiamo fatto squadra tante volte, continuiamo a

supportarci a vicenda anche oggi e di questo vi ringrazio. Ultimi in ordine cronologico, ma con cui ho condiviso momenti meravigliosi, i miei amici italiani e non che ho conosciuto in Austria. Nicola, Kyra, Dorota, Eleonora, Giuliana, Paolo, Dina, Ilaria, Filippo, Leonardo, Francesca, Vasek e Teresa. Con voi ho riso tantissimo e imparato altrettanto.

Un ultimo pensiero per un amico a cui ero molto legato, e la cui partenza ancora non accetto. Caro Enrico, questo momento di gioia a cui tu saresti stato primissimo invitato è dedicato a te.

8. References

Allan, L. (2020, March 18). *Aston Martin Valkyrie: road testing begins ahead of deliveries*. Retrieved from Autocar.co.uk: https://www.autocar.co.uk/car-news/motor-shows-geneva-motor-show/aston-martin-valkyrie-specs-details-pricing

Banvait, H., Anwar, S., & Chen, Y. (2009). A Rule-Based Energy Management Strategy for Plug-in Hybrid Electric Vehicle (PHEV). *American Control Conference*, 3939.

Baroni, L. (2018, November 16). *Hybrid supercar: auto ibride da sogno con prestazioni intelligenti*. Retrieved from autoblog.it: https://www.autoblog.it/post/933317/hybrid-supercar-auto-ibride-da-sogno-con-prestazioni-intelligenti

Bolun, X., Oudalo, A., Ulbig, A., Andersson, G., & Kirschen, D. S. (2018). Modeling of Lithium-Ion Battery Degradation for Cell Life Assessment. *IEEE TRANSACTIONS ON SMART GRID,*, 1137.

Brouk, S., Buey, M., Ly, S., Pedron, M., & Burgalat, S. (2015). Control Strategies for Hybrid Vehicles in Mountainous Areas. *Procedia Computer Science*, 288.

Buzzetti, D. (2014). The Alliance with Boeing against weight. In B. Daniele, *Lamborghini - 50 anni di fascino e passione* (pp. 292-293). Gruppo BPER.

Cordoba-Arenas, A., Onori, S., Guezennec, Y., & Rizzoni, G. (2014). Capacity and power fade cycle-life model for plug-in hybrid electric vehicle lithium-ion battery cells containing blended spinel and layered-oxide positive electrodes. *Journal of Power Sources*, 477. doi:http://dx.doi.org/10.1016/j.jpowsour.2014.12.047

Enang, W., & Bannister, C. (2017). Modelling and control of hybrid electric vehicles. *Renewable and Sustainable Energy Reviews*, 1222.

EUCommission. (2017, November 11). *Proposal for a Regulation of the European Parliament and of the Council setting emission performance standards for new passenger cars and for new light commercial vehicles as part of the Union's integrated approach to reduce CO2 emissions from light-duty*. Retrieved from eur-lex.europa.eu: https://eur-lex.europa.eu/legal-content/EN/TXT/HTML/?uri=CELEX:52017SC0650&from=EN

EUCommission. (2018). *Reducing CO2 emissions from passenger cars - before 2020*. Retrieved from ec.europa.eu: https://ec.europa.eu/clima/policies/transport/vehicles/cars_en

Finesso, R., Spessa, E., & Venditti, M. (2016). Robust equivalent consumption-based controllers for a dual-mode diesel parallel HEV. *Energy Conversion and Management*, 126.

Genta, G. (2009). *The Automotive Chassis.* Turin: Springer.

Harvey, I. (2016, June 23). *The epic story behind Ferrari and Lamborghini Rivalry*. Retrieved from the Vintage News: https://www.thevintagenews.com/2016/06/23/story-behind-ferrari-lamborghinis-rivalry/

Henk, B. (2020, February 6). *2019 (Full Year) Europe: Electric and Plug-In Hybrid Car Sales per EU and EFTA Country*. Retrieved from Car Sales Statistics: https://www.best-selling-cars.com/electric/latest-europe-electric-and-plug-in-hybrid-car-sales-per-eu-and-efta-country/

Jurnecka, R. (2019, February 5). *Original Influencer: The History of the Lamborghini Miura*. Retrieved from www.automobilemag.com: https://www.automobilemag.com/news/1966-1973-lamborghini-miura-history/

Kabitz, S., Gerschler, J. B., Ecker, M., Yurdagel, Y., Emmermacher, B., André, D., . . . Uwe Sauer, D. (2013). Cycle and calendar life study of a graphite | LiNi1/3Mn1/3Co1/3O2 Li-ion high energy system. Part A: Full cell characterization. *Journal of Power Sources*, 582.

Karbowski, D., Pagerit, S., Kwon, J., Rousseau, A., & Freiherr von Pechmann, K.-F. (2009). "Fair" Comparison of Powertrain Configurations for Plug-In Hybrid Operation Using Global Optimization. *SAE International*.

Kriegler, W. (2019). Hybrid Vehicles - Macro Control Strategies. *Advanced Driving Propulsion Technologies course* (p. 70). Graz: FH Joanneum Fahrzeugtechnik.

Kum, D., Peng, H., & Bucknor, N. K. (2010). Optimal Control of Plug-in HEVs for Fuel Economy Under Various Travel Distances. *6th IFAC Symposium Advances in Automotive Control* (p. 258). Munich: International Federation of Automatic Control.

Lanzarotto, D., Marchesoni, M., Passalacqua, M., Pini Prato, A., & Repetto, M. (2018). Overview of different hybrid vehicle architectures. *IFAC Conference Paper Archive* (p. 221). Genova: International Federation of Automatic Control.

Lee, S., Cherry, J., Safoutin, M., McDonald, J., & Olechiw, M. (2018, April 3). Modelling and Validation of 48V Mild Hybrid Lithium-Ion Battery Pack. *SAE International*.

Li, G., & Gorges, D. (2019). Energy Management strategy for parallel hybrid electric vehicles based on approximate dynamic programming and velocity forecast. *Journal of the Franklin Institute*, 9503.

Meng, Y., & Currier, P. (2016). A System Efficiency Approach to Parallel Hybrid Control Strategies. *SAE International*.

Millo, F., & Rolando, L. (2011). Development of a Control Strategy for Complex Light-Duty Diesel-Hybrid Powertrains. *SAE International*.

Moldrich, C. (2020, February 24). *Fastest hybrid cars in 2020*. Retrieved from carmagazine.co.uk: https://www.carmagazine.co.uk/hybrid/fastest-hybrid-car/

Onion, A., Missy, S., & Mullen, M. (2009, November 13). *Luxury car magnate Ferruccio Lamborghini is born*. Retrieved from history.com: https://www.history.com/this-day-in-history/ferruccio-lamborghini-born

Peng, J., He, H., & Xiong, R. (2015). Rule based energy management strategy for a series-parallel plug-in hybrid electric bus optimized by dynamic programming. *Applied Energy*, 1636.

PressRelease. (2019). *Siàn FKP 37 - Ahead of its time*. Retrieved from lamborghini.com: https://www.lamborghini.com/en-en/models/limited-series/sian

PressRelease. (2020, February 12). *Automobili Lamborghini S.p.A MediaCenter*. Retrieved from lamborghini.com: https://media.lamborghini.com/english/corporate/history/automobili-lamborghini-s.p.a./s/2578d5ed-3247-480b-a5e6-fbd36549d463

Prior, M. (2013, November 29). *Porsche 918 Spyder 2013-2015 review* . Retrieved from Autocar.co.uk: https://www.autocar.co.uk/car-review/porsche/918-spyder-2013-2015

Shen, P., Zhao, Z., Zhan, X., Li, J., & Guo, Q. (2018). Optimal energy management strategy for a plug-in hybrid electric commercial vehicle based on velocity prediction. *Energy*, 840.

Smeyers, M. (2015, September 1). *THE HISTORY OF AUTOMOBILI LAMBORGHINI SPA*. Retrieved from LamboCars.com: http://www.lambocars.com/lambonews/the_history_of_automobili_lamborghini_spa.html

Squir Team. (2020). *Lamborghini Sian 2020*. Retrieved from www.squir.com: https://squir.com/lamborghini-sian-2020.html

Stark, A. (2016). *Mild Hybrid Electric Vehicle (MHEV) – architectures*. Retrieved from x-engineer.org: https://x-engineer.org/automotive-engineering/vehicle/hybrid/mild-hybrid-electric-vehicle-mhev-architectures/

Tran, D.-D., Vafaeipour, M., El Baghdadi, M., Barrero, R., Van Mierlo, J., & Hegazy, O. (2019, November 12). Thorough state-of-the-art analysis of electric and hybrid vehicle powertrains: Topologies and integrated energy management strategies. *Renewable and Sustainable Energy Reviews*.

Tufano, D., De Bellis, V., & Malfi, E. (2018). Development of an on-line energy management strategy for hybrid electric vehicle. *Energy Procedia*, 112.

Zhang, B., Chunting Mi, C., & Zhang, M. (2011). Charge-Depleting Control Strategies and Fuel Optimization of Blended-Mode Plug-In Hybrid Electric Vehicles. *IEEE TRANSACTIONS ON VEHICULAR TECHNOLOGY*, 1523.

Zhang, S., Guangqiang, W., & Songlin, Z. (2010). Study on the Energy Management Strategy of DCT-based Series Parallel PHEV. *International Conference on Computing, Control and Industrial Engineering* (p. 27). Shanghai: IEEE Computer Society.

Zhuang, W., Li, S., Zhang, X., Kum, D., Song, Z., Yin, G., & Ju, F. (2020). A survey of powertrain configuration studies on hybrid electric vehicles. *Applied Energy*, 3-4. doi:https://doi.org/10.1016/j.apenergy.2020.114553

9. Appendix

9.1 List of driving cycles

The driving scenarios used to train the strategy and tune its parameters are reported below. Note that the US06 and WLTP cycles were often repeated two or three times in sequence to simulate an homologation test with *charge depleting* and *charge sustaining* phases combined.

9.1.1 US06

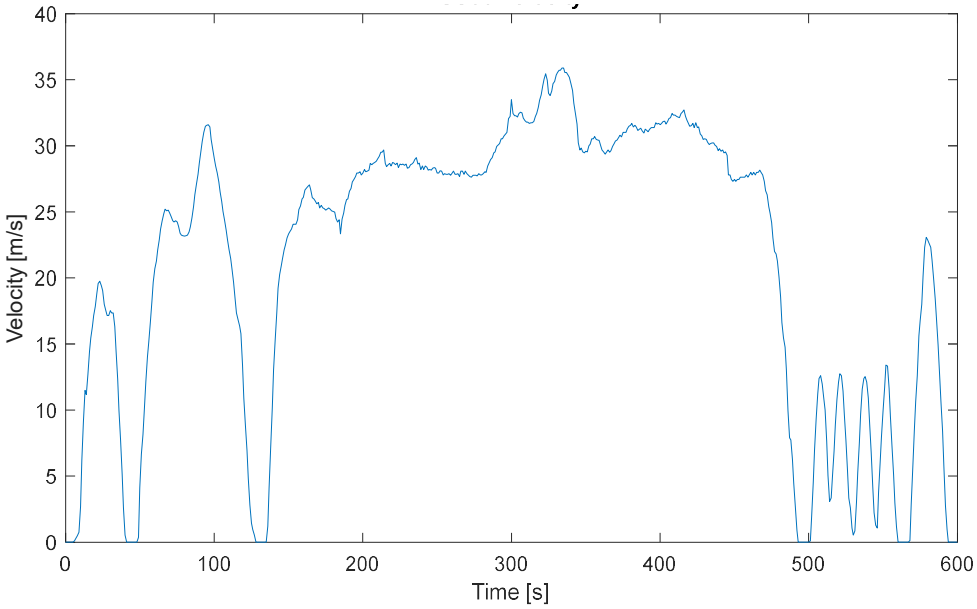

9.1.2 WLTP Class 03

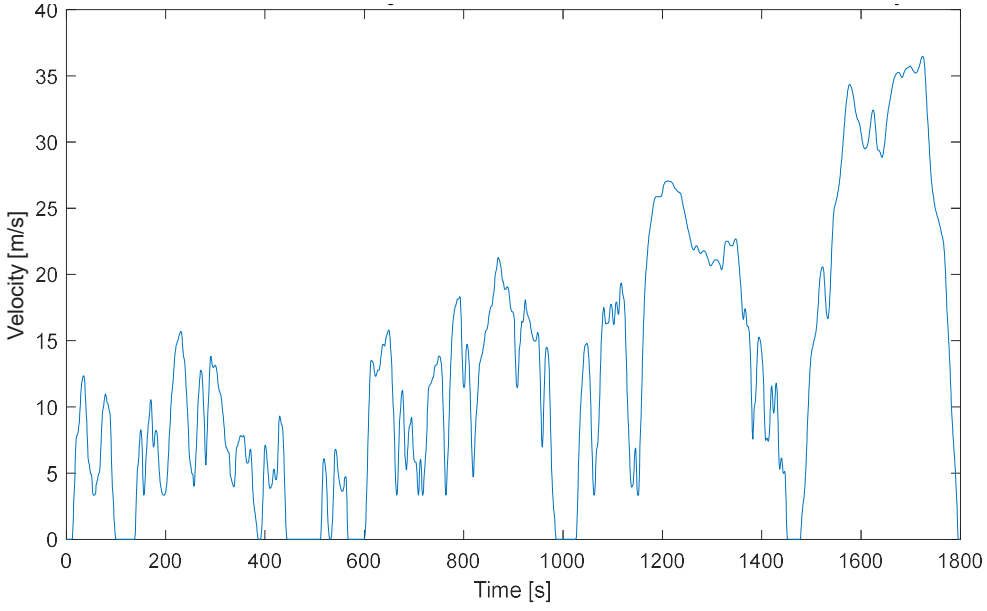

9.1.3 RDE B

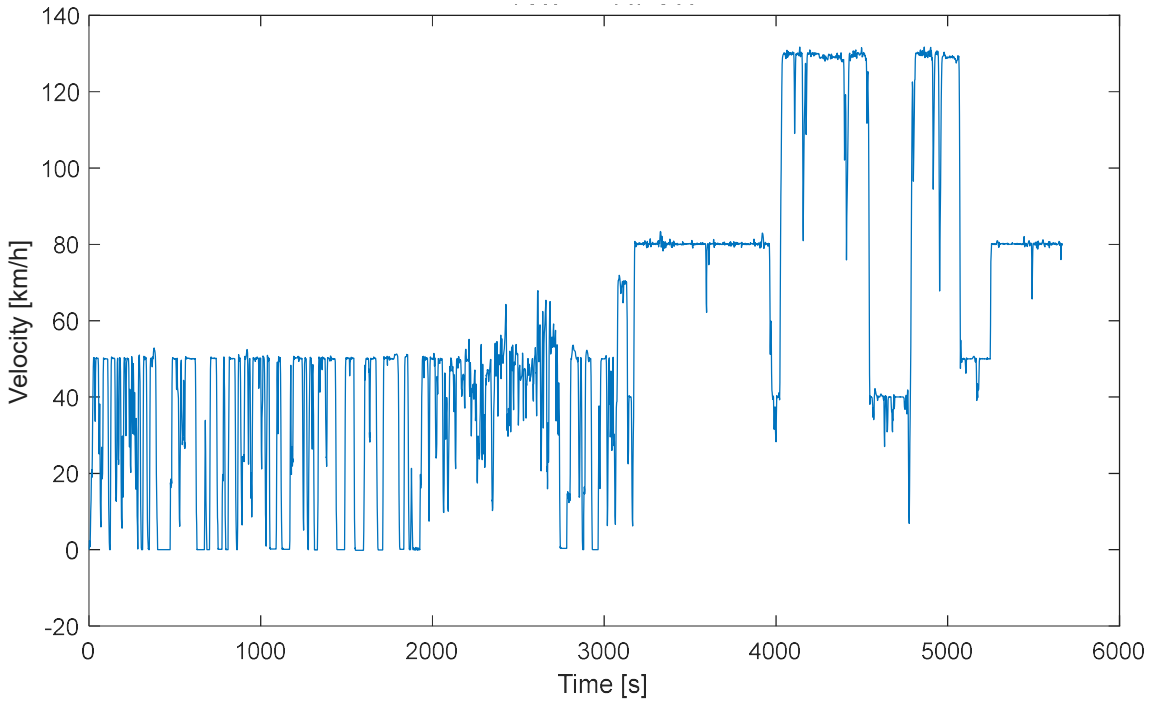

9.1.4 RDE A